

Abstract

Title of Thesis: TWO DIMENSIONAL MAPPING OF THE SODIUM
EMISSION IN EUROPA'S EXOSPHERE

Raquel Fraga-Encinas, Master of Science, 2007

Thesis directed by: Dr. Rosemary M. Killen
Department of Astronomy

We present results of the mapping of Europa's sodium exosphere in two dimensions and through a period of time. We base this research on several observations taken in 2001 and 2002 with the McMath-Pierce Solar Telescope at Kitt Peak, Arizona. We have created sodium emission intensity maps and line of sight column abundance maps of Europa's exosphere in all directions. We include calculations of vertical and tangential column abundances as well as surface densities of sodium relative to the position of Europa and to the Io plasma torus. We find that the sodium exosphere is weakly bound or escaping along the East-West direction, but not to be escaping along the North-South direction. Additionally, we find that the sodium exosphere is energetic enough to extend to a distance of roughly 40,000 km away from the surface of Europa.

**TWO DIMENSIONAL MAPPING OF THE SODIUM EMISSION IN EUROPA'S
EXOSPHERE**

By

Raquel Fraga-Encinas

Thesis submitted to the Faculty of the Graduate School of the
University of Maryland, College Park in partial fulfillment
Of the requirements for the degree of
Master of Science
2007

Advisory Committee:

Professor Douglas P. Hamilton, Chair
Professor Michael F. A'Hearn
Dr. Rosemary M. Killen

© Copyright by
Raquel Fraga-Encinas
2007

Dedication

For Mom, Dad and Luis.

Acknowledgements

These data were acquired at the McMath-Pierce Solar Telescope on Kitt Peak, Arizona. The National Solar Observatory is operated by the Association of Universities for Research in Astronomy, Inc. (AURA) under cooperation agreement with the National Science Foundation. Kitt Peak is on the grounds of the Tohono O’Odham Reservation, which we gratefully acknowledge. We thank Dr. Andrew E. Potter for providing the raw data, data reduction software and guidance. We thank Dr. Floyd Herbert for information about the Io plasma torus.

I would like to express my gratitude to Dr. Rosemary M. Killen for being my advisor and for her invaluable guidance and support throughout this project. I would also like to thank Dr. Douglas P. Hamilton and Dr. Michael F. A’Hearn for their advice, and Dr. Robert H. Herman for his assistance all these years.

I am very thankful to my family for their continuous support during my entire education and to Celsa, Debbie and Paul for their constant encouragement.

Table of Contents

List of Tables	vi
List of Figures	vii
Chapter 1: Introduction	1
1.1 Scientific Motivation	1
Chapter 2: The Physics of Sodium Emission Lines	2
2.1 Origin of the D-lines	2
Chapter 3: The Sodium Exosphere	5
3.1 The Sodium Exosphere Discovery	5
3.2 A New Theory	6
3.3 Other Sodium Exospheres	8
Chapter 4: Europa's Hill Sphere and the Sodium Exobase	9
4.1 Europa's Hill Sphere	9
4.2 The Exobase of the Sodium Exosphere	10
Chapter 5: Observations and Data Reduction	12
5.1 Observations	12
5.2 Data Reduction	13
5.2.1 Extraction of the Sodium D2 Emission	13
Chapter 6: Mapping the Sodium Emission	16
6.1 Sodium Emission Intensity Maps	16
6.2 The Sodium Abundance	23
6.2.1 Line of Sight Sodium Column Abundances	24
6.2.2 Column Abundance relationship with Distance	28
6.2.3 Vertical Sodium Column Abundances and Densities	37
Chapter 7: Uncertainties and Errors	40
7.1 Estimate of Uncertainties and Errors	40
Chapter 8: The Io PlasmaTorus	43
8.1 The Io Plasma Torus	43
8.1.1 Vertical Distance to the Torus	46

Chapter 9: Conclusions	48
9.1 Variability of the Sodium Emission.....	48
9.2 Future Work	49
Appendix A: Detailed Manual for Processing Europa's Data	51
A.1 File Conversion	51
A.2 Cleaning up the Data	51
A.3 Flat Fielding	54
A.4 Trimming the Spectral Image	56
A.5 Correcting the Slope in the Spectra.....	56
A.6 Checking the Zero Level	57
A.7 Geometric Corrections: Registration	57
A.8 Calibration	61
A.9 Fitting the Solar Fraunhofer Line.....	63
A.10 Extracting the Sodium Emission.....	63
A.11 Making the Europa Sodium Emission Image	66
Appendix B: Running VFUDGIT 4.2	67
B.1 Introduction	67
B.2 Using VFUDGIT to extract the Sodium Emission.....	67
Appendix C: Fortran Programs used for the Data Reduction	73
C.1 SKYFLAT.F.....	73
C.2 SPECFLAT.F	76
C.3 CALIBRATION.F.....	80
C.4 PROFIL.F	84
C.5 EUROPANA.F	87
C.6 EUROPAIM.F.....	97
Bibliography	105

List of Tables

3.1	Sodium to potassium ratios in the Solar System.....	7
4.1	Constants used to calculate the Hill Sphere	9
4.2	Constants used to calculate the scale height of the O ₂ atmosphere	10
6.1a	Data from Ephemeris and other calculated quantities	21
6.1b	Data from Ephemeris and other calculated quantities	22
6.2	Values used to calculate the photon scattering coefficient	24
6.3	Line of sight column abundance slopes	36
6.4	Vertical column abundance slopes.....	36
6.5	Tangential column abundance values	38
6.6	Sodium number density abundances	39
6.7	Vertical column abundances values.....	39
7.1	Estimates of the photon noise	41
7.2	Estimates of the continuum level uncertainty	42
7.3	Estimates of the total errors	42
8.1	Europa's vertical distance from the Io plasma torus	47

List of Figures

2.1	Energy level schematic for atomic sodium.....	3
2.2	Contributions to an observed planetary spectrum.....	4
5.1	Sample Voigt fit to the solar Fraunhofer D2 line	15
6.1	Intensity map of sodium D2 emission for obs. 44 on 9/8/2001	17
6.2	Intensity map of sodium D2 emission for obs. 45 on 9/8/2001	17
6.3	Intensity map of sodium D2 emission for obs. 17 on 1/7/2002.....	18
6.4	Intensity map of sodium D2 emission for obs. 12-14 on 2/19/2002.....	18
6.5	Intensity map of sodium D2 emission for obs. 15-17 on 2/19/2002.....	19
6.6	Intensity map of sodium D2 emission for obs. 15-23 on 2/19/2002.....	20
6.7	Line of sight column abundance map for obs. 44 on 9/8/2001.....	25
6.8	Line of sight column abundance map for obs. 45 on 9/8/2001.....	25
6.9	Line of sight column abundance map for obs. 17 on 1/7/2002.....	26
6.10	Line of sight column abundance map for obs. 12-14 on 2/19/2002	26
6.11	Line of sight column abundance map for obs. 15-17 on 2/19/2002	27
6.12	Line of sight column abundance map for obs. 15-23 on 2/19/2002	27
6.13	Col. Abundance vs. East-West Distance – Sept. 8, 2001 – Obs. 44-45.....	29
6.14	Col. Abundance vs. East-West Distance – Sept. 8, 2001 – Obs. 44-45*.....	29
6.15	Col. Abundance vs. North Distance – Sept. 8, 2001 – Obs. 44-45.....	30
6.16	Col. Abundance vs. North Distance – Sept. 8, 2001 – Obs. 44-45*.....	30
6.17	Col. Abundance vs. East-West Distance – Jan. 7, 2002 – Obs. 17.....	31
6.18	Col. Abundance vs. East-West Distance – Jan. 7, 2002 – Obs. 17*.....	31
6.19	Col. Abundance vs. South-North Distance – Jan. 7, 2002 – Obs. 17	32
6.20	Col. Abundance vs. South-North Distance – Jan. 7, 2002 – Obs. 17*.....	32
6.21	Col. Abundance vs. East-West Distance – Feb. 19, 2002 – Obs. 12-14	33
6.22	Col. Abundance vs. East Distance – Feb. 19, 2002 – Obs. 12-14*	33
6.23	Col. Abundance vs. East-West Distance – Feb. 19, 2002 – Obs. 15-17.....	34
6.24	Col. Abundance vs. South-North Distance – Feb. 19, 2002 – Obs. 15-17	34
6.25	Col. Abundance vs. all directions Distance – Feb. 19, 2002 – Obs. 15-23	35
8.1	Europa’s orbital position for obs. 44 and 45 on 9/8/2001.....	44
8.2	Europa’s orbital position for obs. 17 on 1/7/2002 and 12-14 on 2/19/2002	45
8.3	Europa’s orbital position for obs. 15-17 and 22-23 on 2/19/2002	45
A.1	Raw spectrum of Europa	53
A.2	Cosmic ray removed spectrum.....	53
A.3	Sky flat	55

A.4	Flat fielded spectrum of Europa with spurious spikes	55
A.5	Spectrum of Europa with no spikes	56
A.6	Spectrum of Europa with a slope	57
A.7	Columns in the spectrum do not line up	60
A.8	Lines in the spectrum do not line up	61
A.9	Emission extraction	65
A.10	Final intensity map	66
B.1	D2 solar Fraunhofer line	68
B.2	Sample Voigt fit to the solar Fraunhofer line	71
B.3	Sample Voigt fit revealing the D2 emission	72

Chapter 1

Introduction

1.1 Scientific Motivation

In the last thirty years the study of the Galilean moons has developed quite rapidly and especially the field of satellite atmospheres mainly because of the large quantity of new data gathered by the Voyager, Galileo, Hubble and Cassini Missions. It was not long ago, that Io was thought to be the only Galilean moon with an atmosphere.

The research of this paper concentrates on the sodium exosphere of Europa, which is the topmost collisionless layer of an atmosphere. In 1995 an atmosphere composed of oxygen was detected in Europa [Hall et al., 1995]. A year later thanks to the observations of Brown and Hill, the first evidence for a sodium exosphere was presented. With their single observation of Europa along the East-West direction, they were able to make an estimate of the line of sight column abundance of sodium.

In this project we have extended that work by adding a temporal dimension and two spatial dimensions for the mapping of the sodium emission in Europa's exosphere. We based our work on several observations taken in 2001 and 2002 and were able to map the sodium emission in the North-South direction in addition to the East-West direction. We have calculated column abundances and densities of sodium relative to the position of Europa as well as to the Io plasma torus in order to gain a better understanding of the variability of the sodium exosphere over time and location.

Chapter 2

The Physics of Sodium Emission Lines

2.1 Origin of the D-lines

Even though sodium is a trace species in the Solar System compared to hydrogen or helium, we are still able to detect it because of its strong emission lines in the visible part of the spectrum at 5889.95 Å (the so called D2-line) and 5895.92 Å (D1-line). Sodium has 11 electrons, with one valence electron in the 3s shell. The 1s, 2s and 2p shells are filled. The sodium D-lines result from electron transitions between the ground state $3s^2S^{1/2}$ and the first excited state, which is split into $3p^2P^{1/2}$ and $3p^2P^{3/2}$ states due to spin-orbit coupling, resulting in what is called the sodium D-line doublet. If,

$$J=L+S \quad (2.1)$$

where, J = total angular momentum, L = orbital momentum, S = spin

The $P^{1/2}$ and $P^{3/2}$ come from the $1-1/2$ and $1+1/2$.

In addition, hyperfine splitting of the energy levels arises from their preferential alignment in a magnetic field. This causes the D1 line to have four components and the D2 line six components, as seen in the diagram (figure 2.1).

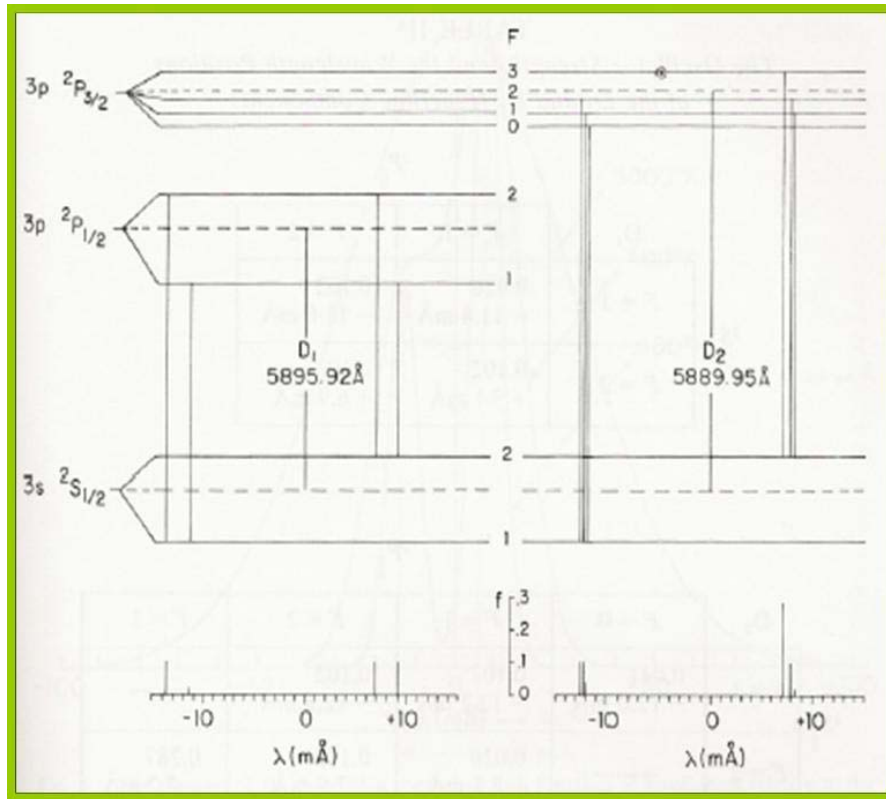


Figure 2.1 – Energy level schematic for atomic sodium: This diagram shows the origin of the D-lines. The D₁ 5895.92 Å and D₂ 5889.95 Å values correspond to the wavelength centroids of the components. [Figure adopted from Brown and Yung, 1976].

The surfaces of planets do not emit light as stars do. We can see them because they reflect light from the sun. The sun itself produces an absorption spectrum (called Fraunhofer) since the photosphere absorbs radiation coming from lower layers which are hotter. Part of this radiation is reflected off the surface of Europa, but its atmosphere also absorbs the sunlight and re-emits it at the same wavelength. This is called solar resonant scattering, which excites the sodium atoms in the exosphere producing emission lines (see figure 2.2). The lines are Doppler shifted with respect to the sodium solar Fraunhofer lines due to the radial velocity of Europa with respect to the sun. The atmosphere of the Earth also introduces additional absorption lines: especially important are water lines and sodium airglow emission. It is important to note that Europa has an icy crust, hence a

very high geometric albedo, about 0.64. So when looking at the surface, the sodium emission from the tenuous exosphere is undetectable since it is overpowered by the reflected surface continuum. In the case of some other exospheres, such as the one above Mercury where the albedo is only about 0.12, we can see emission directly over the disk of the planet.

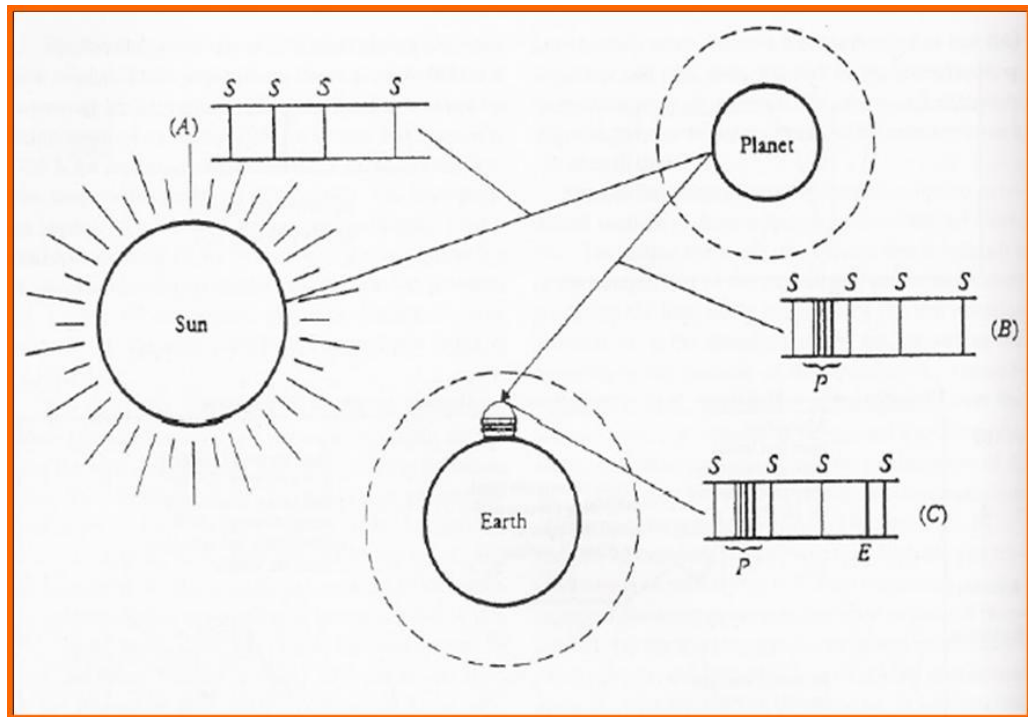


Figure 2.2 – Contributions to an observed planetary spectrum: S-lines represent the solar absorption, P-lines emission or absorption by the planets atmosphere and E-lines possible contribution from the Earth's atmosphere. [Figure adopted from de Pater and Lissauer, 2001].

Chapter 3

The Sodium Exosphere

3.1 The Sodium Exosphere Discovery

The initial discovery of a sodium atmosphere around Europa, with a column density of around $2 \times 10^9 \text{ cm}^{-2}$ and surface density of 70 cm^{-3} , came from the observations of Brown and Hill [1996]. Jupiter's magnetosphere extends beyond Europa's orbit, so energetic ions continually bombard the satellite's surface. Brown and Hill proposed that the sodium found in the exosphere is exogenous to Europa. Io's strong volcanic activity would release great amounts of this element which then would get ionized by the Jovian magnetosphere and finally get trapped into Europa's icy surface. This extended sodium exosphere would then be produced by the process of sputtering. This means that high energy ions originating in the magnetosphere bombard the surface of Europa. There are two types of sputtering: in the first momentum is exchanged. In the second, atoms are first excited to a repulsive electronic state and they subsequently desorb. Sputtering can occur from the surface or atmosphere. Brown and Hill could not measure sodium emission within 5 Europa radii due to the overpowering strength of the surface continuum. However, emission was still detected at a distance of 25 Europa radii, which suggested that these sodium atoms are leaving the surface with velocities larger than 2 km/s. Since Europa's surface only reaches temperatures of about 95 K [Fink and Larson, 1975], sublimation of Na atoms would only yield velocities of about 0.3 km/s which would not be enough to account for the observed extent of the exosphere, as well as

producing a gravitationally bound exosphere. Hence, they concluded that ion sputtering was the mechanism for sodium production and assumed a steady-state mass of the exosphere. The resolution of their long-slit spectra, taken perpendicular to Europa's orbital plane, was 250 mÅ.

3.2 A New Theory

After discovering the presence of potassium in Europa's exosphere [Brown, 1999], further work was carried out to determine the ratios of Na/K in the exospheres of both Europa and Io [Brown, 2001]. The results for Europa were a ratio Na/K \sim 25 and for Io, Na/K \sim 10. Additional analysis of these observations and 3-D Monte Carlo simulations for alkalis (elements comprising Group 1 in the periodic table) in Europa's atmosphere [Leblanc et al., 2002] indicated that the previous assumption of Europa's sodium originating in Io was incorrect. This new work suggested a local origin for both potassium and sodium. The sodium to potassium ratio changes for different bodies in the Solar System. It also varies with time in a given exosphere: the ratio in Mercury's exosphere might vary from 40 to 140 [Potter et al., 2002]. Several sodium to potassium ratios are given in table 3.1. The Na/K value thus may reflect changes of sodium source and loss rates, rather than being a mere indicator of the Na/K ratio on surface rocks.

Besides alkalis, molecular oxygen is also present in Europa's atmosphere as the primary component. Atomic oxygen emission has been detected and it is believed to originate from electron impact dissociation and excitation of atmospheric O₂ [Hall et al., 1995]. Molecular oxygen has not been detected, but its presence has been inferred from the relative intensities of two OI emission lines. This moon has an icy surface so it is not

surprising that the oxygen could be released from the permafrost. However, there has been some struggle to explain exactly how the molecular oxygen gets formed. The latest oxygen-production model suggests a four-step process. Initially, a high energy particle dissociates H₂O into hydrogen and what is called a hydroxyl radical, or OH. Then, two OH molecules react to produce hydrogen peroxide, H₂O₂. Thirdly, another OH molecule reacts with the hydrogen peroxide forming HO₂ (hydrogen coupled to two oxygen atoms), plus a water molecule. Finally, another energetic particle splits an O₂ molecule from the HO₂. This model is based on experiments in which a microscopically thin ice film grown on a platinum surface, under a vacuum, was bombarded with high energy electrons [Kimmel and Petrik, 2006].

Number density at the surface of Europa and column abundance for molecular oxygen are about 10⁸ cm⁻³ and 10¹⁵ cm⁻² respectively [Hall et al., 1995]. In comparison, the O₂ number density at the Earth's surface is about 5 x 10¹⁸ cm⁻³ [U.S. Standard Atmosphere, 1976]. Having an O₂ atmosphere means that the boundary for the sodium exosphere is not the surface of Europa (see section 4.1.2). Any molecules or atoms leaving the surface will be interacting with the oxygen first.

Object	Na/K	Source
Mercury exosphere	40 - 140	Potter et al. 2002
Io exosphere	10	Brown 2001
Europa exosphere	25	Brown 2001
Moon exosphere	6	Potter and Morgan 1988
Lunar crust	7-9	Lodders & Fegley, p. 177
Meteorites	9-12	Lodders & Fegley, p. 311
Earth atmosphere	20 - 150	Gault and Rundle 1969
Earth seawater	27	Lodders & Fegley, p. 164
Earth crust	2	Lodders & Fegley, p. 143
Solar system	15	Lodders & Fegley, p. 80

Table 3.1 - Sodium to potassium ratios in the Solar System.

3.3 Other Sodium Exospheres

In our solar system there have been other observed sodium (as well as potassium) exospheres, such as in Mercury, the Moon and Io. It is believed that the dominant processes for the sodium production and loss at Mercury, the Moon and Io are different from those of Europa. Io's sodium originates in its volcanoes. In the cases of Mercury and the Moon, it is likely that some sodium can be transferred to the surface by meteoritic impacts or be vaporized by those impacts. There is also sodium present in the surface rocks. Ion impact and photo-sputtering are also important at Mercury and the Moon.

Chapter 4

Europa's Hill Sphere and the Sodium Exobase

4.1 Europa's Hill Sphere

Europa's Hill Sphere is the distance from the satellite at which the gravitational force of Europa on a body is comparable to the difference between the tidal forces of Jupiter on Europa and Europa on the body. The size of the Hill Sphere is given by the following equation, where the constants are given in the table below:

$$R_H = \left[\frac{M_{europa}}{3(M_{jupiter} + M_{europa})} \right]^{1/3} a \quad (4.1)$$

Mass of Europa	$M_{europa} = 4.8 \times 10^{22} \text{ kg}$
Mass of Jupiter	$M_{jupiter} = 1.90 \times 10^{27} \text{ kg}$
Mean distance from Jupiter to Europa	$a = 670,900 \text{ km}$

Table 4.1 – Constants used to calculate the Hill Sphere.

Europa's Hill Sphere (R_H) is equal to $13,650 \text{ km}$ which is approximately 8.69 Europa radii or 3.74 arcseconds away from its center, given that Europa's mean angular diameter is about 0.86 arcseconds. Therefore, at distances larger than Europa's Hill Sphere of 3.74 arcseconds, an atom will become the gravitationally influenced by Jupiter.

4.2 The Exobase of the Sodium Exosphere

The exobase is the lower boundary of an exosphere where the mean free path is greater than one scale height. In the case of Europa's sodium exosphere the exobase is not the surface of the satellite but rather inside the oxygen atmosphere. Above the exobase the atmosphere becomes collisionless. Another important parameter of atmospheres is the scale height, which is the distance used to describe how the pressure or density of such atmosphere falls off by one e-folding factor.

Saur et al. [1998] conducted 1-dimensional calculations of the vertical temperature profile of the O₂ atmosphere assuming electron impact heating, heat conduction to the surface and Joule heating, which is heating due to collisions between particles. Their O₂ temperature estimates range from 750 Kelvin to 1000 Kelvin. Assuming an average temperature of the O₂ molecules of 875 Kelvin we can calculate the pressure scale height of the O₂ atmosphere, that is, the height in the atmosphere where the pressure has dropped by a value of 1/e of the atmospheric pressure at the surface. The pressure scale height (*H*) is equal to:

$$H_{O_2} = kT_{O_2} / (g_E \cdot \mu \cdot m_H) \quad (4.2)$$

Boltzman constant	$k = 1.38 \times 10^{-23} \text{ Kelvin/Joule}$
Acceleration of gravity for Europa	$g_E = 1.30 \text{ m/s}^2$
Temperature of oxygen molecules	$T_{O_2} = 875 \text{ Kelvin}$
Mass of hydrogen	$m_H = 1.67 \times 10^{-27} \text{ kg}$
Molecular number for oxygen	$\mu = 32$

Table 4.2 – Constants used to calculate the scale height of the O₂ atmosphere.

Hence, the scale height of the O₂ atmosphere is equal to 174km.

From this value one can calculate the physical height to the exobase (z). Let us assume an exponential decrease of the number density of the O₂ atmosphere given by

$$n(z) \sim n_0 e^{-z/H}, \quad (4.3)$$

where n_0 is the number density of O₂ molecules at the surface of Europa, and take a value for the O₂ column density of $N(O_2) = n_0 H \sim 1.5 \times 10^{15} \text{ cm}^{-2}$ [Hall et al., 1995]. Then, integrating the number density over the distance to which the atmosphere becomes a collision less exosphere (ie. optically thin) will give the answer of the height to the exobase (z):

$$\int_0^z n_0 e^{-z'/H} \cdot dz' = 10^{14} \quad (4.4)$$

In this case, z is approximately 12km. This boundary is too small to be able to be resolved in our observations since the size of 1 pixel is about 3,650km.

Chapter 5

Observations and Data Reduction

5.1 Observations

The sodium emission observations were taken by A. E Potter and R. M. Killen using the 1.6 meter McMath-Pierce solar telescope at Kitt Peak National Observatory. This has a 3 mirror $f/54$ heliostat design in which the heliostat mirrors are used to track the sun, or observable object, and direct the light to the telescope. Europa was observed for a period spanning from the years 1999 until 2004; however, the work presented here includes observations taken between 2001 and 2002. Exposure times ranged from 15 to 30 minutes. A $10''$ by $10''$ Bowen image slicer [Pierce, 1965] which redirects the incoming light to fit a narrow slit without affecting the focal ratio, was used with the Echelle stellar spectrograph with an image stabilizer [Keller & Plymate, 2002]. The CCD camera, with dimensions 800 by 800 pixels, was cooled with liquid nitrogen. Each spatial pixel has an area of $1''$ (in the North-South direction) by $0.3''$ (in the East-West direction), but they were co-added to create $1''$ by $1''$ size pixels. The spectral resolution of each pixel corresponds to about $20.5 \text{ m}\text{\AA}$, which is an improvement from Brown & Hill's $250 \text{ m}\text{\AA}$, allowing us to work closer to the surface of the satellite since our value for the smallest wavelength difference we can measure is smaller reducing the continuum to emission ratio. From the spectrum of each individual pixel, we extracted the sodium D2 emission line producing a $10''$ by $10''$ map of the D2 emission intensity. We only disregard the pixel directly above Europa, when the emission is swamped by the surface reflection.

5.2 Data Reduction

The following is an overview of how the data were reduced. For much more detailed information see Appendix A. The data were cleaned of bad pixels, cosmic ray hits (which become a problem during such long exposures) and the zero level was subtracted. The process of flat fielding is carried out in order to correct for the uneven efficiency of individual pixels. Normally, the spectrum of a lamp is used to flat-field the data. However, in our observations sky spectra were used in the process of flat-fielding because the flat from the lamp does not illuminate the field in the same way as the object we are observing does, therefore it creates an undesirable slope in the observed spectra. The data were then corrected for any misalignments due to imperfect alignments of the CCD position, in the process called registration. After that, the number of kilorayleighs (which are defined as $10^{13} \text{ photons}/m^2 \cdot s$) per count was calculated to be used as a calibration constant for the intensity, based on the known albedo of Europa.

5.2.1 Extraction of the Sodium D2 Emission

In our observations the D1 emission line signal is too noisy to be of any use. This is because even for the simplest case in which there is no continuum and for an optically thin atmosphere the ratio $D2/D1 \sim 1.66$ [Killen, 2006]. Hence, all of our work is concentrated on the stronger D2 line. The observed emission is a combination of sunlight reflection and the actual sodium emission from Europa's exosphere. The latter was extracted by fitting the solar Fraunhofer line profile at the peak of the Europa reflection, since sodium emission cannot be detected there due to the overwhelming brightness of the continuum. Next this profile was

scaled to the spectra away from the center of the satellite where emission becomes apparent. This fit, created by the VFUDGIT routine (see appendix B), was then subtracted from the observed emission in order to get the intrinsic emission from the exosphere (see figure 5.1). From those emissions, we mapped the emission spatially to create a map of the sodium emission intensity around Europa. The calibration factor was obtained by looking at the continuum outside the Fraunhofer lines and using values for the V-band magnitude of Europa (see appendix A).

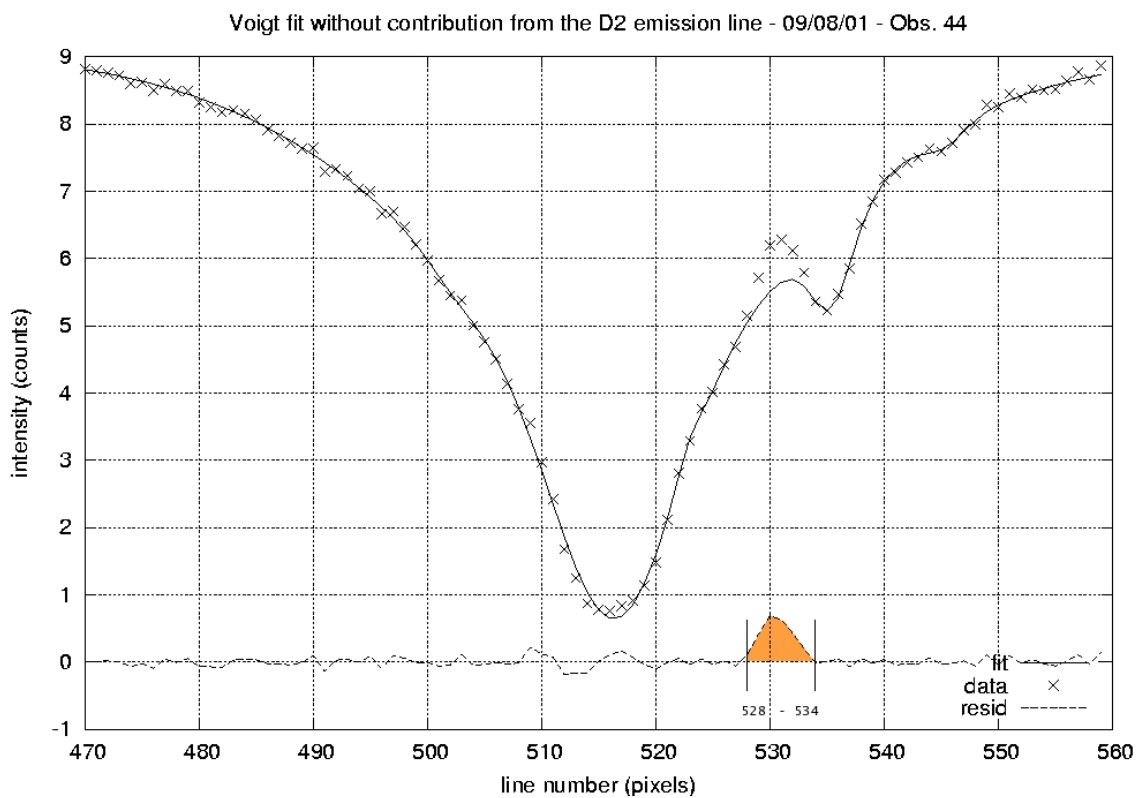
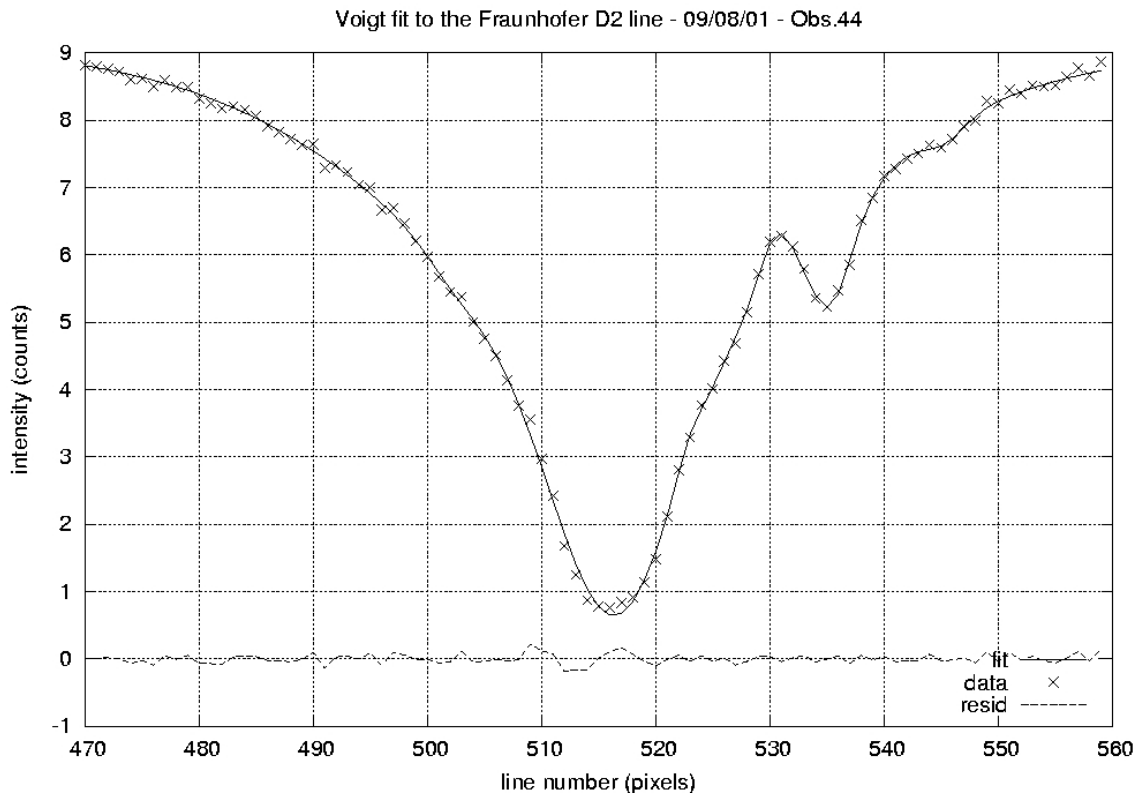


Figure 5.1 – Sample Voigt fit to the solar Fraunhofer D2 line (top) and fit neglecting the emission (bottom).

Chapter 6

Mapping the Sodium Emission

6.1 Sodium Emission Intensity Maps

The following figures are maps of the intensity of the D2 sodium emission line of Europa's exosphere. In each of them, the image of the surface reflection is on the left and Europa's D2 sodium emission is on the right. The color bar indicates intensity values given in units of kilorayleighs (kR). In several of the maps (figures 6.4, 6.5 and 6.6) a number of observations had to be averaged together to improve the signal to noise ratio. The scale is 1'' per pixel and the coordinates are East to the left of the image and South to the top. The black circle in the center of each image represents the size of Europa, which is slightly less than 1'' (see tables 6.1a and 6.1b at the end of this section). For all of these observations Jupiter is located to the East of Europa.

The aperture of the image slicer is 10'' by 10''. However, most of the maps presented here (with the exception of figure 6.3 which is 10''x 10'') end up with slightly different dimensions. For all the February 19, 2002 observations (figures 6.4, 6.5 and 6.6) and the September 8, 2001 observations (figures 6.1 and 6.2), the data in the first slice was very noisy and partially cut-off so this first slice had to be discarded during the process of data reduction, as a consequence those maps are only 9'' wide in the South-North direction. The seeing is also indicated in each map, ranging from 1.0'' to 3.1''. Figure 6.6 is a special case. In this map we combined an image centered on Europa (average of observations 15-17 taken on February 19, 2002) with another image (average of

observations 22-23 taken on February 19, 2002) in which the telescope was pointing 8'' West of the satellite in order to get a larger field of view. As a result, the dimension in the East-West direction is 18''.

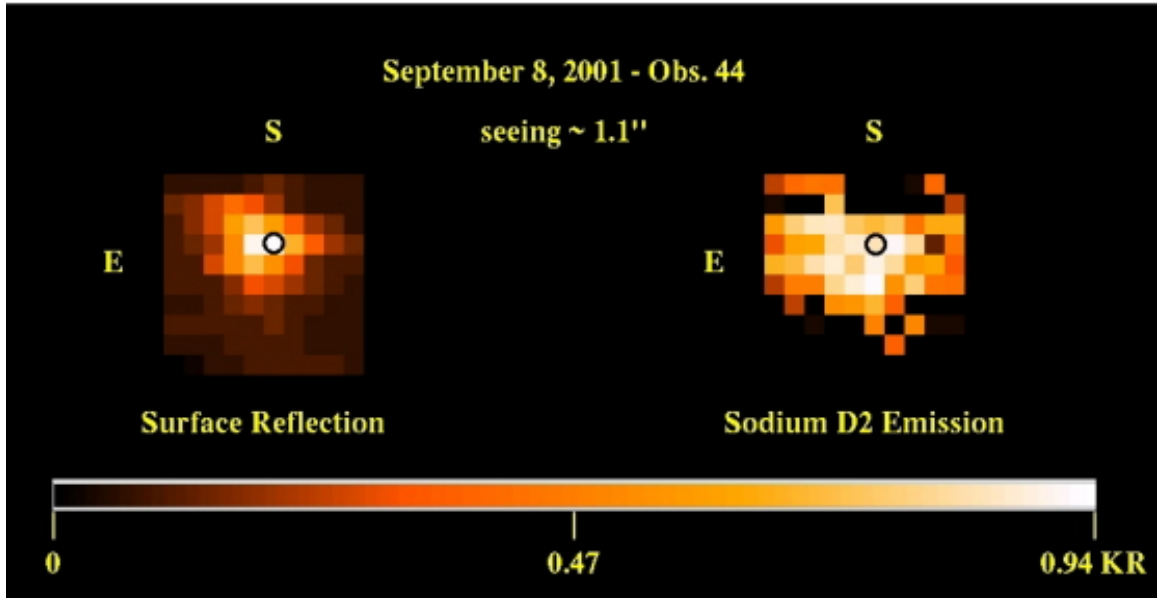


Figure 6.1 – Intensity map of sodium D2 emission for obs. 44 on 9/8/2001: Continuum is to the left, emission to the right. The black circle is at Europa's position and represents its angular size. Intensity scale is in kilorayleighs. Single observation with exposure time of 20 minutes.

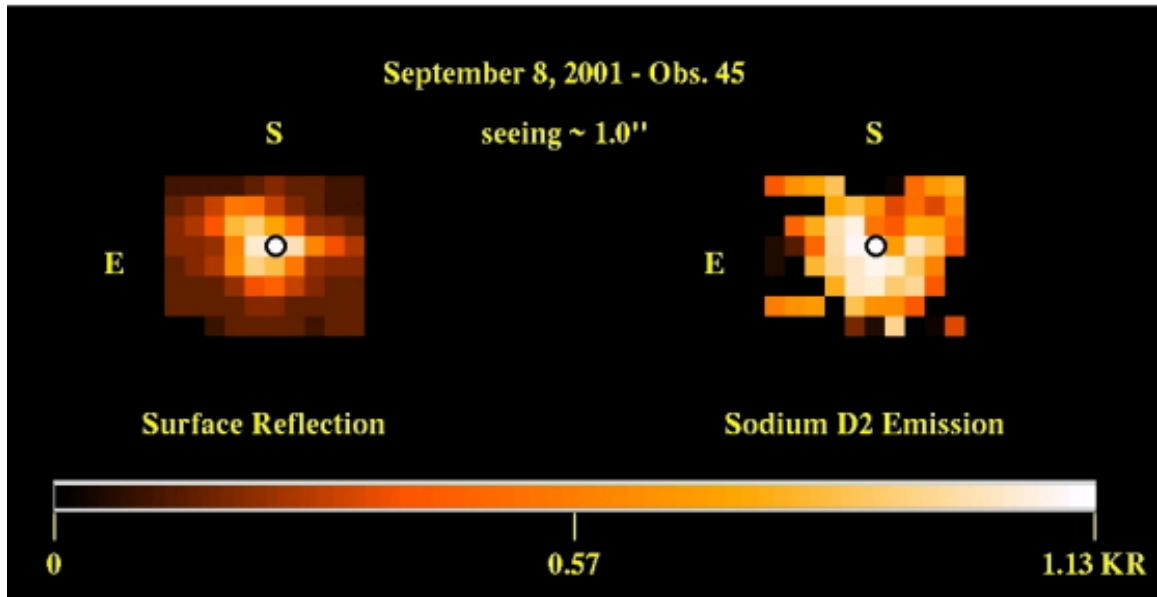


Figure 6.2 – Intensity map of sodium D2 emission for obs. 45 on 9/8/2001: Single observation with exposure time of 20 minutes.

The general trend in these maps is that the sodium intensity decreases as we move away from Europa. For all maps except the January 7, 2002 observation (figure 6.3), there seems to be an enhancement of the emission intensity in the South-East to North-West diagonal direction. This issue will be discussed further in the next section (see 6.2).

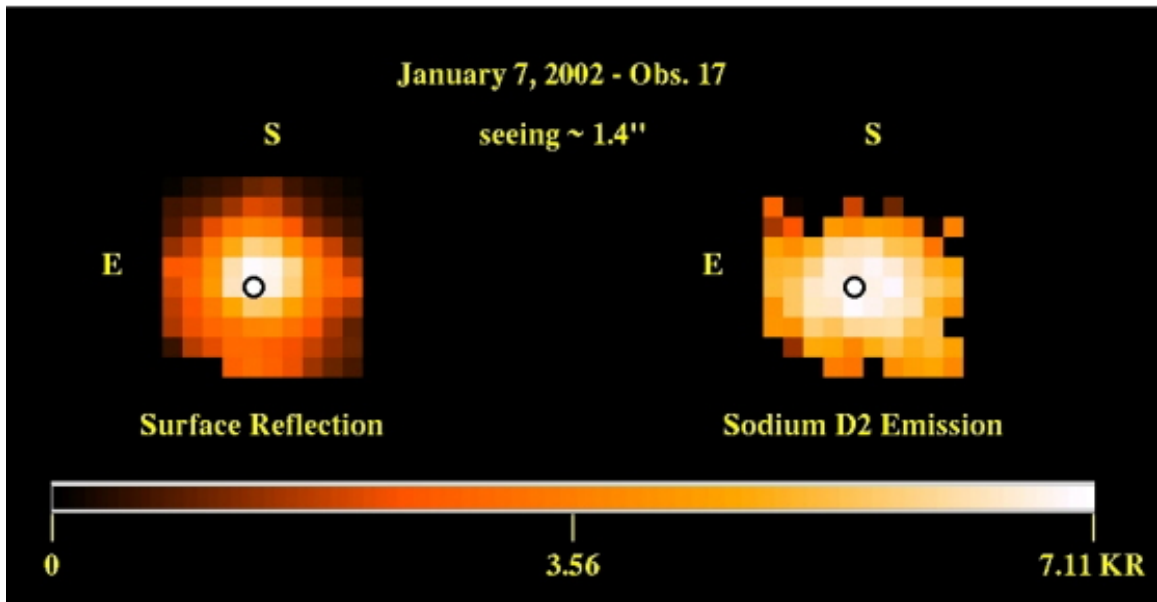


Figure 6.3 – Intensity map of sodium D2 emission for obs. 17 on 1/7/2002: Exposure time is 30 minutes.

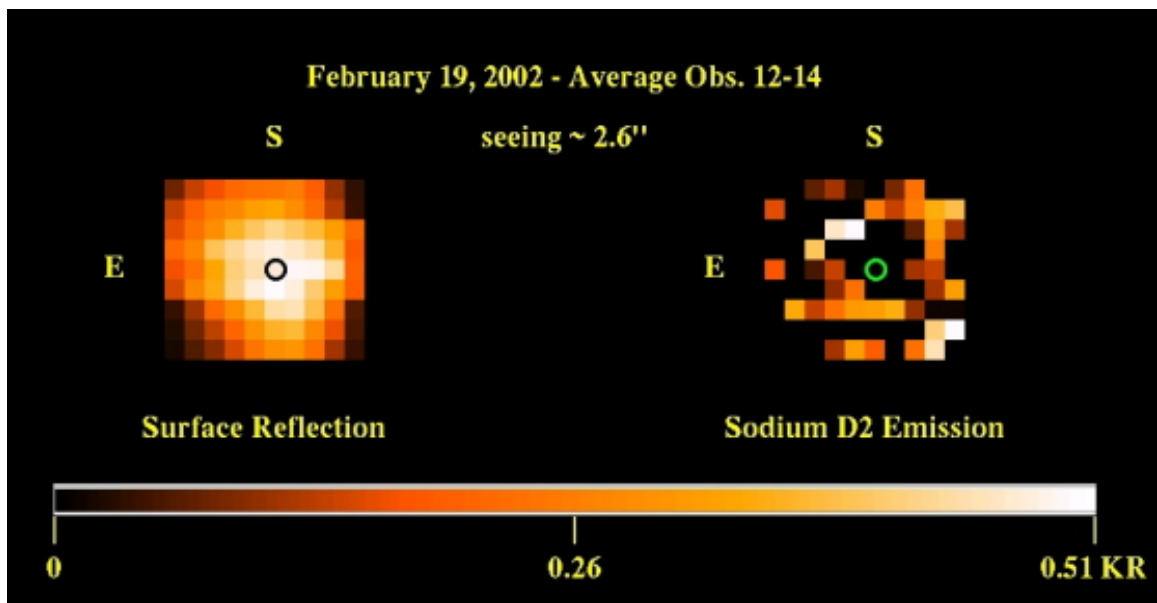


Figure 6.4 – Intensity map of sodium D2 emission for obs. 12-14 on 2/19/2002: This map is an average of consecutive observations 12, 13 and 14 with exposure time of 15 minutes each.

There is a quite interesting feature in figure 6.4 above. The map for these first set of observations taken on February 19, 2002, shows a hole around the disk of Europa but it is not present in subsequent observations taken that day (see figures 6.5 and 6.6). For some reason it appears that there is a lack of sodium around the satellite but also an enhancement in the South-East to North-West directions several pixels away from the disk. Europa's diameter is 3138 km and its angular size at the time of this observation was $0.95''$. Given that the largest hole we see is 2 pixels across (South direction), the distance from the surface of Europa to the center of the next pixel with emission is about $2.525''$ or 8340 km. If the time span from the end of observation 14 to the beginning of observation 15 is 185 seconds, this implies a velocity of 45 km/s for a sodium atom leaving the surface which corresponds to a temperature of 2.8×10^6 Kelvin. It is physically unlikely that the neutral sodium atoms could be at such high temperatures. Hence, we must infer that this lack of sodium around the satellite is an artifact of the data reduction rather than due to destruction of sodium atoms.

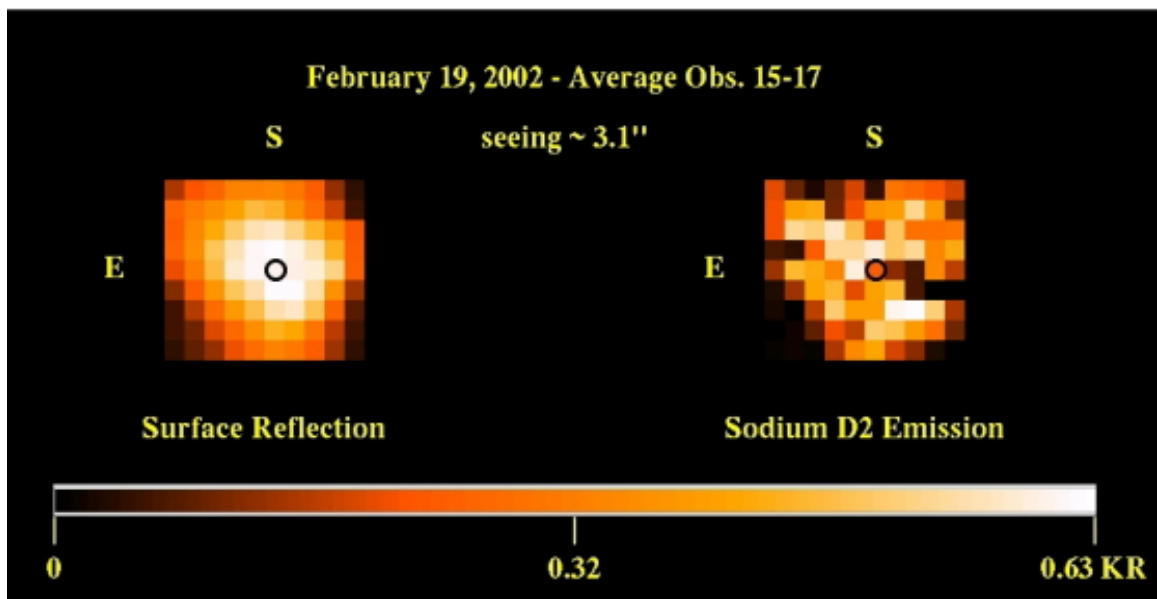


Figure 6.5 – Intensity map of sodium D2 emission for obs. 15-17 on 2/19/2002: This map is an average of consecutive observations 15, 16 and 17 with exposure time of 15 minutes each.

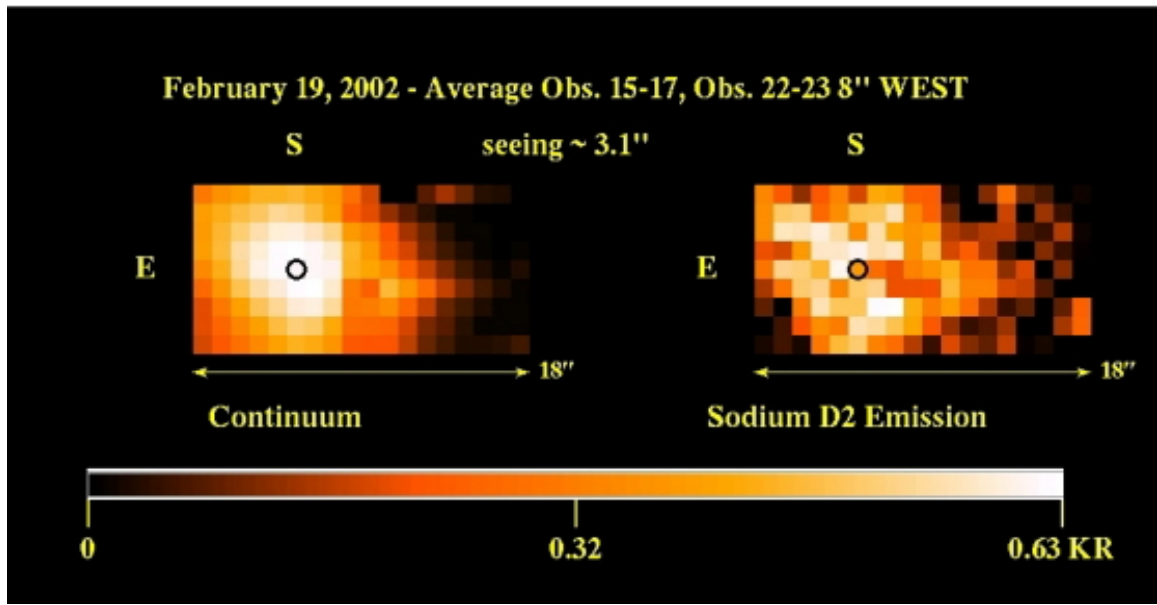


Figure 6.6 – Intensity map of sodium D2 emission for obs. 15-23 on 2/19/2002: This map combines the average of observations 15-17 with the average of observations 22-23 taken 8'' West of Europa. The exposure time is 30 minutes.

In figure 6.6 we can see that the sodium emission extends well beyond the location of Europa and it is still detectable 12'' West of the disk. As previously mentioned, Europa's diameter is 3,138 km and the angular size of its disk in these observations is roughly 0.95''. Therefore, the sodium exosphere extends to a distance of about 39,600 km away from the disk towards the West with an error around 23% (see chapter 7 for error calculations). This is comparable to the extent of Mercury's sodium "tail" anti-sunward of Mercury.

Date	N	UT1 (start)	UT2 (end)	exp(')	ZD(o)	air	Vmag	ccd	angD('')
Sep 8,2001	44	2001-09-08, 10:59:49'	11:19:49'	20	54.3	1.71	5.91	ti4	0.787
Sep 8,2001	45	2001-09-08, 11:21:05'	11:41:05'	20	49.8	1.55	5.91	ti4	0.787
Jan 7,2002	17	2002-01-07,07:14:02'	07:44:02'	30	9.25	1.01	5.36	ti4	1.028
Feb19,2002	12	2002-02-19,02:48:03'	03:03:03'	15	17.23	1.05	5.53	ti5	0.947
Feb19,2002	13	2002-02-19,03:05:03'	03:20:03'	15	14.1	1.03	5.53	ti5	0.947
Feb19,2002	14	2002-02-19,03:21:52'	03:36:52'	15	11.35	1.02	5.53	ti5	0.947
Feb19,2002	15	2002-02-19,03:39:57'	03:54:57'	15	9.21	1.01	5.53	ti5	0.947
Feb19,2002	16	2002-02-19,03:56:36'	04:11:57'	15	8.52	1.01	5.53	ti5	0.947
Feb19,2002	17	2002-02-19,04:14:15'	04:29:15'	15	9.45	1.01	5.54	ti5	0.947
Feb19,2002	22	2002-02-19,05:41:18'	06:11:18'	30	24.84	1.10	5.54	ti5	0.946
Feb19,2002	23	2002-02-19,06:13:12'	06:43:12'	30	31.52	1.17	5.54	ti5	0.946
avg. 22-23		2002-02-19,05:57:15'	06:27:15'	30	28.18	1.14	5.54	ti5	0.946
Date	N	rdot1	rdot2	rdot(km/s)	r1	r2	r (AU)	sysIII(o)	
Sep 8,2001	44	14.0317	13.9673	13.9995	5.1300	5.1301	5.1301	62.120	
Sep 8,2001	45	13.9639	13.8911	13.9275	5.1301	5.1302	5.1302	73.330	
Jan 7,2002	17	14.1711	14.0545	14.1128	5.1741	5.1743	5.1742	138.370	
Feb19,2002	12	12.7078	12.5792	12.6435	5.1912	5.1913	5.1913	-55.310	
Feb19,2002	13	12.5618	12.4285	12.4951	5.1913	5.1914	5.1913	-46.240	
Feb19,2002	14	12.4121	12.2744	12.3432	5.1914	5.1915	5.1914	-37.250	
Feb19,2002	15	12.2456	12.1030	12.1743	5.1915	5.1915	5.1915	-27.595	
Feb19,2002	16	12.0871	11.9402	12.0136	5.1916	5.1916	5.1916	-18.695	
Feb19,2002	17	11.9138	11.7624	11.8381	5.1916	5.1917	5.1917	-9.275	
Feb19,2002	22	10.9832	10.6345	10.8089	5.1920	5.1922	5.1921	41.235	
Feb19,2002	23	10.6120	10.2490	10.4305	5.1922	5.1923	5.1922	58.265	
avg. 22-23		10.7976	10.4417	10.6197	5.1921	5.1922	5.1922	49.750	
Date	N	Ob-lonJ1	Ob-lonJ2	Ob-lonJ(o)	Ob-lonE1	Ob-lonE2	Ob-lonE(o)		
Sep 8,2001	44	149.44	161.53	155.485	272.66	274.07	273.365		
Sep 8,2001	45	162.13	174.22	168.175	274.14	275.55	274.845		
Jan 7,2002	17	235.55	253.69	244.62	285.19	287.31	286.25		
Feb19,2002	12	70.05	79.12	74.585	309.37	310.42	309.895		
Feb19,2002	13	80.32	89.39	84.855	310.57	311.62	311.095		
Feb19,2002	14	90.49	99.56	95.025	311.75	312.8	312.275		
Feb19,2002	15	101.42	110.49	105.955	313.02	314.08	313.55		
Feb19,2002	16	111.49	120.56	116.025	314.19	315.25	314.72		
Feb19,2002	17	122.16	131.22	126.69	315.44	316.49	315.965		
Feb19,2002	22	174.78	192.92	183.85	321.56	323.67	322.615		
Feb19,2002	23	194.06	212.20	203.13	323.81	325.92	324.865		
avg. 22-23		184.42	202.56	193.49	322.685	324.795	323.74		

Table 6.1a – Data from Ephemeris and other calculated quantities: In the three sections of this table the date and observation number are included. The following parameters are indicated for each section of the table.

Top section: *UT start, end* – Universal Time; *exp* – exposure time in minutes; *Vmag* – visual magnitude; *ZD* – zenith angle in degrees; *air* – air mass; *ccd* – name of the CCD used; *angD* – angular diameter in arcseconds.

Middle section: *rdot1 & rdot2* – heliocentric velocity of Europa at the beginning and end of the observation in km/s; *rdot* – average of those values; *r1 & r2* – average distance from the sun at the beginning and end of the observation in Astronomical units; *r* – average of those values; *sysIII* – system angle in degrees.

Bottom section: *Ob-lonJ1 & Ob-lonJ2* – observer’s longitude of Jupiter at the beginning and end of the observation in degrees; *Ob-lonJ* – average of those values; *Ob-lonE1 & Ob-lonE2* – observer’s longitude of Europa at the beginning and end of the observation in degrees; *Ob-lonE* – average of those values.

Date	N	deldot1 E	deldot2 E	deldot E	rdot1 Io	rdot2 Io	rdot Io(km/s)	
Sep 8,2001	44	-10.622	-10.613	-10.618	5.979	5.164	5.571	
Sep 8,2001	45	-10.613	-10.610	-10.611	5.123	4.297	4.710	
Jan 7,2002	17	17.488	17.418	17.453	-16.611	-16.723	-16.667	
Feb19,2002	12	33.701	33.565	33.633	-7.545	-6.972	-7.259	
Feb19,2002	13	33.546	33.407	33.477	-6.895	-6.895	-6.895	
Feb19,2002	14	33.390	33.246	33.318	-6.238	-5.643	-5.940	
Feb19,2002	15	33.216	33.069	33.143	-5.519	-4.914	-5.216	
Feb19,2002	16	33.053	32.901	32.977	-4.847	-4.233	-4.540	
Feb19,2002	17	32.874	32.719	32.796	-4.124	-3.503	-3.813	
Feb19,2002	22	31.923	31.566	31.744	-0.460	0.821	0.180	
Feb19,2002	23	31.543	31.171	31.357	0.902	2.180	1.541	
avg. 22-23		31.733	31.369	31.551	0.221	1.500	0.861	
Date	N	deldot1 Io	deldot2 Io	deldot Io	Ob-lon1	Ob-lon2	Ob-lon Io(o)	
Sep 8,2001	44	-16.080	-16.825	-16.453	331.920	334.740	333.330	
Sep 8,2001	45	-16.862	-17.623	-17.243	334.880	337.700	336.290	
Jan 7,2002	17	-13.313	-13.337	-13.325	84.940	89.180	87.060	
Feb19,2002	12	17.097	17.735	17.416	161.000	163.120	162.060	
Feb19,2002	13	17.821	18.467	18.144	163.410	165.530	164.470	
Feb19,2002	14	18.546	19.199	18.872	165.780	167.910	166.845	
Feb19,2002	15	19.334	19.993	19.663	168.340	170.460	169.400	
Feb19,2002	16	20.065	20.728	20.397	170.700	172.820	171.760	
Feb19,2002	17	20.846	21.512	21.179	173.190	175.310	174.250	
Feb19,2002	22	24.715	26.033	25.374	185.500	189.740	187.620	
Feb19,2002	23	26.116	27.412	26.764	190.010	194.260	192.135	
avg. 22-23		25.416	26.723	26.069	187.755	192.000	189.878	
Date	N	$\Delta\lambda E(mA)$	D2(pix)	D1(pix)	mA/pix	$\Delta\lambda E(pix)$	$\Delta\lambda Io(mA)$	$\Delta\lambda Io(pix)$
Sep 8,2001	44	-275.371	516.171	225.767	20.558	-13.395	-109.590	-5.331
Sep 8,2001	45	-273.953	516.1291	225.677	20.554	-13.328	-92.650	-4.508
Jan 7,2002	17	-277.599	511.37	220.180	20.502	-13.540	327.834	15.990
Feb19,2002	12	-248.698	-	-	-	-	-	-
Feb19,2002	13	-245.780	494.002	203.727	20.567	-11.950	135.616	6.594
Feb19,2002	14	-242.792	-	-	-	-	-	-
Feb19,2002	15	-239.468	-	-	-	-	-	-
Feb19,2002	16	-236.308	488.19	198.245	20.590	-11.477	89.298	4.337
Feb19,2002	17	-232.856	-	-	-	-	-	-
Feb19,2002	22	-212.610	-	-	-	-	-	-
Feb19,2002	23	-205.167	-	-	-	-	-	-
avg. 22-23		-208.889	488.626	199.184	20.626	-10.128	-16.927	-0.821

Table 6.1b – Data from Ephemeris and other calculated quantities:

Top section: *deldot1 E & deldot2 E* – apparent range-rate of Europa’s center with respect to the observer at the beginning and end of the observation in units of km/s; *deldotE* – average of those values; *rdot1 Io & rdot2 Io* – heliocentric velocity of Io at the beginning and end of the observation in km/s; *rdot Io* – average.

Middle section: *deldot1 Io & deldot2 Io* – apparent range-rate of Io’s center with respect to the observer at the beginning and end of the observation in units of km/s; *deldot Io* – average of those values; *Ob-lon1 & Ob-lon2* – observer’s longitude of Io at the beginning and end of the observation in degrees; *Ob-lon Io* – average of those values.

Bottom section: $\Delta\lambda E(mA)$ – Expected Doppler shift of Europa’s sodium D2 emission line in mÅ; *D2* – location of the solar Fraunhofer D2 line in pixels; *D1* – location of the solar Fraunhofer D1 line in pixels; mA/pix – number of milliångstroms per pixel; $\Delta\lambda E(pix)$ – Expected Doppler shift of Europa’s sodium D2 emission line in pixels; $\Delta\lambda Io(mA)$ – Expected Doppler shift of Io’s sodium D2 emission line in mÅ; $\Delta\lambda Io(pix)$ – Expected Doppler shift of Io’s sodium D2 emission line in pixels.

6.2 The Sodium Abundance

Using the intensities from the maps in the previous section (see 6.1), we calculated the line of sight column abundance (also known as tangential column abundance) of sodium in the exosphere. This is the number of sodium atoms in a thin cylinder with cross section of 1 cm^2 along the line of sight to the observer.

Intensity is in kilorayleighs (kR) and the column abundance, N_T , in atoms/cm².

$$N_T = \frac{\text{Intensity} \times 10^9}{g} \quad (6.1)$$

The *g-factor* is the photon scattering coefficient at a distance R and it is given by

$$g = \gamma \cdot (\pi \cdot F_s) \cdot \left(\frac{\lambda^2}{c} \right) \cdot \left(\frac{\pi \cdot e^2}{m \cdot c} \right) f_{D_2} \left(\frac{1}{R} \right)^2, \quad (6.2)$$

where $(\pi \cdot F_s) = 5.46 \times 10^{13} \frac{\text{photons}}{\text{cm}^2 \cdot \text{s} \cdot \text{\AA}}$ is the solar flux at Earth's orbit. The third factor

$\frac{\pi \cdot e^2}{m \cdot c} = 2.647 \times 10^{-2} \frac{\text{cm}^2}{\text{s}}$ is the integrated absorption coefficient per atom for unit *f-*

value. The oscillator strength of the D2 line is $f_{D_2} = 0.655$. If c is the speed of light, λ is

the wavelength of the sodium D2 line at 5889.95 Å and e the electron charge, then

$$\left(\frac{\lambda^2}{c} \right) = \frac{(5889.95 \text{\AA})^2}{2.998 \times 10^{18}} = 1.157 \times 10^{-11} \text{\AA} \cdot \text{s} \quad (6.3)$$

$$g = 10.95 \cdot \gamma \cdot \left(\frac{1}{R} \right)^2 \frac{\text{photons}}{\text{atom} \cdot \text{s}}, \quad (6.4)$$

where R is Europa's distance from the sun in AU and γ is the fraction of the continuum at the rest wavelength; γ can be interpolated from table I of Brown & Yung [1976], once

we have calculated $\Delta\lambda$ for each observation, where $\frac{\Delta\lambda}{\lambda} = \frac{v}{c}$ in which v is the radial velocity with respect to the sun, $r\text{-dot}$, with values given in table 6.2 below.

Date	Observation	R (AU)	rdot (km/s)	$\Delta\lambda$ (mÅ)	$\gamma\text{-D2}$	fraction dist.	g-factor
09/08/01	44	5.1301	14.000	275.048	0.5361	1.0274	0.2232
09/08/01	45	5.1302	13.927	273.614	0.5334	1.0274	0.2221
01/07/02	17	5.1742	14.113	277.268	0.5405	1.0100	0.2212
02/19/02	12-14avg	5.1913	12.495	245.480	0.5006	1.0034	0.2036
02/19/02	15-17avg	5.1916	12.014	236.030	0.4910	1.0032	0.1996
02/19/02	22-23avg	5.1922	10.620	208.643	0.4572	1.0030	0.1858

Table 6.2 – Values used to calculate the photon scattering coefficient, $g\text{-factor}$: where R is the distance from Europa to the sun in Astronomical Units, $r\text{-dot}$ is the radial velocity, $\Delta\lambda$ is the Doppler shift, $\gamma\text{-D2}$ is the fraction of the continuum at the rest wavelength for the D2 emission line and $fraction\ dist.$ is the ratio $(5.2/R)^2$.

6.2.1 Line of Sight Sodium Column Abundances

In this section we present maps of the integrated line of sight Na column abundance (figures 6.7 to 6.12). The black circle represents the size of Europa and coordinates are defined with East to the left and South to the top. The color bar indicates the column abundance in units of sodium atoms per cm^2 .

All maps except the January 7, 2002 observation (figure 6.9), show an enhancement of the column abundance along the South-East to North-West diagonal direction compared with the South-West to North-East direction. A possible explanation for this asymmetry is that the enhancement could be due to interactions of the sodium atoms with Io's plasma torus such that in some areas of the exosphere the sodium could be getting destroyed. In order to answer this question we need to look at the relative positions of Io, the plasma torus and Europa for each of the observations which shall be explored in chapter 8.

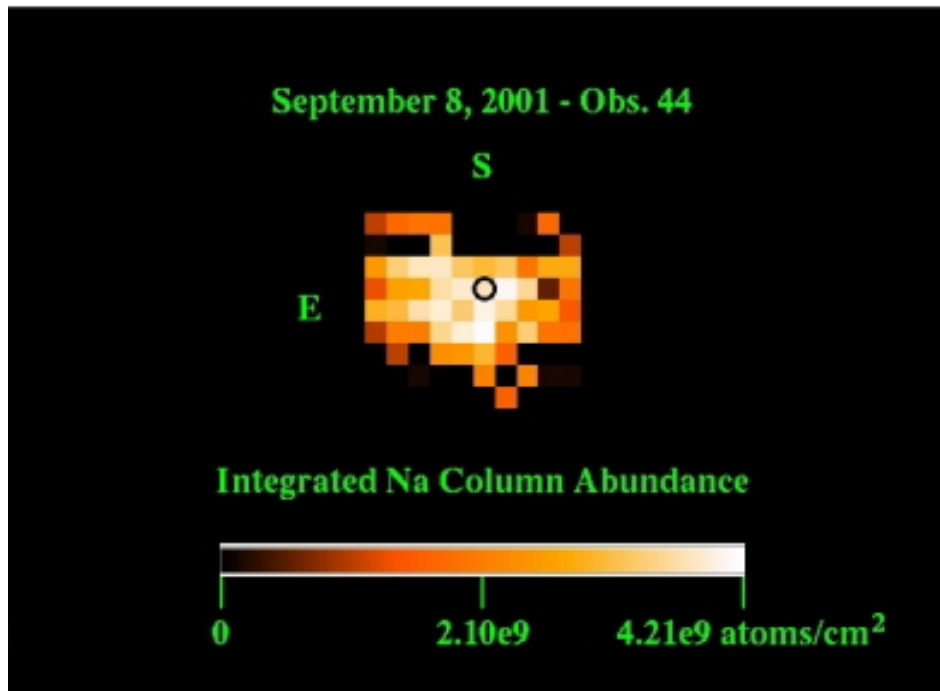


Figure 6.7 – Line of sight column abundance map for obs. 44 on 9/8/2001: Exposure time of 20 minutes. The black circle is at Europa's position and represents its angular size. Column abundance scale is in sodium atoms/cm².

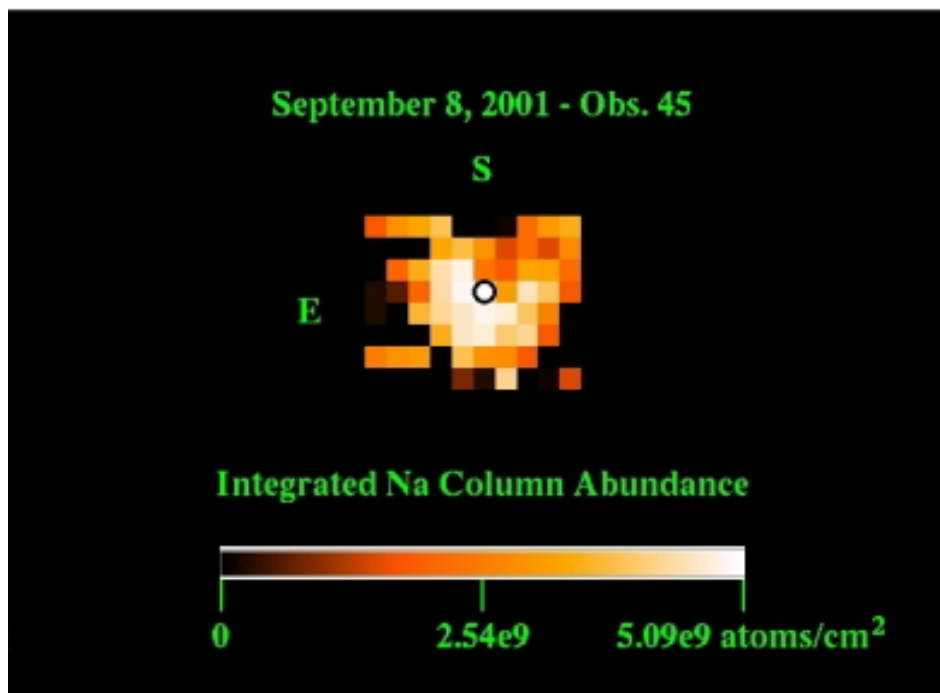


Figure 6.8 – Line of sight column abundance map for obs. 45 on 9/8/2001: Exposure time of 20 minutes.

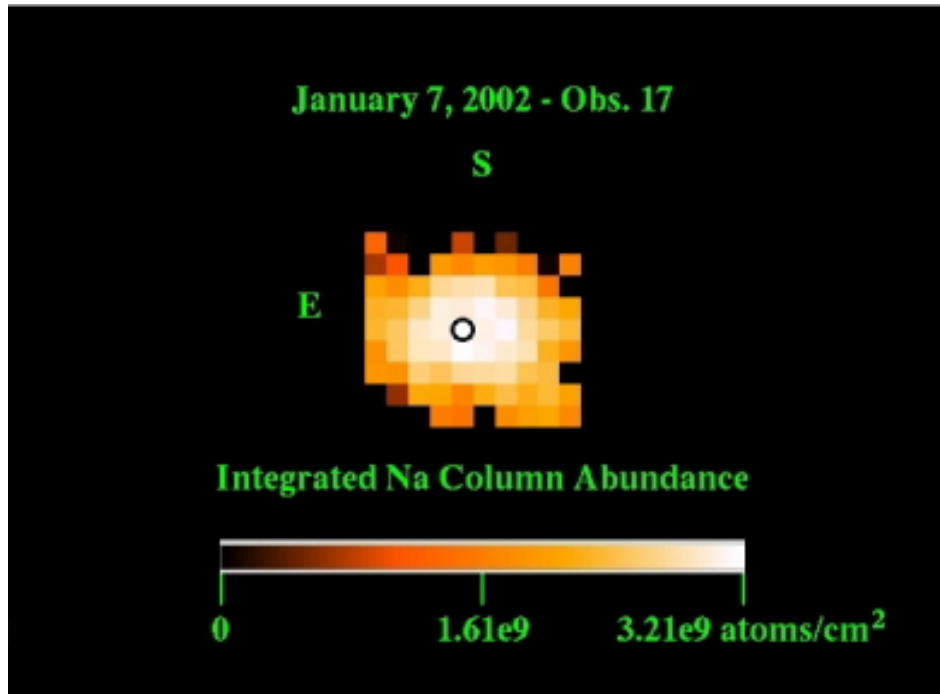


Figure 6.9 – Line of sight column abundance map for obs. 17 on 1/7/2002: Exposure time of 30 minutes.

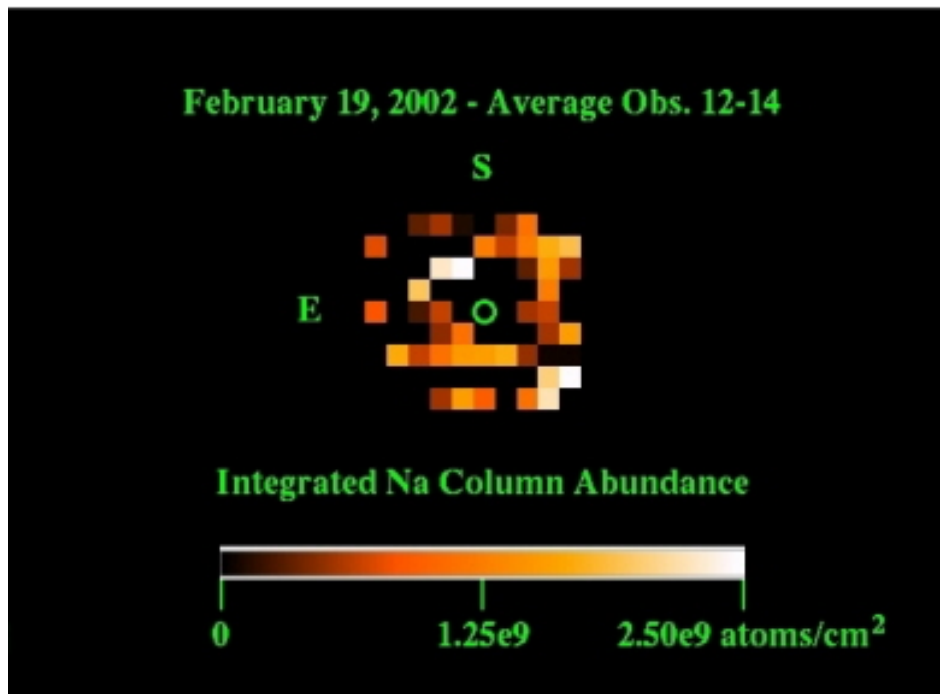


Figure 6.10 – Line of sight column abundance map for obs. 12-14 on 2/19/2002: This is an average of consecutive observations 12, 13 and 14 with exposure time of 15 minutes each.

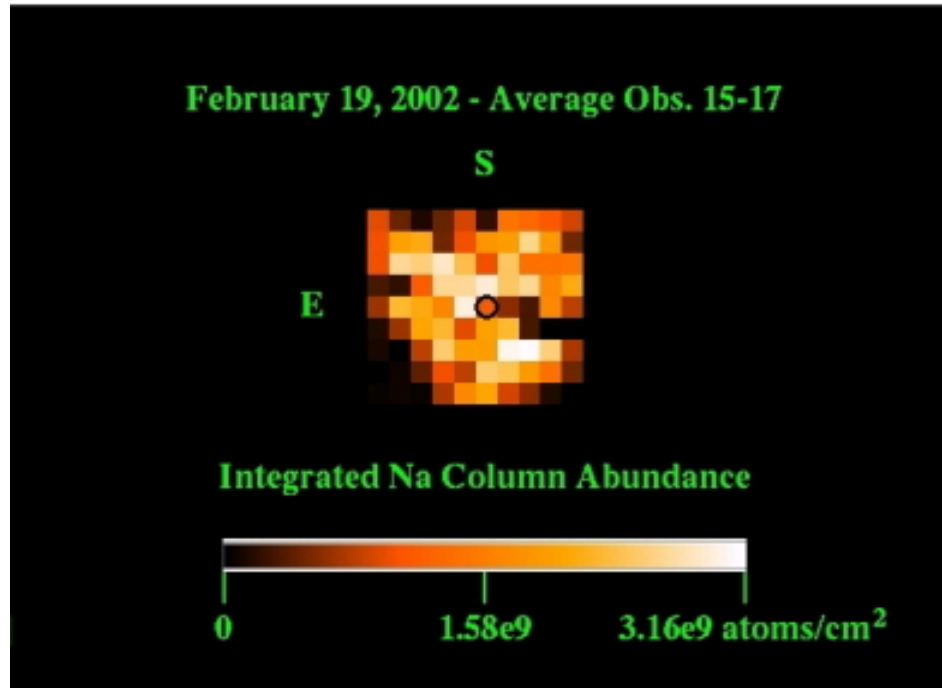


Figure 6.11 – Line of sight column abundance map for obs. 15-17 on 2/19/2002: This is an average of consecutive observations 15, 16 and 17 with exposure time of 15 minutes each.

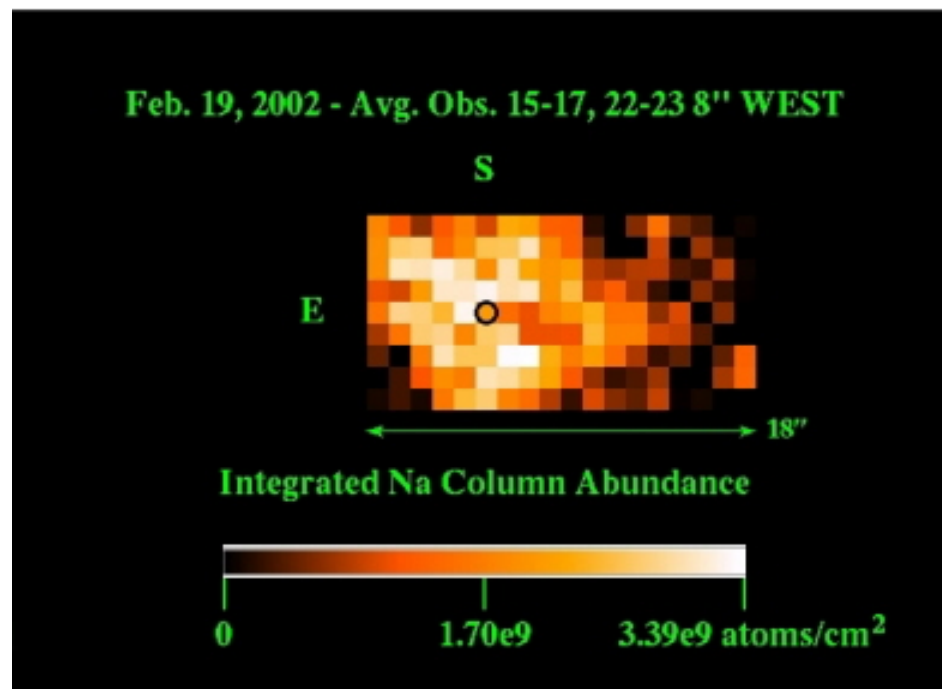


Figure 6.12 – Line of sight column abundance map for obs. 15-23 on 2/19/2002: This map combines the data from figure 6.11 above with the average of obs. 22-23 taken 8'' West of Europa.

6.2.2 Column Abundance relationship with Distance

A useful relationship that can be obtained from the maps in the previous section is how the line of sight column abundance is related to the distance away from Europa. The graphs in this section (figures 6.13 to 6.25) are log-log plots of abundances versus distance from Europa in the East, West, South and North directions. Data is represented by dashed lines and linear best fits by solid lines. The boundary of the Hill Sphere, which is where Europa's gravitational influence on a body is taken over by Jupiter's influence, is indicated by a vertical grey dashed line. Data points to the left of this line are within the Hill Sphere.

For a number of graphs (figures 6.14, 6.16, 6.18, 6.20 and 6.22), the first pixel away from the surface of Europa in a given direction has been neglected when doing the fits. It is interesting to compare how the fits change from those including all data. It is possible that the first pixel around Europa in all directions does not show all the sodium emission present because the strong continuum from the surface has not been perfectly subtracted and bleeds into this first neighboring pixel. In addition, abundance values for the pixel centered on Europa's disk are not considered because the surface reflection overpowers the D2 emission over the satellite.

In general the overall trend for most figures is that the line of sight column abundance falls with distance away from Europa, however it falls at different rates for each direction as seen from the slopes indicated on each graph.

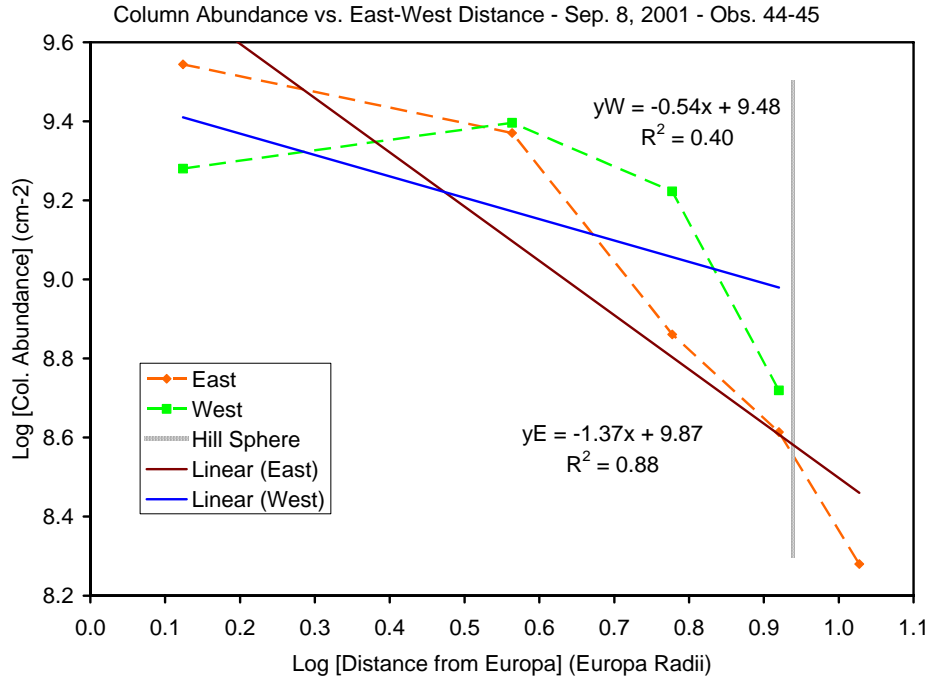


Figure 6.13 – Log-log plot of the column abundance in the East (orange dashed line) and West (green dashed line) directions away from Europa. The boundary of Europa’s Hill sphere is marked by the grey line. The best linear fits of the data are represented by solid lines. The line of sight column abundance falls as $r^{-1.37}$ towards the East and as $r^{-0.54}$ towards the West. The observations were taken Sep. 8, 2001.

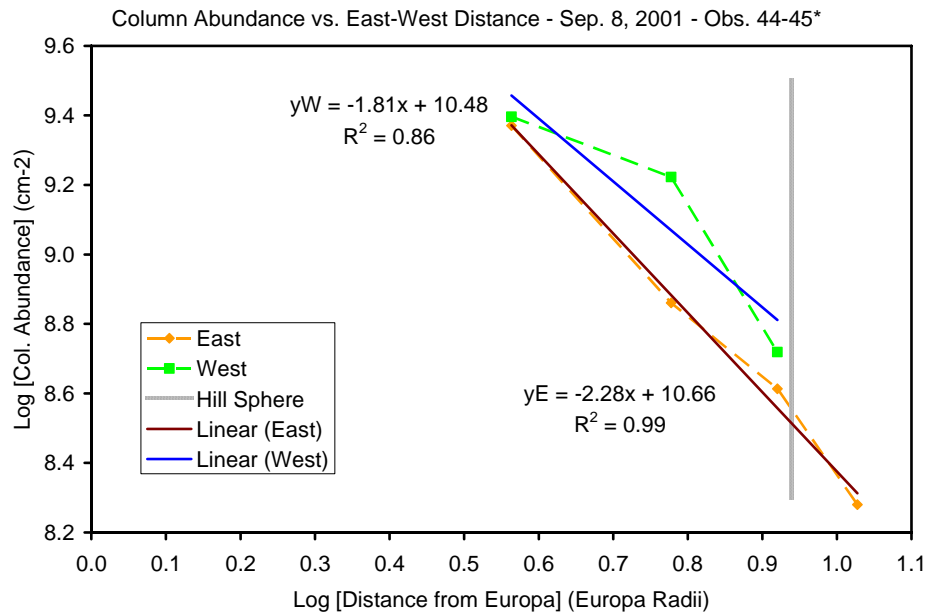


Figure 6.14 – Log-log plot of the column abundance in the East (orange dashed line) and West (green dashed line) directions away from Europa. The boundary of Europa’s Hill sphere is marked by the grey line. The best linear fits of the data are represented by solid lines. The line of sight column abundance falls as $r^{-2.28}$ towards the East and as $r^{-1.81}$ towards the West. In these fits, the 1st pixel away from Europa has been neglected. The observations were taken Sep. 8, 2001.

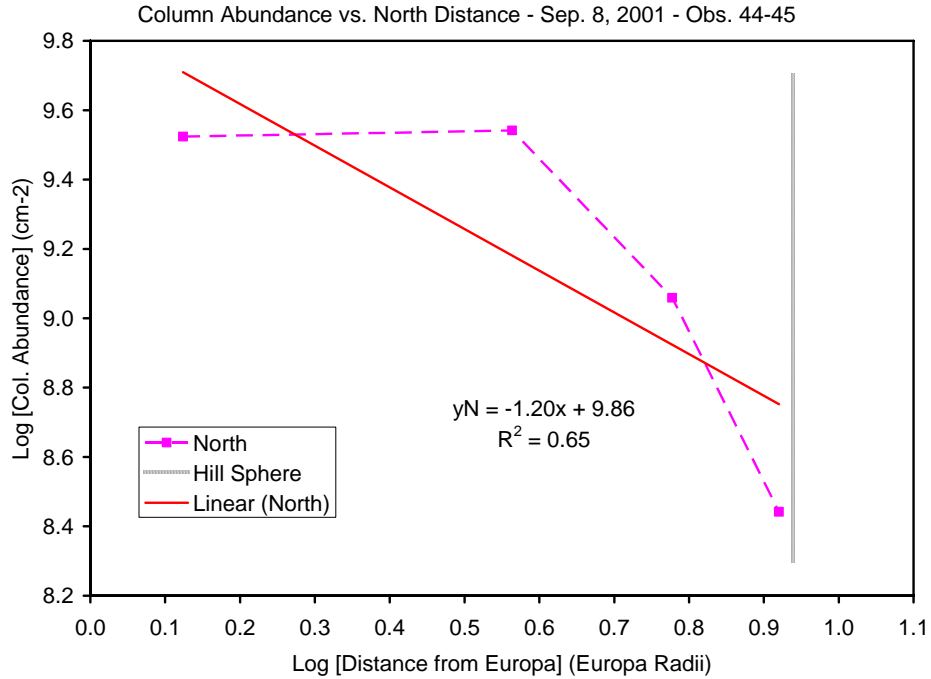


Figure 6.15 – Log-log plot of the column abundance in the North direction (pink dashed line) away from Europa. The boundary of Europa’s Hill sphere is marked by the grey line. The best linear fit of the data is represented by the red solid line. The line of sight column abundance falls as $r^{-1.20}$ towards the North. South direction is not shown because there are not enough data points for a meaningful fit. The observations were taken Sep. 8, 2001.

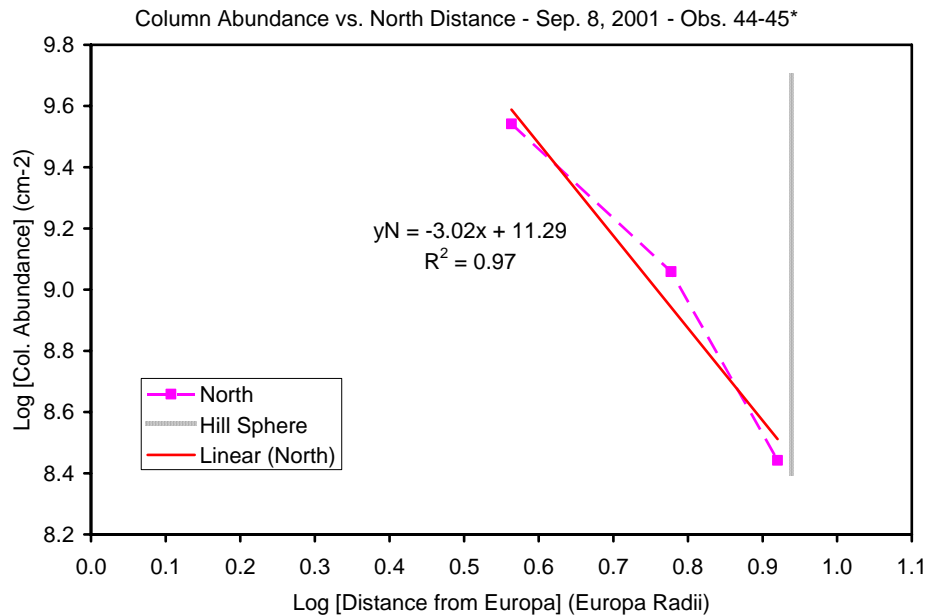


Figure 6.16 – Log-log plot of the column abundance in the North direction (pink dashed line) away from Europa. The boundary of Europa’s Hill sphere is marked by the grey line. The best linear fit of the data is represented by the red solid line. The line of sight column abundance falls as $r^{-3.02}$ towards the North. South direction is not shown because there are not enough data points for a meaningful fit. In this fit, the 1st pixel away from Europa has been neglected. The observations were taken Sep. 8, 2001.

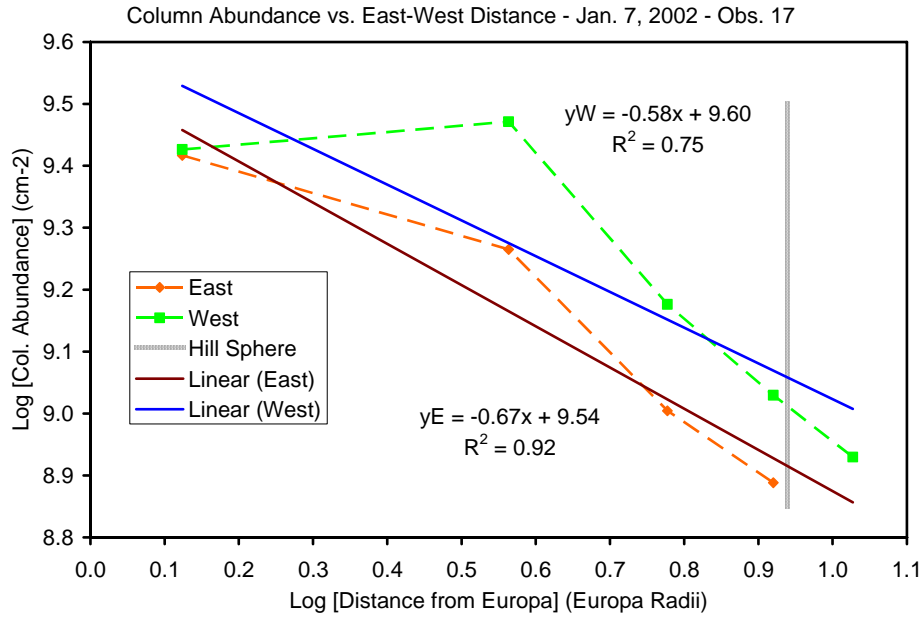


Figure 6.17 – Log-log plot of the column abundance in the East (orange dashed line) and West (green dashed line) directions away from Europa. The boundary of Europa’s Hill sphere is marked by the grey line. The best linear fits of the data are represented by solid lines. The line of sight column abundance falls as $r^{-0.67}$ towards the East and as $r^{-0.58}$ towards the West. This observation was taken Jan. 7, 2002.

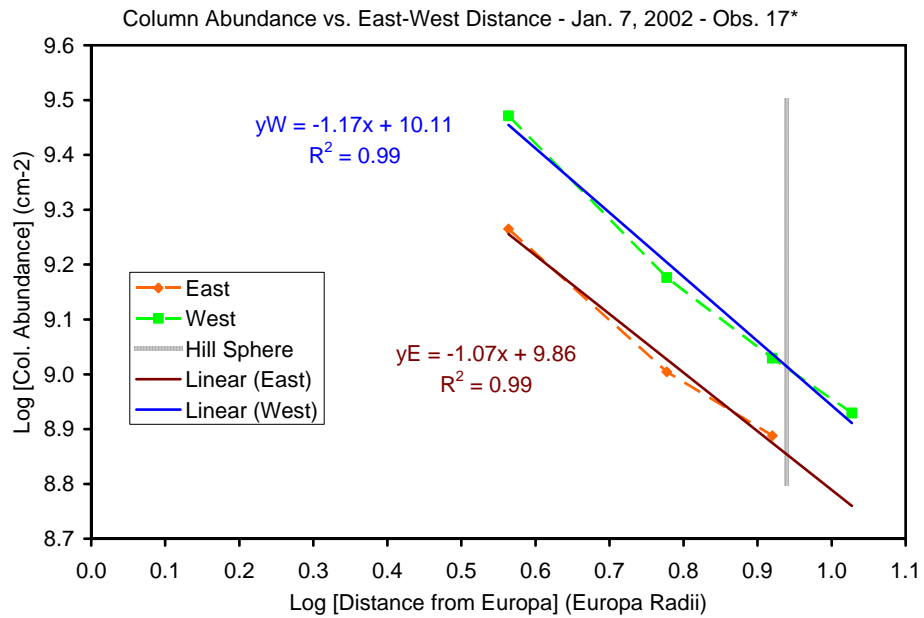


Figure 6.18 – Log-log plot of the column abundance in the East (orange dashed line) and West (green dashed line) directions away from Europa. The boundary of Europa’s Hill sphere is marked by the grey line. The best linear fits of the data are represented by solid lines. The line of sight column abundance falls as $r^{-1.07}$ towards the East and as $r^{-1.17}$ towards the West. In these fits, the 1st pixel away from Europa has been neglected. This observation was taken Jan. 7, 2002.

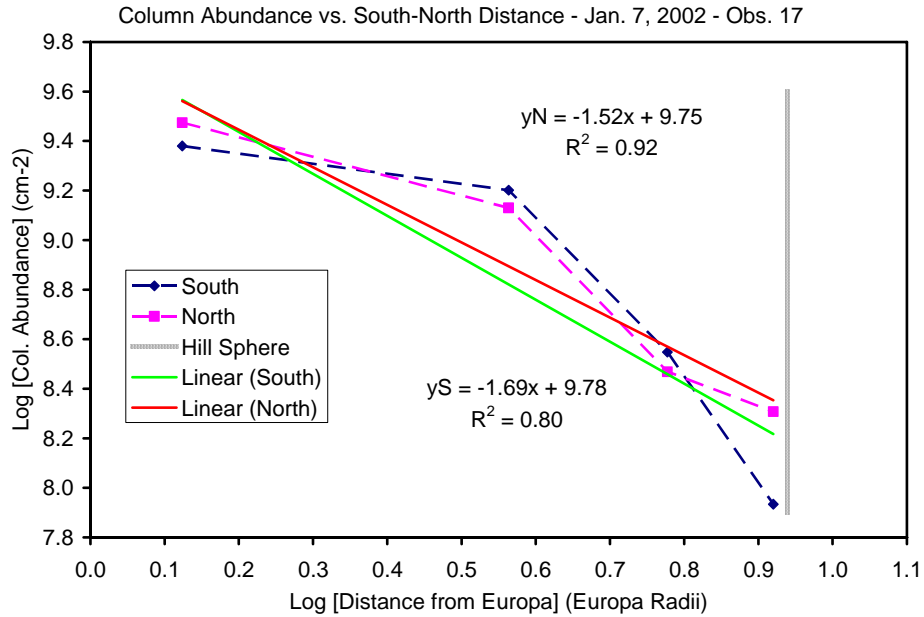


Figure 6.19 – Log-log plot of the column abundance in the South (blue dashed line) and North (pink dashed line) direction away from Europa. The boundary of Europa’s Hill sphere is marked by the grey line. The best linear fit of the data is represented by solid lines. The line of sight column abundance falls as $r^{-1.69}$ towards the South and as $r^{-1.52}$ towards the North. This observation was taken Jan. 7, 2002.

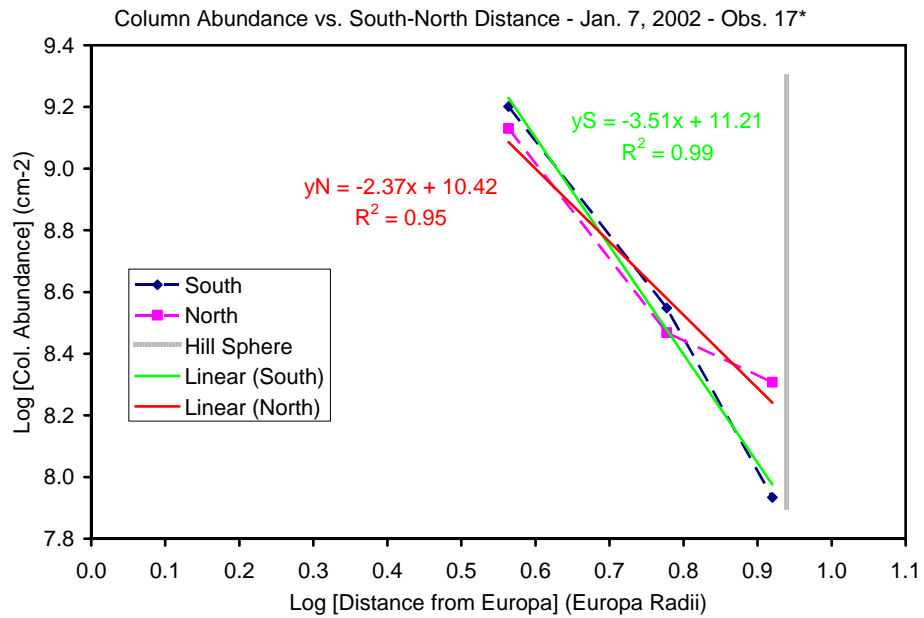


Figure 6.20 – Log-log plot of the column abundance in the South (blue dashed line) and North (pink dashed line) direction away from Europa. The boundary of Europa’s Hill sphere is marked by the grey line. The best linear fit of the data is represented by solid lines. The line of sight column abundance falls as $r^{-3.51}$ towards the South and as $r^{-2.37}$ towards the North. In these fits, the 1st pixel away from Europa has been neglected. This observation was taken Jan. 7, 2002.

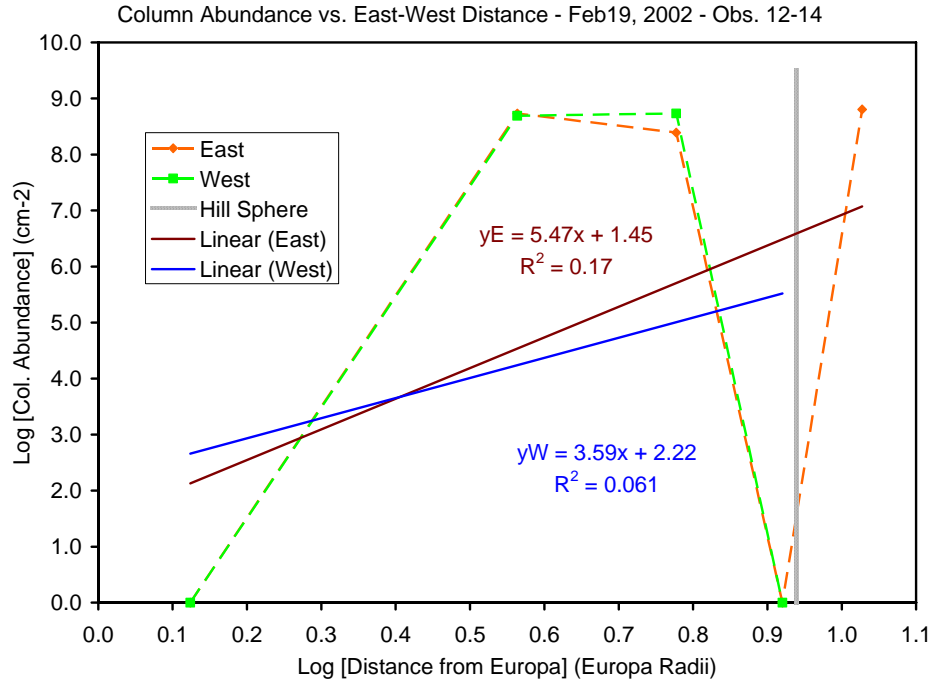


Figure 6.21 – Log-log plot of the column abundance in the East (orange dashed line) and West (green dashed line) directions away from Europa. The boundary of Europa’s Hill sphere is marked by the grey line. The best linear fits of the data are represented by solid lines. The line of sight column abundance falls as $r^{5.47}$ towards the East and as $r^{3.59}$ towards the West. The observations were taken Feb. 19, 2002.

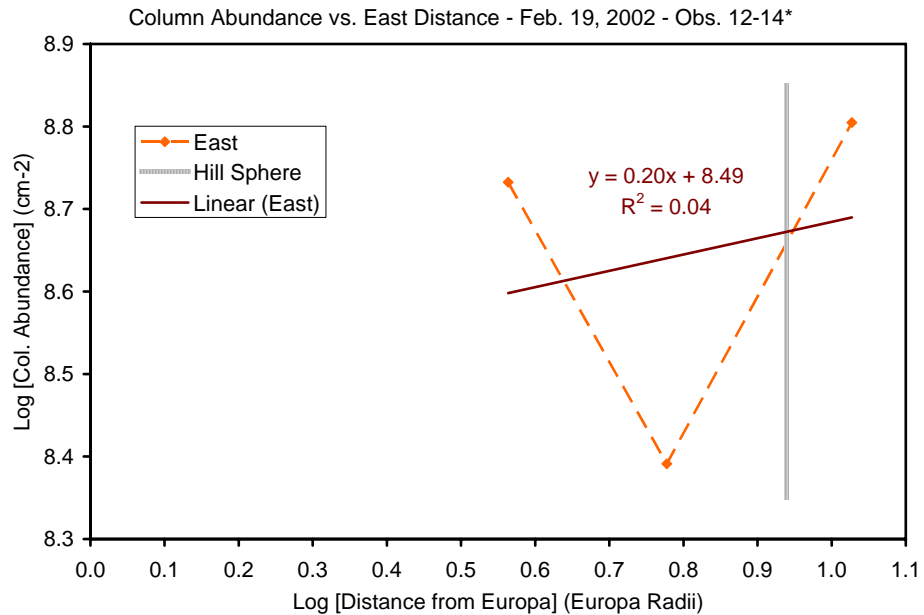


Figure 6.22 – Log-log plot of the column abundance in the East (orange dashed line) and West (green dashed line) directions away from Europa. The boundary of Europa’s Hill sphere is marked by the grey line. The best linear fits of the data are represented by solid lines. The line of sight column abundance falls as $r^{0.20}$ towards the East. In these fit, the 1st pixel away from Europa has been neglected. West, North and South directions are not represented because there are not enough data points for a meaningful fit. The observations were taken Feb. 19, 2002. The sodium map for this data presents a hole which is an artifact.

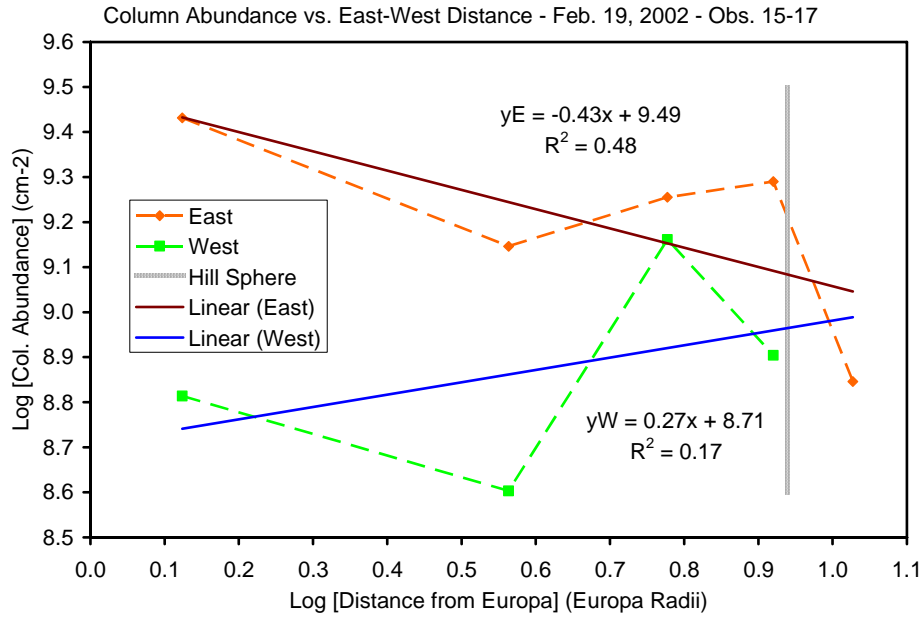


Figure 6.23 – Log-log plot of the column abundance in the East (orange dashed line) and West (green dashed line) directions away from Europa. The boundary of Europa’s Hill sphere is marked by the grey line. The best linear fits of the data are represented by solid lines. The line of sight column abundance falls as $r^{-0.43}$ towards the East and as $r^{0.27}$ towards the West. The observations were taken Feb. 19, 2002.

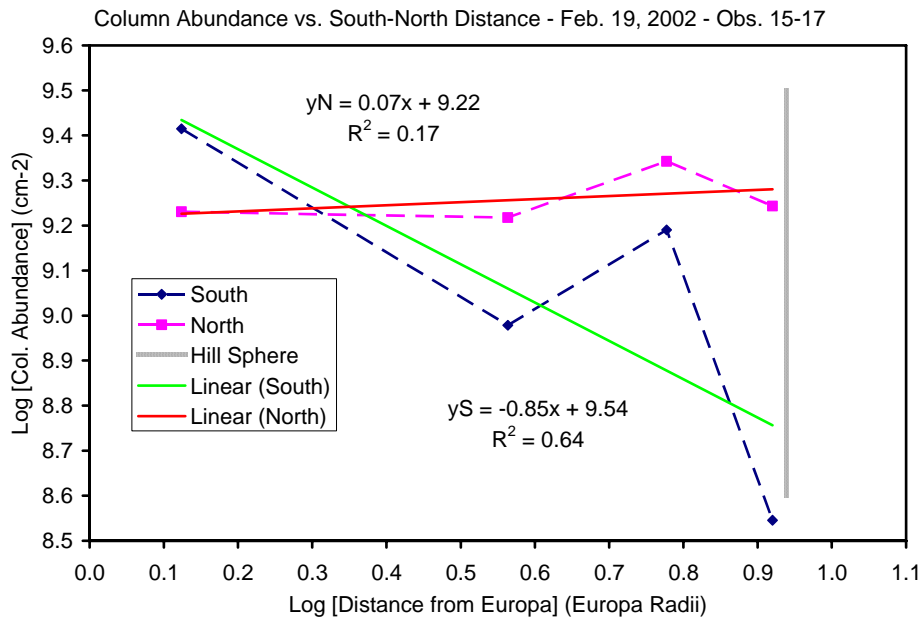


Figure 6.24 – Log-log plot of the column abundance in the South (blue dashed line) and North (pink dashed line) direction away from Europa. The boundary of Europa’s Hill sphere is marked by the grey line. The best linear fit of the data is represented by solid lines. The line of sight column abundance falls as $r^{-0.87}$ towards the South and as $r^{0.07}$ towards the North. The observations were taken Feb. 19, 2002.

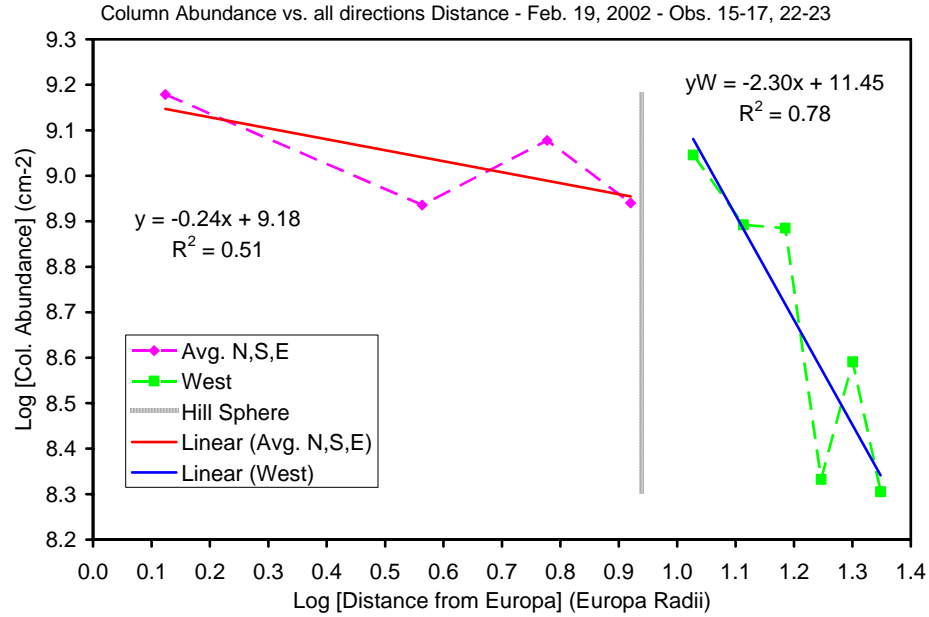


Figure 6.25 – Log-log plot of the column abundance and distance from Europa taken along all directions. The data within the Hill sphere (grey line) of North, South and East directions was averaged and plotted against the West direction outside of the Hill sphere. The best linear fit of the data is represented by solid lines. The line of sight column abundance falls as $r^{-0.24}$ within the Hill sphere and as $r^{-2.30}$ outside of it. As seen in the abundance map (fig. 6.12), observations 22-23 point 8'' away from Europa in the West direction, therefore we have information outside of the Hill sphere going West from Europa.

The following tables 6.3 and 6.4 summarize information from the graphs above.

The line of sight (or tangential) column abundance, N_T , falls as $r^{(slope\ graph)}$, where r is the distance away from Europa. The vertical (or zenith) column abundance, N_V , which will be discussed in the next section (see 6.2.3), falls as $r^{(-1+slope)}$.

Brown and Hill [1996] obtained a slope of -1.5 for their log-log plot of the line of sight sodium column abundance going along the East-West direction. Our values range from slopes of -3.51 to 0.40 (table 6.3) if we neglect the results for the February 19, 2002 observations 12-14 in which we already determined there is an artifact in the image. Vertical column abundances fall as distance to the power ranging from -4.51 to -0.60, again neglecting our observations 12-14. Brown and Hill's vertical column abundance falls as r to the -2.5.

OBSERVATION	East	West	South	North		
Sep. 8, 2001 - 44-45	-1.37	-0.54	NA	-1.20		
Jan. 7, 2002 - 17	-0.67	-0.58	-1.69	-1.52		
Feb. 19, 2002 - 12-14	5.47	3.59	NA	NA		
Feb. 19, 2002 - 15-17	-0.43	0.27	-0.85	0.07		
Feb. 19, 2002 - 15-23	-0.43	0.40	-0.85	0.07		
OBSERVATION	East2	West2	South2	North2	N,S,E	Outside Hill
Sep. 8, 2001 - 44-45	-2.28	-1.81	NA	-3.02	NA	NA
Jan. 7, 2002 - 17	-1.07	-1.17	-3.51	-2.37	NA	NA
Feb. 19, 2002 - 12-14	0.29	NA	NA	NA	NA	NA
Feb. 19, 2002 - 15-17	NA	NA	NA	NA	NA	NA
Feb. 19, 2002 - 15-23	NA	NA	NA	NA	-0.24	-2.30

Table 6.3 – Line of sight column abundance slopes: This table includes values for the exponent of r in the relationship: line of sight column abundance $N_T \propto r^A$. This constant A is given for each direction *East*, *West*, *South* and *North* as the slope determined in the log-log plots. Values for *East2*, *West2*, *South2* and *North2* correspond to slopes of the best linear fits for the graphs in which the 1st pixel away from Europa was neglected (figures 6.14, 6.16, 6.18, 6.20 and 6.22). The column *N, S, E* and *Outside Hill* only applies to figure 6.25 where the slope was calculated within the Hill sphere for North, South and East and outside of the Hill sphere towards the West.

OBSERVATION	East	West	South	North		
Sep. 8, 2001 - 44-45	-2.37	-1.54	NA	-2.20		
Jan. 7, 2002 - 17	-1.67	-1.58	-2.69	-2.52		
Feb. 19, 2002 - 12-14	4.47	2.59	NA	NA		
Feb. 19, 2002 - 15-17	-1.43	-0.73	-1.85	-0.93		
Feb. 19, 2002 - 15-23	-1.43	-0.60	-1.85	-0.93		
OBSERVATION	East2	West2	South2	North2	N,S,E	Outside Hill
Sep. 8, 2001 - 44-45	-3.28	-2.81	NA	-4.02	NA	NA
Jan. 7, 2002 - 17	-2.07	-2.17	-4.51	-3.37	NA	NA
Feb. 19, 2002 - 12-14	-0.71	NA	NA	NA	NA	NA
Feb. 19, 2002 - 15-17	NA	NA	NA	NA	NA	NA
Feb. 19, 2002 - 15-23	NA	NA	NA	NA	-1.24	-3.30

Table 6.4 – Vertical column abundance slopes: This table includes values for the exponent of r in the relationship: vertical column abundance $N_V \propto r^B$. This constant B is given for each direction *East*, *West*, *South* and *North* and it corresponds to $B = (-1 + A)$, where A is the slope determined in the log-log plots above with summary values also given in table 6.3. Values for *East2*, *West2*, *South2* and *North2* correspond to slopes of the best linear fits for the graphs in which the 1st pixel away from Europa was neglected (figures 6.14, 6.16, 6.18, 6.20 and 6.22). The column *N, S, E* and *Outside Hill* only applies to figure 6.25 where the slope was calculated within the Hill sphere for North, South and East directions and outside the Hill sphere towards the West.

For gas that is gravitationally bound to a planet the vertical column abundance falls faster than $1/r^2$. Then, Brown and Hill's value shows that the sodium is weakly bound to Europa but there is a tail in the distribution of sodium atom's

velocities so many atoms are still escaping. Our results indicate that in the East and West directions sodium seems to be escaping or to be weakly bound. It is interesting to note that for the observation which extended 8'' West of the disk, the data outside of the Hill sphere indicates that the gas is depleted possibly by electron impact ionization. It is possible that in this region the sodium atoms are being destroyed by high energy particles causing the abundance to decrease rapidly. In the North and South directions the sodium appears to be bound during the September 2001 and January 2002 observations, but escaping in the February 2002 observations.

In section 4.2 of this paper we calculated the scale height and physical height to the exobase assuming that molecular oxygen densities fall exponentially. This is a good approximation for the bound O₂ atmosphere, but our data shows that the sodium exosphere is escaping or weakly bound.

6.2.3 Vertical Sodium Column Abundances and Densities

The previous section focused on our results for the line of sight, or tangential, column abundance of sodium around Europa. Assuming that the number density of sodium atoms is inversely proportional to the distance from Europa squared, where R is the distance from Europa, R_0 the radius of the satellite and $n(R_0)$ the number density at its surface, also known as n_0 . Then:

$$n(R) = n(R_0) \cdot \left(\frac{R_0}{R} \right)^2 \quad (6.5)$$

Integrating along the line of sight dl direction, the tangential column abundance, N_T , can be derived:

$$N_T = \int n(R_l) \cdot dl, \quad (6.6)$$

where $R_l = R_0 \cdot \sec \theta$, and $l = R_0 \cdot \tan \theta$ with derivative $dl = R_0 \sec^2 \theta \cdot d\theta$. Thus,

$$N_T = \int_{-\pi/2}^{\pi/2} n(R_0) \cdot \left(\frac{R_0}{R_0 \sec \theta} \right)^2 \cdot (R_0 \sec^2 \theta \cdot d\theta) = \pi \cdot n_0 \cdot R_0 \quad (6.7)$$

is the tangential column abundance at the surface of Europa in units of *atoms/cm²*.

In the case of the vertical column abundance, N_V , the number density is integrated radially away from the surface and has also units of *atoms/cm²*. Therefore,

$$N_V = \int n(R) \cdot dR = \int_{R_0}^{\infty} n(R_0) \cdot \left(\frac{R_0}{R} \right)^2 \cdot dR = n_0 \cdot R_0 \quad (6.8)$$

Using the values of the tangential column abundance obtained from our maps, the vertical column abundance and density of sodium at the surface of Europa can be calculated along the East, West, South and North directions as shown in the series of tables 6.5, 6.6 and 6.7.

Observation	East (N_T)	West (N_T)	South (N_T)	North (N_T)
Sept. 8, 2001 - 44	3.09E+09	3.67E+09	1.70E+09	3.23E+09
Sept. 8, 2001 - 45	3.96E+09	9.90E+08	4.95E+08	3.46E+09
Jan. 7, 2002 - 17	2.61E+09	2.67E+09	2.40E+09	2.98E+09
Feb. 19, 2002 - 12-14	NA	NA	NA	NA
Feb. 19, 2002 - 15-17	2.70E+09	6.51E+08	2.60E+09	1.70E+09
Feb. 19, 2002 - 15-23	2.91E+09	6.70E+08	2.80E+09	1.83E+09

Table 6.5 – Tangential column abundance values: N_T is in units of sodium atoms/cm² and was obtained from the abundance maps in section 6.2.1.

Observation	East $n(h)$	West $n(h)$	South $n(h)$	North $n(h)$
Sept. 8, 2001 - 44	2.47	2.93	1.36	2.58
Sept. 8, 2001 - 45	3.16	0.79	0.40	2.76
Jan. 7, 2002 - 17	2.72	2.78	2.50	3.11
Feb. 19, 2002 - 12-14	NA	NA	NA	NA
Feb. 19, 2002 - 15-17	2.59	0.63	2.50	1.63
Feb. 19, 2002 - 15-23	2.80	0.64	2.69	1.76

Observation	East n_0	West n_0	South n_0	North n_0
Sept. 8, 2001 - 44	15.93	18.92	8.76	16.65
Sept. 8, 2001 - 45	20.42	5.10	2.55	17.84
Jan. 7, 2002 - 17	10.30	10.54	9.47	11.76
Feb. 19, 2002 - 12-14	NA	NA	NA	NA
Feb. 19, 2002 - 15-17	11.57	2.79	11.14	7.28
Feb. 19, 2002 - 15-23	12.47	2.87	12.00	7.84

Table 6.6 – Sodium number density values: This table includes values for the sodium number density $n(h)$, the first pixel away from the disk of Europa in all directions (top section). Those values of the number density are interpolated to obtain the density of sodium atoms at the surface of Europa (n_0) in units of sodium atoms/cm³ (bottom section).

Observation	East (N_V)	West (N_V)	South (N_V)	North (N_V)
Sept. 8, 2001 - 44	2.50E+09	2.97E+09	1.38E+09	2.61E+09
Sept. 8, 2001 - 45	3.20E+09	8.01E+08	4.00E+08	2.80E+09
Jan. 7, 2002 - 17	1.62E+09	1.65E+09	1.49E+09	1.85E+09
Feb. 19, 2002 - 12-14	NA	NA	NA	NA
Feb. 19, 2002 - 15-17	1.82E+09	4.38E+08	1.75E+09	1.14E+09
Feb. 19, 2002 - 15-23	1.96E+09	4.50E+08	1.88E+09	1.23E+09

Table 6.7 – Vertical column abundance values: N_V is in units of sodium atoms/cm² and was calculated using the surface densities n_0 from table 6.6. These are values at the surface of Europa.

We can see that the values for the vertical column abundance are slightly smaller than those of tangential column abundance. This is expected since for the line of sight column abundances as we move tangentially we are integrating over more gas in the exosphere than if we were to look radially down.

Chapter 7

Uncertainties and Errors

7.1 Estimate of Uncertainties and Errors

There are several types of uncertainties introduced in the results of this work.

While observing an object our resolution is limited by the seeing, σ , which is affected by atmospheric turbulence and it causes the intensities of individual pixels to bleed off into neighboring ones. For the observations presented on this paper the seeing of the data varied between values of 1.0'' to 3.1''. In addition, we need to take into account the pixel uncertainty which is 1/3''. The total error introduced by the seeing σ_T becomes:

$$\sigma_T = (\sigma^2 + (1/3)^2)^{1/2}, \quad (7.1)$$

where σ is the seeing of the atmosphere in arcseconds.

A systematic error introduced during the process of data reduction is determining the level of the continuum in order to perform the continuum subtraction. The true continuum level at a point is:

$$I_{cont} = \frac{I_0}{\sqrt{2\pi} \cdot \sigma_T} \exp\left(-\Delta x^2 / 2\sigma_T^2\right), \quad (7.2)$$

where I_0 is the true value of the continuum without atmospheric seeing which comes from the surface reflection of Europa; σ_T is the seeing in arcseconds and Δx is the physical distance away from the pixel centered on Europa in units of arcseconds. Therefore, we can estimate the percentage our continuum level deviates from the value of the true continuum by calculating $I(\sigma_T)$.

Another systematic error comes from the fitting of the Voigt profile of the solar Fraunhofer line used to extract the sodium emission from the data. The VFUDGIT routine uses the Levenburg-Marquardt method for estimating parameters and their “goodness of fit” by minimizing $\chi^2 = \sum_{i=1}^N ((y_i - y(x_i))/\sigma_i)^2$, where $y(x)$ is the intensity of the continuum, with an implementation taken from Numerical Recipes, which allows for parameters to be free or fixed [Press et al., 1986].

There is also an error intrinsic to the data which is the noise level of each observation. It depends on the photon statistics of the line. The error of counting photons, or photon noise, is equal to \sqrt{N} , where N is the number of photons (i.e. the strength of the signal measured). Consequently, the signal to noise ratio for the data is $SNR = N/\sqrt{N} = \sqrt{N}$. Away from the center of Europa the photon noise level remains the same, but the SNR decreases. However, near the center of Europa pixels are contaminated by the surface reflection, so there is a trade off in the errors between the photon noise and continuum scattering (see values in tables 7.1, 7.2 and 7.3). Additionally, another source of uncertainty is the presence of telluric water lines in our spectra. One of these water absorption lines appears slightly blue shifted from the location of the D2 sodium emission and it is present in all of our observations, to some extent.

Observation	Noise over E	Noise away E	SNR over E	SNR away E
Sept. 8, 2001 - 44	32.6%	36.1%	43.39	2.06
Sept. 8, 2001 - 45	34.6%	36.1%	43.96	2.35
Jan. 7, 2002 - 17	8.8%	10.3%	57.33	2.12
Feb. 19, 2002 - 12-14	25.5%	31.4%	23.83	3.52
Feb. 19, 2002 - 15-23	21.8%	22.4%	18.70	7.13

Table 7.1 – Estimates of the photon noise: the photon noise level over Europa is *Noise over E*; photon noise level 4.52’’ away from Europa is *Noise away E*; the signal to noise ratio over Europa is *SNR over E*, and the signal to noise ratio 4.52’’ away from Europa is *SNR away E*.

Observation	σ	σ_T	$I(\sigma_T)$ near E	$I(\sigma_T)$ away E
Sep. 8, 2001 - 44	1.10	1.15	21.4%	0.015%
Sep. 8, 2001 - 45	1.00	1.05	21.3%	0.004%
Jan. 7, 2002 - 17	1.40	1.44	20.3%	0.200%
Feb. 19, 2002 - 12-14	2.60	2.62	13.8%	3.436%
Feb. 19, 2002 - 15-23	3.10	3.12	12.0%	4.467%

Table 7.2 – Estimates of the continuum level uncertainty: σ is the seeing for a given observation in arcseconds; σ_T is the total seeing taking into account the $1/3''$ per pixel, given in units of arcseconds; $I(\sigma_T)$ near E is the uncertainty in the determination of the continuum $1.13''$ away from Europa given as a percentage of the true value of the continuum I_0 ; $I(\sigma_T)$ away E is the uncertainty in the determination of the continuum $4.52''$ away from Europa given as a percentage of the true value of the continuum I_0 .

Observation	Total Errors near E	Total Errors away E
Sep. 8, 2001 - 44	39.0%	36.1%
Sep. 8, 2001 - 45	40.6%	36.1%
Jan. 7, 2002 - 17	22.2%	10.3%
Feb. 19, 2002 - 12-14	29.0%	31.6%
Feb. 19, 2002 - 15-23	24.9%	22.8%

Table 7.3 – Estimates of the total errors: *Total Errors near E* is the total error due to photon noise and continuum level uncertainty $1.13''$ away from Europa. *Total Errors away E* is the total error due to photon noise and continuum level uncertainty $4.52''$ away from Europa,.

Our errors range from 8.8% to 36.1%. At $1.13''$ away from the disk of Europa the errors due to the continuum determination and photon noise are comparable. In contrast, at $4.52''$ away from the disk the errors due to photon noise clearly dominate.

Finally, it is important to note that in this project we have assumed that there is no multiple scattering of light by the sodium exosphere. We have taken the pixel centered on Europa as reference of the true value of the continuum level. Because of scattered light there are photons we are unable to see. The error from scattering becomes larger the closer we are to the disk of Europa. In the future it would be important to review the radiative processes in Europa's exosphere and make the necessary corrections to the level of the continuum in order to account for multiple scattering [Killen, 2006].

Chapter 8

The Io Plasma Torus

8.1 The Io Plasma Torus

Jupiter has a very powerful magnetic field and the magnetosphere is so large that sometimes it extends past the orbit of Saturn. For that reason, all the Galilean moons lie deep inside the Jovian magnetosphere. In addition, Io is known to be the most volcanically active body in the Solar System and interacts strongly with Jupiter's magnetic field. Through several processes, such as sputtering by ions from the Jovian magnetosphere, particles from Io's surface and atmosphere gain enough energy to escape the moon. This combination of ions and neutrals is further ionized in Jupiter's magnetosphere by electron impact ionization and photoionization resulting in a build up of ions and electrons around the orbit of Io into what is known as the Io plasma torus. The main species present are ions of oxygen, sulfur, sulfur dioxide and chlorine.

Jupiter rotates just less than 10 hours but it takes Io 1.77 days to complete one orbit as it moves at 17 km/s. Therefore, the Io plasma which is rotating at 74 km/s overtakes Io with a relative velocity of 57 km/s [Saur et al., 2004]. The Io torus is comprised of a cold inner region (temperature in the order of a few eV) within 5.7 Jupiter radii, and a hotter outer component (around 100 eV) that extends up to 8 Jupiter radii. Densities of a few particles cm^{-3} have been detected up to a distance of 20 Jupiter radii [de Pater and Lissauer, 2001]. In the torus numbers for the plasma density range from 1000 to 3600 cm^{-3} depending on the flyby measurement [Frank and Paterson, 2000, 2001 and 2002].

It is important to know the position of Europa with respect to Io and the Io torus in order to determine how this plasma can be interacting with Europa's sodium exosphere.

The following figures (8.1, 8.2 and 8.3) indicate the position of Europa and Io in their orbital planes for each of our observations.

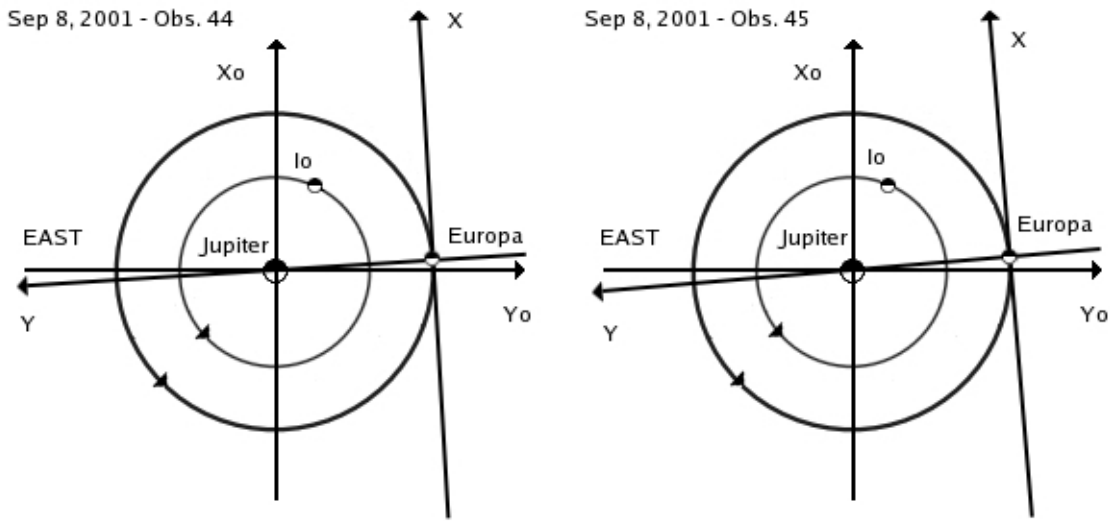


Figure 8.1 – Europa's and Io's orbital position for obs. 44 and 45 on 9/8/2001: East and West directions of the observer are indicated. North pole is towards the reader. The Sun and the Earth are located in the negative x_0 direction. The x - y axis represents the position of Europa as it orbits around Jupiter which is located to the East of Europa for all our observations. The diagram on the left corresponds to observation # 44 taken on September 8, 2001 at 10:59:49 Universal Time. The one on the right corresponds to observation # 45 taken on September 8, 2001 at 11:21:05 UT.

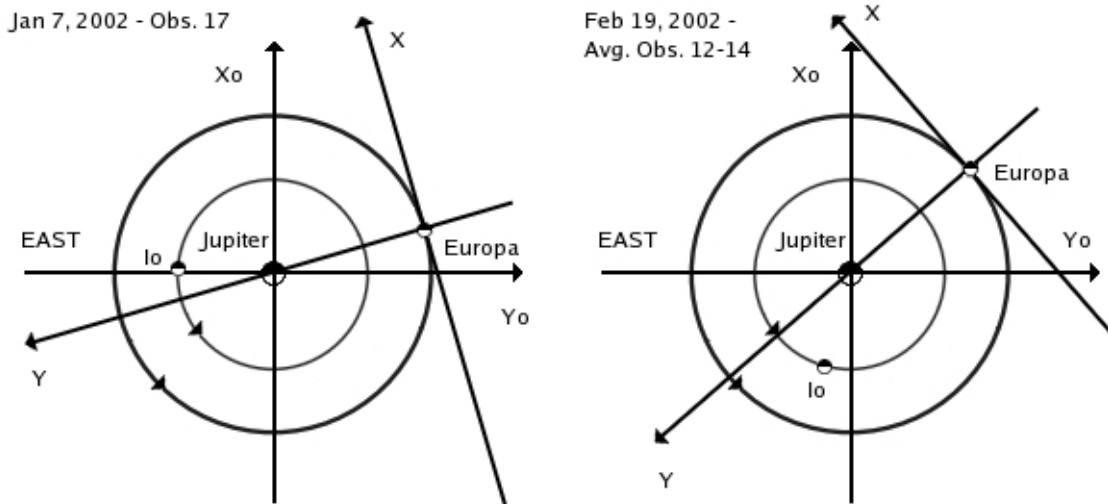


Figure 8.2 – Europa’s and Io’s orbital position for obs. 17 on 1/7/2002 and obs. 12-14 on 2/19/2002: Coordinates are as described in figure 8.1. The diagram on the left corresponds to observation # 17 taken on January 7, 2002 at 07:14:02 UT. The one on the right corresponds to the average of consecutive observations # 12-14 taken on February 19, 2002 with average UT of 03:05:03.

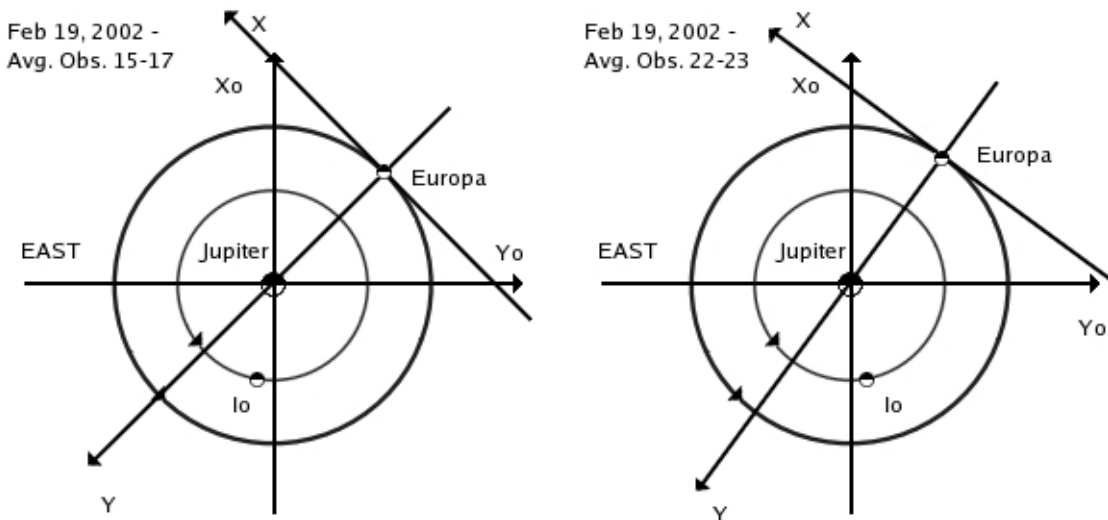


Figure 8.3 – Europa’s and Io’s orbital position for obs. 15-17 on 2/19/2002 and obs. 22-23 on 2/19/2002: Coordinates are as described in figure 8.1. The diagram on the left corresponds to the average of consecutive observations # 15-17 taken on February 19, 2002 with average UT of 03:56:36. The one on the right corresponds to the average of consecutive observations # 22-23 taken on February 19, 2002 with average UT of 05:57:45.

8.1.1 Vertical Distance from the Io Torus

In order to calculate the vertical distance of Europa from the Io plasma torus (see values in table 8.1) we need to determine the location of the line of nodes for the plasma torus. This line is given by the intersection of the plane of the Io torus with the Jovian spin equator at two points: the ascending and descending nodes. The location where the Io torus crosses upward the spin equator is called the ascending node, and where it crosses it down is called the descending node.

Jupiter's magnetic dipole is inclined 10 degrees towards a System III longitude of 200 degrees, so the magnetic equator crosses the spin equator at 110 and 290 degrees Jovian longitudes. By convention 290 is the longitude of the ascending node and 110 the longitude of the descending node. The Io torus is in the plane of the centrifugal equator, and the latter is tilted 2/3 of the way from the spin equator towards the magnetic equator, so the torus has the same nodes as the magnetic equator, 290 and 110 degrees of longitude. If we let λ_{EP} be the angle between Europa and the ascending node of the plasma torus, then

$$\lambda_{EP} = \lambda_E - 290, \quad (8.1)$$

where λ_E is the longitude of Europa. Therefore, the distance going radially outward along the perpendicular to the line of nodes, R_p , is given by

$$R_p = R_E \cdot \sin \lambda_{EP}, \quad (8.2)$$

where R_E is Europa's orbital distance. However, Europa's orbital plane is inclined by 7 degrees with respect to the centrifugal equator, so the overall distance from the plane of the Io torus to Europa's orbital plane can be written as:

$$D_{plane} = R_p \cdot \sin \gamma \quad (8.3)$$

$$D_{plane} = R_E \cdot \sin \lambda_{EP} \cdot \sin \gamma \quad (8.4)$$

Observation (yes)	Long J (o)	O-P-T (o)	λ_E (o)	λ_{EP} (o)	$\sin[\lambda_{EP}]$ (o)	D_{plane} (R_E)	Direction
Sep. 8, 2001 - 44	155.49	90.133	65.35	-224.65	0.703	0.0857	North
Sep. 8, 2001 - 45	168.18	91.613	76.56	-213.44	0.545	0.0664	North
Jan. 7, 2002 - 17	244.62	103.2965	141.32	-148.68	-0.520	-0.0634	South
Feb. 19, 2002 - 12-14	84.85	129.6127	-44.76	-334.76	0.426	0.0520	North
Feb. 19, 2002 - 15-17	116.03	133.29	-17.27	-307.27	0.796	0.0970	North
Feb. 19, 2002 - 22-23	193.49	141.93	51.56	-238.44	0.852	0.1039	North
Observation (weak)	Long J (o)	O-P-T (o)	λ_E (o)	λ_{EP} (o)	$\sin[\lambda_{EP}]$ (o)	D_{plane} (R_E)	Direction
Sep. 11, 2001 - 9	252.715	36.068	216.65	-73.35	-0.128	-0.016	South
Sep. 11, 2001 - 10	262.265	37.165	225.10	-64.90	-0.906	-0.110	South
Jan. 3, 2002 - 4	343.245	55.52	287.73	-2.27	-0.040	-0.005	South
Dec. 19, 2002 - 17	112.790	134.66	-21.87	-311.87	0.745	0.091	North
Dec. 19, 2002 - 18	132.790	132.29	0.50	-289.50	0.943	0.115	North
Observation (none)	Long J (o)	O-P-T (o)	λ_E (o)	λ_{EP} (o)	$\sin[\lambda_{EP}]$ (o)	D_{plane} (R_E)	Direction
Sep. 9, 2001 - 27	325.445	104.128	221.32	-68.68	-0.932	-0.114	South
Sep. 10, 2001 - 28	97.155	64.64	32.52	-257.49	0.976	0.119	North
Jan. 3, 2002 - 5	353.515	113.459	240.06	-49.94	-0.795	-0.097	South
Jan. 5, 2002 - 15	207.375	108.687	98.69	-191.31	0.196	0.024	North
Feb. 19, 2002- 20	159.125	138.915	20.21	-269.79	1.000	0.122	North
Feb. 20, 2002 - 13	224.725	129.547	95.18	-194.82	0.256	0.031	North

Table 8.1 – Europa’s vertical distance from the Io plasma torus:

Long J corresponds to the observer’s longitude of Jupiter in units of degrees. *O-P-T* is the Observer-Jupiter-Europa angle in units of degrees. λ_E is the longitude of Europa and λ_{EP} is the angle between Europa and the ascending node also in degrees. The resulting distance, D_{plane} , has units of Europa orbital radii, R_E . Positive distances mean Europa is to the North of the torus and negative numbers mean Europa is to the South of the Io torus. The top section of the table indicates the observations presented in this paper with measured Na emission. The middle section indicates observations with weak emission in which the signal to noise ratio was too small to obtain sodium maps. The bottom section indicates observations with no measured emission.

We can see that for our set of observations the distance of Europa from the plane of the plasma torus did not change dramatically, values range from 0.05 to 0.1 Europa orbital radii North of the torus plane and for the January 2002 observation the distance is 0.06 Europa orbital radii South of the torus. Using this information we can now look back at the maps and calculations of sodium column abundances and densities and see if the position of Europa with respect to the torus can explain the asymmetries and abundance variations we described in chapter 6.

Chapter 9

Discussion and Conclusions

9.1 Variability of the Sodium Emission and Abundances

One factor that can cause the sodium D-line emission intensity to change is Doppler shift. Emission lines are Doppler shifted depending on the velocity of Europa with respect to the sun (heliocentric velocity). The larger the Doppler shift, the stronger the emission line is, since there will be more solar flux in the atom's rest frame at Europa.

However, what it is interesting are the changes in sodium abundances due to variations in the sodium sources and sinks.

The loss by electron or ion impact ionization of neutral sodium changes due to the ambient plasma. If we compare our results of the vertical column abundances (lower section of table 6.4) with the position of Europa relative to the torus, we can clearly see that for the September 2001 observations, the sodium scale height is smallest towards the North (with $N_V \propto r^{-4.0}$) and in the January 2002 observation the opposite is occurring, where the scale height is smaller in the Southward direction (with $N_V \propto r^{-4.5}$). The top section of table 8.1 indicates how the distance of Europa from the torus in September 2001 is between 0.085 and 0.069 Europa orbital radii North of the torus. For the January 2002 observation the distance is 0.063 Europa orbital radii South of the plasma torus. This is suggestive that sodium atoms may be lost due to ionization by the electrons or ions in the ambient plasma.

Another conclusion our data supports is that the sodium exosphere around Europa is weakly bound or escaping along the East-West direction, which agrees with Brown and Hill's result [1996]. However, it seems not to be escaping along the North-South direction, or it is being destroyed there. For observations in which the signal to noise ratio was too low to create any sodium maps (middle section of table 8.1) and observations without any sodium emission (bottom section of table 8.1), distances range from 0.05 to 0.12 Europa orbital radii away from the plasma torus. There is no clear pattern that could explain the lack of sodium emission. Another possible factor is that the Jovian gravity field adds approximately an additional 1/3 of Europa's gravity along the North-South direction (Hamilton, personal communication).

Our determined values for the sodium surface number density n_0 range from 2 to 20 atoms/cm³, and column abundances are in the order of 10⁹ atoms/cm². These are quite small values compared to the surface density of molecular oxygen in Europa, about 10⁸ molecules/cm³, and column abundance of 10¹⁵ molecules/cm² [Hall et al., 1995]. Hence, the sodium exosphere is extremely tenuous.

In addition, we can say that the sodium exosphere is energetic enough to extend to a distance of at least 39,600 km away from the surface of the satellite, which is comparable to the sodium tail Mercury presents in the anti-sunward direction.

9.2 Future Work

An important issue that this work could not answer and that should be investigated further are asymmetries of the sodium cloud present in the leading and trailing hemispheres of Europa. Unfortunately, for all the observations included in this paper the

orbital position of Europa is always to the West of Jupiter. It would be useful to reduce data at other orbital locations in order to examine if the pile up of magnetic flux on Europa's trailing hemisphere would yield different ionization rates on the leading and trailing hemispheres as suggested by Parnicas et al., 2000.

In the future, data reduction and analysis of observations taken from 1999 to 2001 and since 2002 will be undertaken. It is also of importance to analyze observations as far away from the surface of Europa as possible, in order to establish the physical extent of this energetic sodium exosphere. It is quite possible that it might extend beyond our observed 39,600 km.

Furthermore, it is important to include in future work the effects of multiple scattering near the disk of Europa. Our findings will be also used to model the sources and losses of sodium and its temporal variations with respect to the position of Europa relative to the Io plasma torus and Jovian System III longitudes, as well as calculating the velocity distribution for the sodium emission. Finally, we should gain a better knowledge of the energy flow into the surface and how it affects the surface chemistry of Europa and explore how it could be related to loss of volatiles.

Appendix A

Detailed Manual for Processing Europa's Data

A.1 File Conversion

Start IRAF by typing **cl**. Convert all the raw data (*.fits* files) into IRAF files (*.imh* files) using the **rfits** command. Any UNIX commands to be run under IRAF should be preceded by the character “!”. ”.

```
>rfits *.fits (when asked for the extension enter “ “)
```

Make a list of all the file names and all the file headers to know what type of observations we are dealing with: sky, Europa, zero, etc

```
>dir *.imh > files.lst
```

```
>imheader *.imh > filehdrs.lst
```

A.2 Cleaning up the Data

Zero bias, cosmic rays and bad pixels should be removed. Create a list of all the zero files in order to make a zero average file which will be subtracted from all the data.

```
>!emacs zero.lst
```

```
>imcombine @zero.lst zero
```

In some cases, exposure times are short due to atmospheric instabilities (ie. 15 minutes compared to 30 minutes). Therefore, noise levels in the raw data are high and it is necessary to average 2 or more consecutive Europa observations. For instance, the

following example required averaging observations 12, 13 and 14 taken in February 19, 2002.

There are often hot pixels and cosmic ray hits in the CCD. Make a bad pixel file with an editor such as EMACS (i.e. “badpixels”). It should follow the following format:

start column stop column start line stop line

For the example observation the “badpixels” file looks like this:

```
176  180  1    800
27   31  45   47
216  220  84   86
305  311  275  279
44   47  319  322
```

The routine **fixpix** interpolates across bad regions and removes the cosmic rays.

```
>!emacs badpixels    (badpixel file is created)
>fixpix feb19avg12-14average.imh badpixels
>fixpix zero.imh badpixels
```

Cosmic rays are harder to eliminate with **fixpix** because they create clusters of bad pixels.

The routine **cosmicrays** should be used instead. It uses the ratio (as a percentage) of the mean neighboring pixel flux to the candidate cosmic ray pixel for rejection. This process overwrites the input image so it is a good idea to make a copy of the initial image.

```
>imcopy feb19avg12-14average.imh feb19avg12-14CR.imh
>imcopy zero.imh zeroCR.imh
>noao.imred.ccdred.crutil    (navigates to the location of cosmicrays routine)
>cosmicrays feb19avg12-14CR.imh
```

>*cosmicrays zeroCR.imh* (quits the interactive mode by typing “q”)

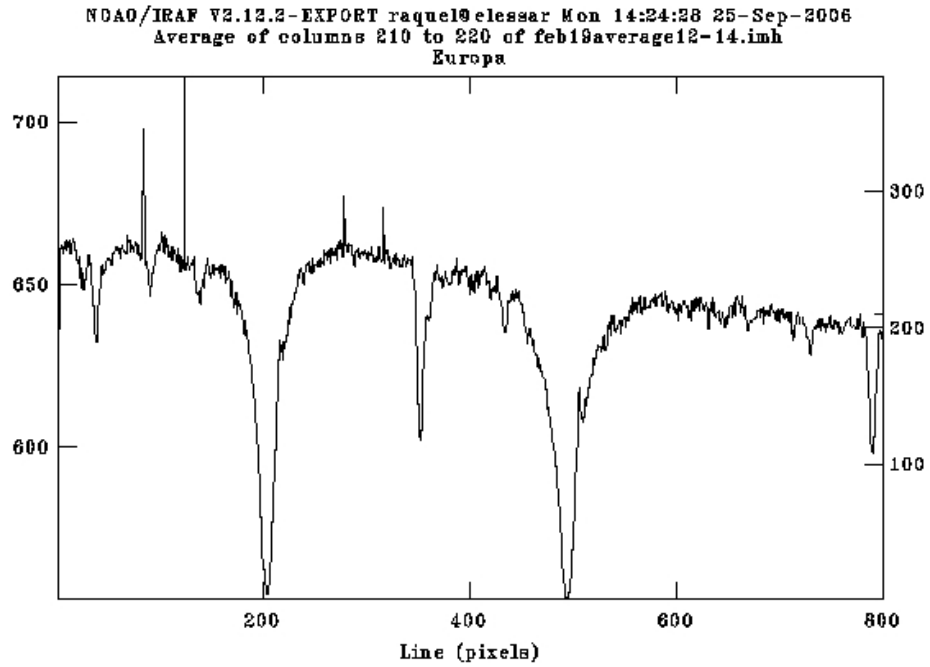


Figure A.1 – Raw spectrum of Europa.

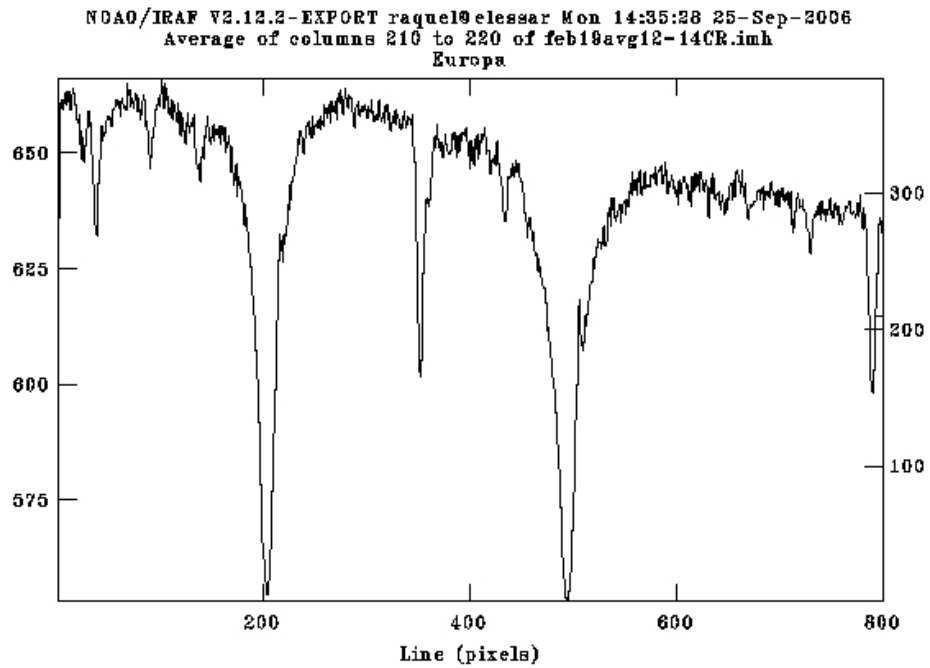


Figure A.2 – Cosmic ray removed spectrum.

A.3 Flat Fielding

For this kind of data, pixel efficiency variations are much less important than those caused by the optics of the slicer. Therefore, a sky spectrum (made from a combination of several good sky files) is used for flat fielding. The file *sky.lst* can be created with EMACS. It lists several good sky observations to be averaged with the routine **imcombine**, thus producing the file *sky.imh*.

```
>imcombine @sky.lst sky
```

```
>cosmicrays sky.imh      (removing cosmic rays from the sky file as well)
```

Subtract the bias from both the Europa observation and sky average.

```
>imarith feb19avg12-14CR.imh – zeroCR.imh feb19avg12-14bias.imh
```

```
>imarith sky.imh – zeroCR.imh skybias.imh
```

To create a sky flat apply the program **skyflat.f** (see Appendix C for details) to the bias corrected sky spectrum and with the resulting file flat field the Europa spectral image.

```
>!(directory with fortran codes)/skyflat.e  (navigate to the executable file)
```

```
>imdivide feb19avg12-14bias.imh skyflat.imh feb19avg12-14flat.imh
```

This process will produce some spurious spikes at the edges or between the slices. Create another bad pixel file and interpolate across the bad data.

```
>fixpix jan070017flat.imh badspikes
```

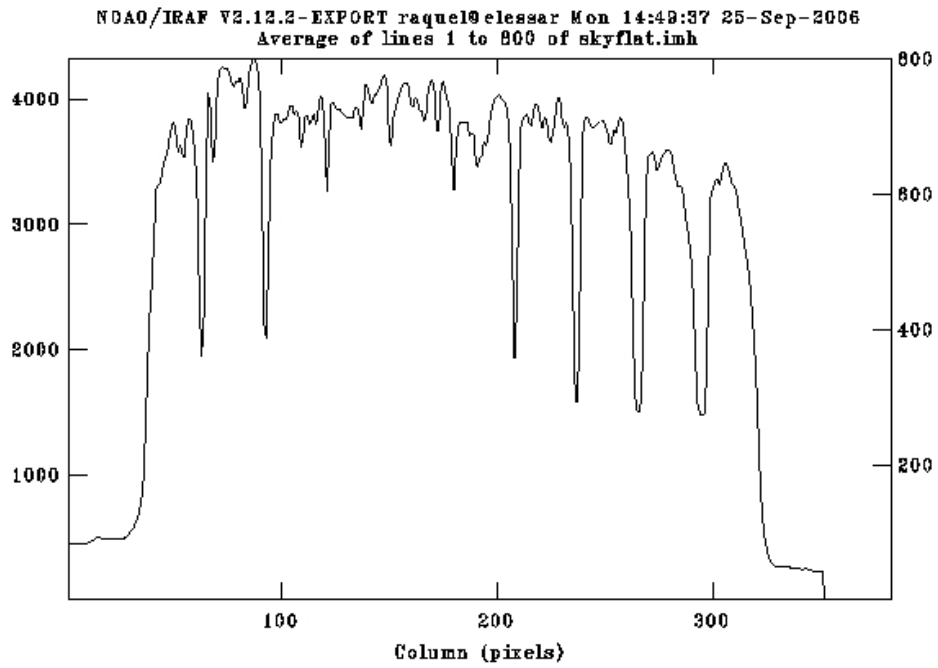



Figure A.3 – Sky flat.

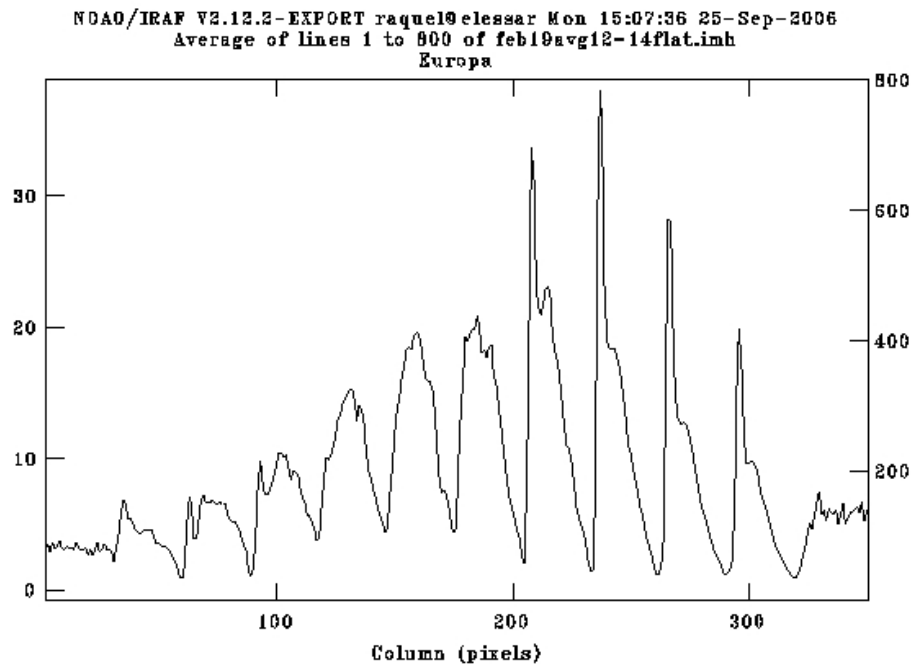


Figure A.4 – Flat fielded spectrum of Europa with spurious spikes.

A.4 Trimming the Spectral Image

Another side effect of the flat fielding process is the introduction of lots of noise at both ends of the slices. To eliminate these parts make a plot averaging over all the lines, identify the edge of the first slice and last slice and crop the image.

```
>implot feb19avg12-14flat.imh    (“CTRL-C” indicates pixel location)
```

```
>imcopy feb19avg12-14flat.imh[31:319,*] feb19avg12-14flat_crop.imh
```

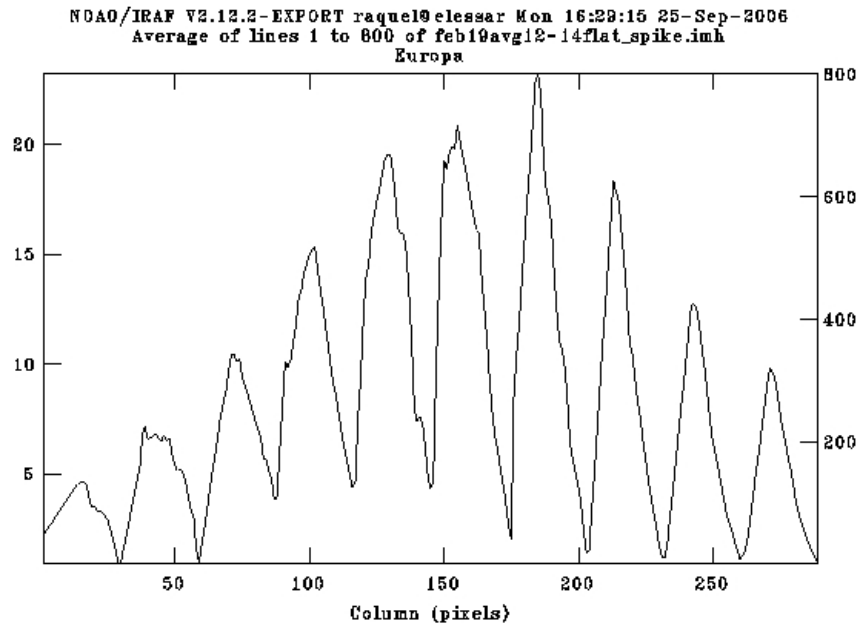


Figure A.5 – Spectrum of Europa with no spikes: Here the edges of the slices have been cropped.

A.5 Correcting the Slope in the Spectra

Inspection of the flat fielded spectral image generally shows an evident downward slope. This distortion poses a problem if one were interested in comparing the relation between the Sodium D2 and D1 lines. Therefore, correct it by applying the program **specflat.f** (see appendix C) to the spectral image. A wide range of columns from the central bright slice should be chosen to get a good average correction.

```
>!(directory with fortran codes)/specflat.e
```

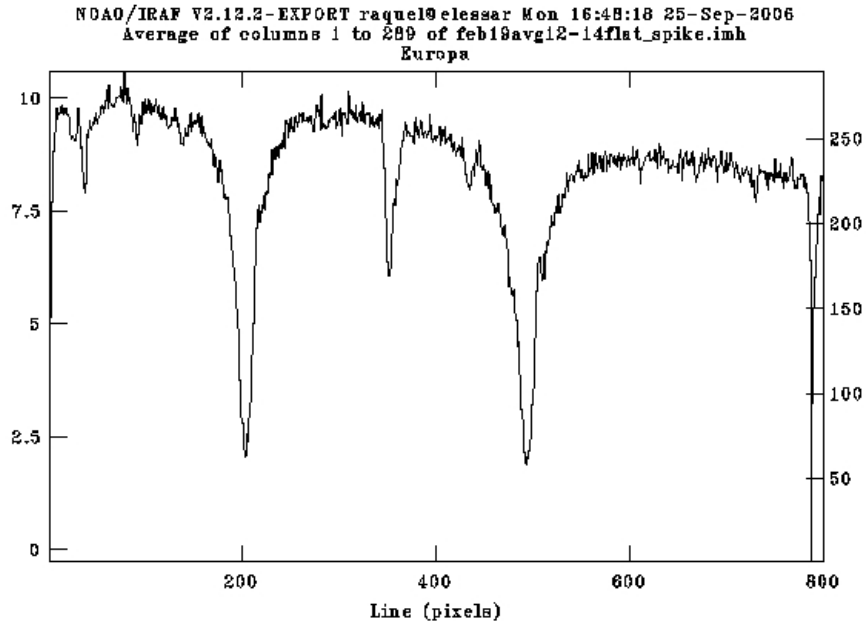


Figure A.6 – Spectrum of Europa with a slope: Note the downward trend towards the right side of the plot.

A.6 Checking the Zero Level

Sometimes the slices outside the emission regions do not go down to a zero level. If this is the case, subtract or add a constant to bring them to zero. For this example no corrections were needed, but one could do:

```
(>imarith imagename.imh - constant leveled_image.imh)
```

A.7 Geometric Corrections: Registration

This step corrects the image for misalignments in either, or both, lines and columns. Start by plotting the spectrum from one end of the image (type “:c” in the interactive mode), expand it around an absorption line and overlay the spectrum from the other end (typing

“o” permits over plotting). If the spectrum does not line up, the IRAF registration programs must be applied. Alignment of the slices is checked by the same procedure, but plotting lines (by typing “:l”) instead of columns (by typing “:c”). There are two routines that will allow such corrections: **geomap** and **geotran**. The first program calculates the coordinate transformation necessary to register the image, the second applies such transformation.

The **geomap** program requires input tables which indicate how the image should be transformed. The first step is to plot the spectrum at a column at the low end of the spectrum, for instance column 97 (type “:c 97”). Then, the spectrum is expanded around a sharp absorption line as noted above, and the line number at its minimum is recorded. For example, the number at column 97 is 351.94. Next repeat the procedure at the other end of the slicer. In this case column 243 has that same absorption line minimum at line 354.07. The column halfway between them is 170. Then the assumption that the spectral line will fall halfway in between the two is made and its value is the average of both extremes, 353.01. Hence, everything is registered to the middle column 170. All this yields the first three lines for the first input file. Going to a different spectral feature at the opposite end of the spectrum will yield another three lines. For instance, column 97 with absorption line minimum located at line 201.69, then column 243 with the same line placed at 204.44 will result in the middle column location of 203.07. An input file with all this information should be created (see table below). The first pair of numbers in the table are the output (desired position) and the second pair are for input (actual position of the lines before registration). Note that the second numbers in the output pairs are the same in each set of three.

>!emacs input1

97 353.01 97 351.94

170 353.01 170 353.01

243 353.01 243 354.07

97 203.07 97 201.69

170 203.07 170 203.07

243 203.07 243 204.44

The same step is repeated in order to register the lines. The markers used in this case are either the the minimums or the peaks between slices.

>!emacs input2

114.12 10 114.67 10

114.12 405 114.12 405

114.12 800 113.57 800

230.96 10 231.03 10

230.96 405 230.96 405

230.96 800 230.89 800

The **geomap** routine requires as inputs firstly, the file called “input1” discussed above, secondly the name of the output data file (“database1”) and thirdly, the dimensions of the image. The command **imheader** indicates dimensions of files. It is necessary for the dimensions to include decimal points so one must type “800.” instead of just 800.

>images.immatch (navigate to the routine directory)

```
>geomap input1 database1 1. 289. 1. 800.
```

```
>geomap input2 database2 1. 289. 1. 800.
```

After this, the coordinate transformation can be performed in two steps.

```
>geotran feb19avg12-14specflat.imh feb19avg12-14tran1.imh database1 input1
```

```
>geotran feb19avg12-14tran1.imh feb19avg12-14tran2.imh database2 input2
```

```
>imcopy feb19avg12-14tran2.imh feb19avg12-14reg.imh
```

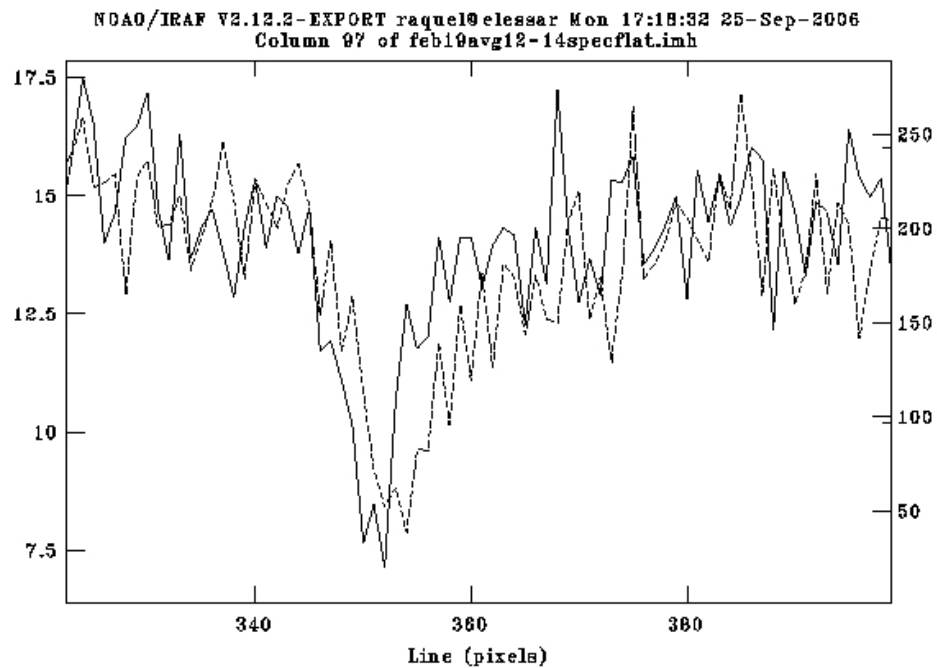


Figure A.7 – Columns in the spectrum do not line up: This is an overlay of columns 97 and 243 showing how the location of absorption and emission lines does not match.

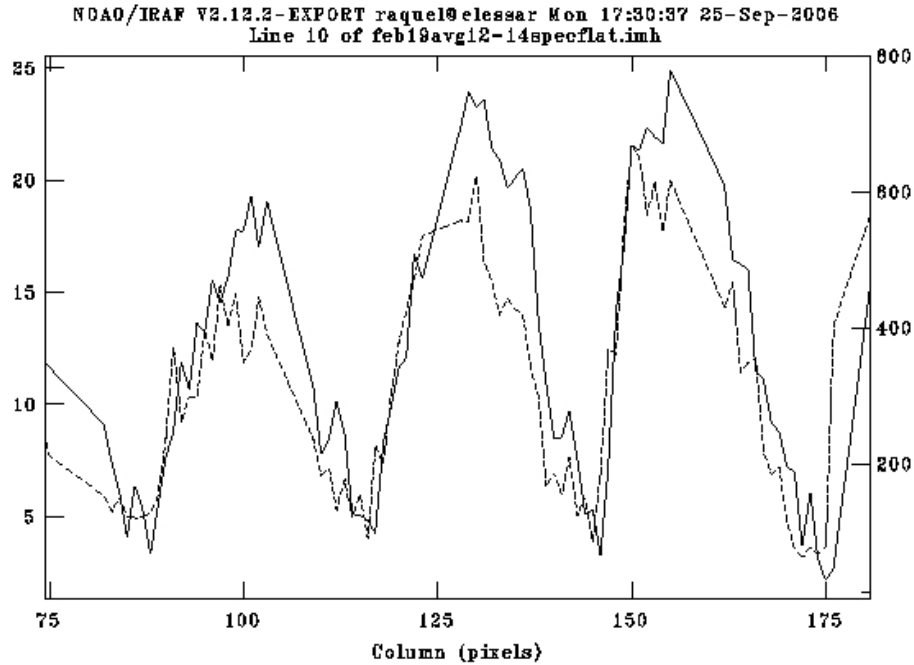


Figure A.8 – Lines in the spectrum do not line up: This is an overlay of lines 10 and 800 showing how the peaks and edges of slices do not match.

A.8 Calibration

This next step calculates the calibration constants for the now clean and registered spectrum of Europa with the program **calibration.f** (see appendix C). Along with the calibration factor, system III longitude, seeing and G-factor are also calculated. The following is an example of how the program runs:

`>!(directory with fortran codes)/calibration.e` (navigate to executable)

Enter V magnitude of satellite

Enter maximum continuum value

Enter continuum FWHM, units of pixels

Enter number of pixels in one slice

Enter step size in spectrum, milliangstroms

Enter observer longitude of Jupiter

Enter observer longitude of satellite

Enter rdot, radial velocity of satellite

Enter distance AU of satellite from Sun

Enter name of output file

You will get an output to the screen of the following results. These numbers are all copied into the output file, and are displayed just to see that everything was normal with the calculation.

G-FACTOR, photons/cm² sec per atom = .239001408

System III longitude = 313.400024

Seeing (FWHM), arc seconds = 3.04608178

Calibration factor, kilorayleighs/count = 0.00647792779

For the *feb19avg12-14* data this are the input values:

5.53 *V-magnitude of Europa found in the JPL ephemeris.*

28 *(No decimals points are allowed) implot the column with highest intensity from the brightest slice and choose the maximum level of the continuum signal. (Usually a flat region between the D1 and D2 Fraunhofer absorption lines).*

13.58 *Full Width Half Maximum of the continuum signal. Averaging several lines of the bright central slice gives a clean display of the slices. Cursor command p-p in the implot routine will display the FWHM value of that brightest slice.*

29 *(No decimal points are allowed). The average number of points in each slice.*

20.56 *Number of milliangstrom per step in the spectrum.*

This number is calculated using the spacing between the D1 and D2 lines:

(D2-D1) pixels / 5.97 Angstrom.

(494.022-203.728) pixels / 5.97 Angstrom = 48.625 pixels / Angstrom.

$1 / (48.625 \text{ pixels per Angstrom}) \times 1000 = 20.56 \text{ milliAngstrom per pixel.}$

84.85 The Observer Longitude for Jupiter as given by the JPL ephemeris.

311.09 The Observer Longitude for Europa as given by the JPL ephemeris.

12.49 This is r-dot, the radial velocity of the satellite relative to the Sun as given by the JPL ephemeris.

4.9697 This is the distance of the satellite from the Sun in AU as given by the JPL ephemeris.

calib.dat This is the name of the output calibration file.

A.9 Fitting the Solar Fraunhofer Line

In this step we want to create a good fit of the D2 Fraunhofer line profile in an area with as little sodium emission as possible, so then a spectral profile with no emission can be created and later on used as a template to extract the sodium out of the data. (For more details see the VFUDGIT routine instructions included in appendix B).

A.10 Extracting the Sodium Emission

Now the spectral dimension of the slicer data file needs to match the spectrum in the template file created above:

```
>imcopy feb19avg12-14reg.imh[*;454:534]feb19avg12-14range.imh
```

The following is an example of inputs for the **europana.f** program:

feb19avg12-14range.imh *Europa input image matching the template's range.*

<i>calib.dat</i>	<i>Calibration file created in step A.8.</i>
<i>feb19avg12-14vf.vft</i>	<i>Template file produced by the VFUDGIT routine.</i>
<i>81</i>	<i>Number of lines in template file.</i>
<i>feb19avg12-14na</i>	<i>Name of the output sodium D2 image.</i>
<i>47,55</i>	<i>Start, stop points for emission as seen in the residual.</i>
<i>1</i>	<i>Starting column in the image file.</i>
<i>9</i>	<i>Number of slices.</i>
<i>29</i>	<i>Pixels per slice, same value as used during calibration.</i>
<i>1</i>	<i>Edge locations for each of the slices. Separate with return.</i>
<i>29</i>	
<i>58</i>	
<i>87</i>	
<i>116</i>	
<i>145</i>	
<i>172</i>	
<i>203</i>	
<i>232</i>	
<i>261</i>	
<i>feb19avg12-14na.dat</i>	<i>Output data summary file name.</i>
<i>feb19avg12-14na.img</i>	<i>Output image data file name</i>

It is crucial to get the slicer edge locations accurately, as well as the extent of the sodium emission seen from the residuals of the VFUDGIT fit. In some cases the output image will show spurious lines at different locations from where the sodium emission would be,

usually the emission can be followed across most of the image. Sometimes it is necessary to run this step again in order to get a good estimate of the emission span and slice edges. This will tell if the emission extraction has been successful. There may be several artificial lines, but the sodium is the one that can be followed almost all the way across the image.

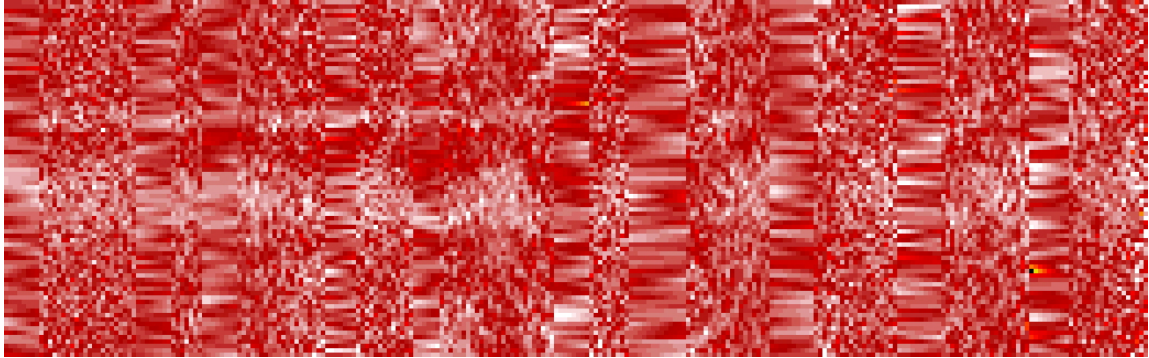


Figure A.9 – Emission extraction: Spatial-spectral image obtained from subtracting the template reflection spectrum from the 10-slicer Europa data.

Slicer edge locations

In order to get a good final image, one should choose the slicer edge locations carefully. A good method is to work with the maximum values in the slicer, rather than the minima between the slices. Locate the maxima for each slice using “*ctrl/c*”, and make a list of them. Calculate the differences between each pair of slices. Average the differences to get a value for the average number of elements in each slice. Subtract half that value from the location of each of the maxima to get the start point for each slice.

The *.dat* and *.img* files will each contain a header that gives the date and time of the observation, the average kR in the image, the exposure time, the calibration in terms of kR per count, the g-factor, the system III longitude, and the seeing. The *.dat* file lists all

the emission data points from the initial spectral image, and the *.img file lists emission data points resampled to a 10 x 10 arcsecond matrix.

A.11 Making the Europa Sodium Emission Image

At last, we can make a Europa sodium emission image. For this final step, the program used is **europaim.f** (see appendix C). Inputs to the program are self-explanatory. First input is the name of the *.img file you generated using **europana.f**. Second is the number of slices, third is the directory for the pixels, and last is the name of the sodium image. The header of the image will contain all the information from the header of the *.img file.

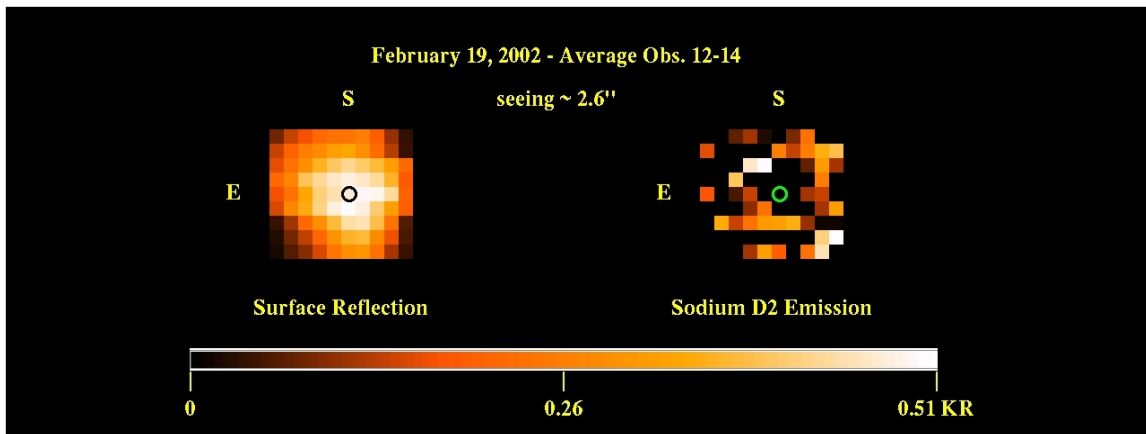


Figure A.10 – Final intensity map: The surface reflection image is on the left, the sodium D2 emission image is on the right.

Appendix B

Running VFUDGIT 4.2

B.1 Introduction

The VFUDGIT 4.2 routine was built around another data fitting program called FUDGIT. This package was modified in order to make least-squares fittings of Voigt functions simpler and allow components of some Voigt profiles to be linked to other Voigt profiles. VFUDGIT uses GNUPLOT as a graphical interface [Woodward, R.C., 1998].

B.2 Using VFUDGIT to extract the Sodium Emission

This routine creates a Voigt profile fit. This profile is the product of the convolution of Lorentzian and Gaussian distributions. The first due to pressure broadening of the line, the second due to the thermal Doppler broadening. In the case of Europa, Doppler broadening dominates over pressure broadening because we are dealing with a collisionless atmosphere.

The main goal here is to create a good fit for the spectral profile of the solar Fraunhofer D2 line without the emission, in other words the spectrum of the reflection from Europa with no contribution from the sodium emission. Using the program **profil.f** (see appendix C) a spectrum with the best signal-to-noise ratio is created by averaging about 10 columns around the highest intensity location. This is around the peak of the brightest slice. The result is an ascii file with data of the spectrum averaged over those columns.

VFUDGIT does not work inside IRAF. One must start the package by typing *vf* in a separate terminal.

% vf

V-Fudgit> pmode set grid (sets a grid for the plot)

V-Fudgit> getdat europad2.dat (loads the ascii file created by profil.f)

V-Fudgit> plotdat (plots the Europa data)

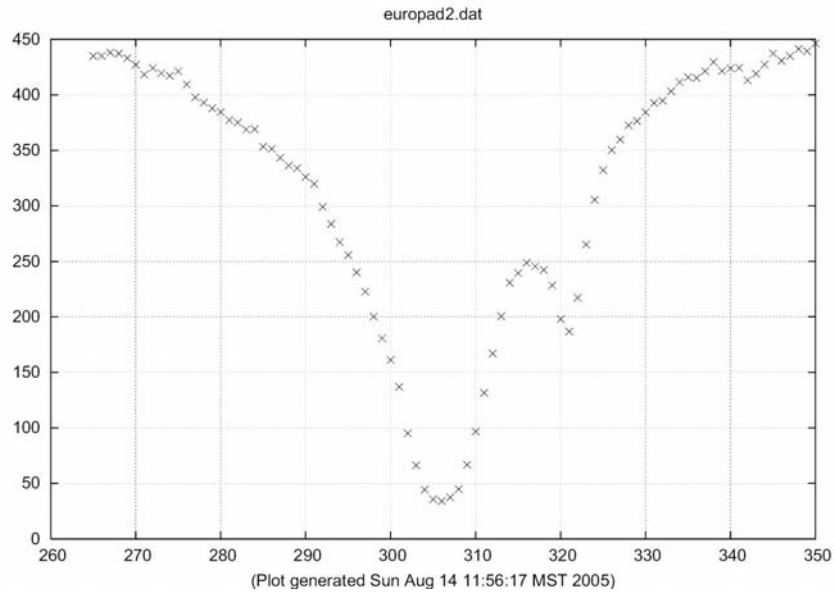


Figure B.1 – D2 solar Fraunhofer line: Here the central 10 brightest columns have been averaged.

This spectrum shows the D2 Fraunhofer line, a water line around line 320, and a barely visible sodium emission line somewhere to the left of the water absorption. To start a good fit for this spectrum, one must find out where the sodium emission line should be located. Using the radial velocity of Europa with respect to the Sun, *r-dot* (given by the JPL ephemeris), the shift of the D2 emission from the minimum of the solar Fraunhofer line can be calculated:

– \dot{r} \times 19.647 milliångstroms.

For this example, an observation taken on August 15, 1998, the radial velocity was 9.69km/sec, so the shift was approximately -190 milliångstroms. Knowing the scale of the spectrum from the spacing between the two D lines (see calculation for input 5 in section A.8 of appendix A), the number of milliångstroms per step can be determined. For this data it was 25.5. Hence, the emission line should be located at -190/25.5 or -7.45 steps away from the minimum of the solar D2 Fraunhofer line. It is important to remember that these spectra are reversed, with blue (small wavelengths) on the right instead of left. So the emission will be we about 7.45 pixels to the right of the Fraunhofer minimum, which is located around line 306. Therefore the sodium emission should be around lines 313 or 314.

The fit for this spectrum is going to be a convolution of Gaussian and Lorentzian functions. The solar Fraunhofer line fit is composed of 2 absorption lines separated a few lines apart near the minimum of the Fraunhofer line we see. There is also an absorption water line near 320 and the D2 emission around lines 313 or 314 as calculated above. Therefore the fit needs at least 4 Voigt parameters. This is an example of command used for fitting the example spectrum:

```
V-Fudgit> setmod 4 1          (setting up 4 Voigt parameters to a maximum of 11)
V-Fudgit> setv 1             (First Fraunhofer Voigt component. Enter guesses)
Centroid:    0      1 Read?   305    1      (1 indicates this is a free parameter)
Dop. width:  1      1 Read?    3      1
Lor. width:  1      1 Read?   20     1
Area:        10     1 Read?  -4000  1      (negative areas mean absorption)
```

V-Fudgit> setv 2 (Second Fraunhofer component parameters)

Centroid: 305 1 Read? 307 1

Dop. width: 3 1 Read? 3 1

Lor. Width: 20 1 Read? 20 1

Area: -4000 1 Read? -4000 1

V-Fudgit> setv 3 (Parameters for the D2 emission line)

Centroid: 307 1 Read? 313 1

Dop. width: 3 1 Read? 3 1

Lor. width: 20 1 Read? 3 1

Area: -4000 1 Read? 40 1

V-Fudgit> setv 4 (Parameters for the water absorption line)

Centroid: 312 1 Read? 320 1

Dop. width: 3 1 Read? 3 1

Lor. width: 3 1 Read? 8 1

Area: 40 1 Read? -200 1

V-Fudgit> setc (Estimate the continuum level)

Continuum: 0 1 Read? 400 1

V-Fudgit> fitv (attempts a fit to the spectrum

which will convergence after several iterations)

V-Fudgit> plotf (overlays the calculated fit over the data)

The parameters to *setv* 1, 2, 3, and 4 must be changed until one gets a good fit. This procedure takes a lot of trial and error. After each modification to the Voigt parameters, *fitv* and *plotf* must be repeated. Once a good fit is reached the parameters can be saved.

V-Fudgit> **savepar** (a *.par file will be created)

V-Fudgit> **getpar filename.par** (restore those Voigt parameters)

A good fit can go very bad even with a small change in one of the Voigt functions so saving good parameters frequently is recommended. The figure below is an example of a good fit.

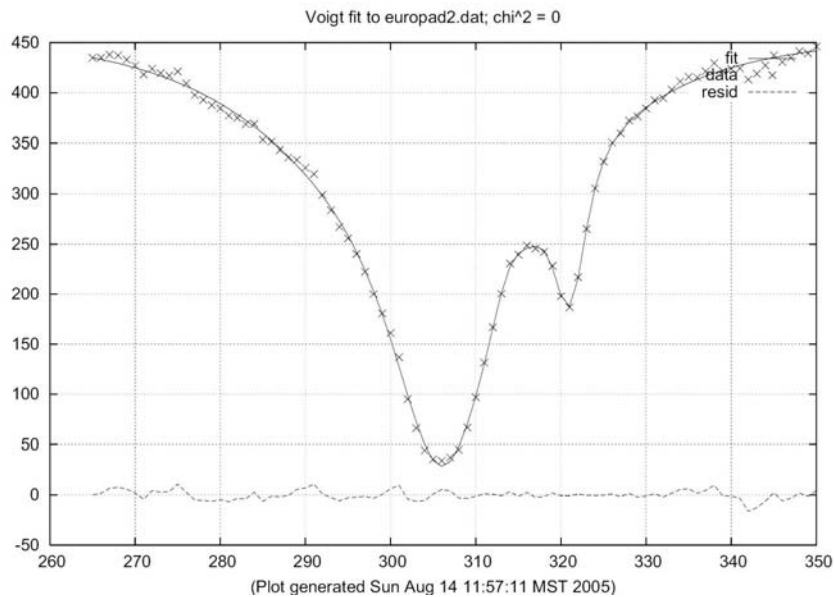


Figure B.2 – Sample Voigt fit to the solar Fraunhofer line: The fit is indicated by a solid line and the data by crosses. Residuals are shown at the bottom (dashed line).

While doing a fit one must keep track of the location of the D2 emission line to make sure it does not wander away from where it should be. The next step is to uncover Europa's D2 emission line. This is done by editing the Voigt parameter for that emission line. The emission intensity (area parameter) should be set to 1 (zero values are not allowed), and the fit plotted again using *plotf*. The result will be as follows:

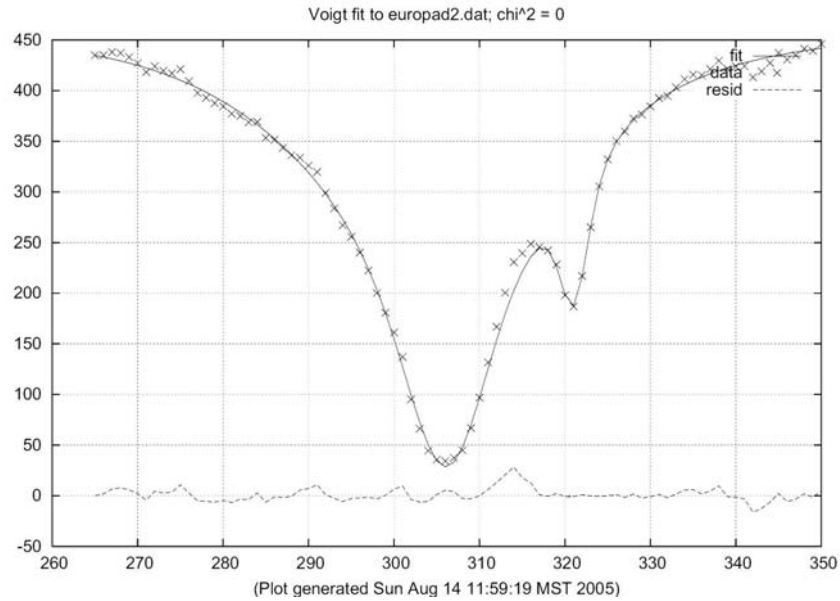


Figure B.3 – Sample Voigt fit revealing the D2 emission: The fit is indicated by a solid line and the data by crosses. Residuals show the location of the D2 emission at the bottom (dashed) around line 313.5.

The emission line appears in the residuals (dashed line) around line 313.5. This fit is the spectral profile without the emission line which will be used as a template to extract the sodium D2 emission from the data. Then the fit can be saved:

V-Fudgit> **savefit** filename.vft.

This ascii file has comments that must be edited out in order to be able to be used as the third input in **europa.f** for the following step in the data reduction (see step A.10 in appendix A).

Appendix C

Fortran Programs used for the Data Reduction

All coding by Dr. Andrew E. Potter

C.1 SKYFLAT.F

SKYFLAT.F will average each spectral line in a sky spectrum to make a new spectral image which can be used to flatten Europa spectral images in the spatial direction.

```
character*80 image1,pixdir,pixdir,imav
integer naxis,pixtype,axlen(7),nim,oim,ier,dtype
real array1(512,1024),array2(512,1024),array3(512,1024)
10 format(i6)
15 format(80a)
20 format(i6,i6)
c Read in the image
write(6,*)' Name the input image'
read(5,15)image1
c Open the sky image and read in the data
call imopen(image1,3,nim,ier)
call imgsiz(nim,axlen,naxis,pixtype,ier)
write(6,*)' Columns = ',axlen(1)
write(6,*)' Lines = ',axlen(2)
if(pixtype.eq.6)then
```

```

        write(6,*)' Pixels are in real format'
    endif

    if(pixtype.eq.3)then
        write(6,*)' Pixels are in short format'
    endif

    call imgs2r(nim,array1,1,axlen(1),1,axlen(2),ier)
    call imclos(nim,ier)

c    Arrange the data array to conventional format

    do 30 i=1,axlen(1)

        do 30 j=1,axlen(2)

            k=(j-1)*axlen(1)+i

            array2(i,j)=array1(k,1)

30    continue

c    Average the spectrum for each line

        do 130 i=1,axlen(1)

            specav=0

            do 120 j=1,axlen(2)

                specav=array2(i,j)+specav

120    continue

            specav=specav/axlen(2)

            do 122 j=1,axlen(2)

                array2(i,j)=specav

122    continue

```

130 *continue*

c Re-arrange the array to iraf image format

do 140 i=1,axlen(1)

do 140 j=1,axlen(2)

*k=(j-1)*axlen(1)+i*

array3(k,1)=array2(i,j)

140 *continue*

write(6,)'Name the output image'*

read(5,15)imav

c Create the output image

dtype=6

call clargc(3,pixdir,ier)

if(ier.eq.0)then

pixdir='HDR\$pixels/'

call immdir(pixdir)

endif

call imcrea(imav,axlen,naxis,dtype,ier)

call imopen(imav,3,oim,ier)

c Write in the data

call imps2r(oim,array3,1,axlen(1),1,axlen(2),ier)

call imclos(oim,ier)

stop

end

C.2 SPECFLAT.F

SPECFLAT.F extracts a profile through an iraf image of the sky along the line dimension and uses it to correct a linear slope in the spectral dimension. If the spectrum is normalized to unity. The Fraunhofer lines should be symmetrically disposed in the spectrum and the spectrum should be wide enough so that the continuum is reached at the beginning and end of the spectrum. Otherwise, an improper tilt will be introduced into the spectrum.

```
character*40 image1,image2,time,ut,keywrd
character*80 pixdir
integer naxis,pixtype,axlen(7),nim,oim,ier,dtype
real array1(600,1000),array2(600,1000),array3(600,1000)
real ina(1000),expt
10 format(80a)
15 format(40a)
20 format(i6,i6)
25 format(2a)
write(6,*)' Name the input image'
read(5,15)image1
c write(6,*)'Name the output file'
c read(5,15)ofile
write(6,*)'Enter start,stop columns for averaging'
read(5,20)istrt,istop
call imopen(image1,3,nim,ier)
```

```

call imgsiz(nim,axlen,naxis,pixtype,ier)
write(6,*)' Columns = ',axlen(1)
write(6,*)' Lines = ',axlen(2)
if(pixtype.eq.6)then
    write(6,*)' Pixels are in real format'
endif
if(pixtype.eq.3)then
    write(6,*)' Pixels are in short format'
endif
call imgs2r(nim,array1,1,axlen(1),1,axlen(2),ier)

```

c Extract keywords to identify the data

```

KEYWRD='DATE-OBS'
CALL IMGKWC (NIM,KEYWRD,TIME,IER)
keywrд='exptime'
call imgkwr(nim,keywrд,expt,ier)
KEYWRD='UT'
CALL IMGKWC (NIM,KEYWRD,UT,IER)
call imclos(nim,ier)

```

c Rearrange array to conventional format

```

do 30 i=1,axlen(1)
do 30 j=1,axlen(2)
k=(j-1)*axlen(1)+i
array2(i,j)=array1(k,1)

```

```

30  continue

    do 50 j=1,axlen(2)

        ina(j)=0
50  continue

    do 100 j=1,axlen(2)

        do 100 i=istrt,istop

            ina(j)=ina(j)+array2(i,j)
100 continue

    specmax=0.0

    do 110 j=1,axlen(2)

        ina(j)=ina(j)/(istop-istrt+1)

        if((j.gt.3).and.(j.lt.axlen(2)-3)) then

            if (specmax.lt.ina(j))then

                specmax=ina(j)

            endif

        endif
110 continue

c  Low end of spectrum

    do 130 i=20,40

        sumlow=sumlow+ina(i)
130 continue

    sumlow=sumlow/20

    ilow=30

```


c High end of spectrum

```
do 140 i=axlen(2)-60,axlen(2)-40
```

```
sumhi=sumhi+ina(i)
```

```
140 continue
```

```
sumhi=sumhi/20
```

```
ihi=axlen(2)-50
```

c Normalize spectrum to average value

```
specav=(ina(ihi)+ina(ilow))/2
```

```
a=(sumhi-sumlow)/(float(ihi-ilow))
```

```
b=sumhi-a*float(ihi)
```

```
do 150 i=1,axlen(1)
```

```
do 150 j=1,axlen(2)
```

```
array2(i,j)=array2(i,j)*specav/(a*j+b)
```

```
150 continue
```

c Re-arrange the array to iraf image format

```
do 160 i=1,axlen(1)
```

```
do 160 j=1,axlen(2)
```

```
k=(j-1)*axlen(1)+i
```

```
array3(k,1)=array2(i,j)
```

```
160 continue
```

```
write(6,*)'Name the output image'
```

```
read(5,15)image2
```

c Create the output image

```

dtype=6

naxis=2

call clargc(3,pixdir,ier)

call immdir ('HDR$pixels/')

call imcrea(image2,axlen,naxis,dtype,ier)

call imopen(image2,3,oim,ier)

c Write in the data

call imps2r(oim,array3,1,axlen(1),1,axlen(2),ier)

c Input keywords to identify the data

call imakwc(oim,'DATE-OBS',time,' ',ier)

call imakwc(oim,'UT',ut,' ',ier)

call imakwr(oim,'EXPTIME',expt,' ',ier)

c Close the image

call imclos(oim,ier)

stop

end

```

C.3 CALIBRATION.F

CALIBRATION.F calculates the calibration factor for satellites. It is based on the procedure outlined in "Io, its atmosphere and optical emission" by R.A. Brown and Y.L. Yung -- pages 1104-1108 in the book "Jupiter" edited by Gehrels. The output is a calibration factor in terms of kilorayleighs per count in the spectrum of the satellite.

DIMENSION PIX(1),nlam(100),dtwo(100),done(100)
*character*48 dfile,ofile*

10 *format(48a)*

WRITE(6,)'Enter V magnitude of satellite'*

READ(5,)vmag*

WRITE(6,)'Enter maximum continuum value '*

READ(5,)contmax*

WRITE(6,)'Enter continuum FWHM, units of pixels '*

READ(5,)sigma*

WRITE(6,)'Enter number of pixels in one slice '*

READ(5,)xnum*

WRITE(6,)'Enter step size in spectrum, milliangstroms'*

READ(5,) pix(1)*

WRITE(6,)'Enter observer longitude of Jupiter'*

READ(5,)OBJUP*

WRITE(6,)'Enter observer longitude of satellite'*

READ(5,)OBSAT*

c Calculate the System III longitude

SYS3=180+OBJUP-OBSAT

write(6,)'Enter rdot,radial velocity of satellite'*

read(5,)rdot*

write(6,)'Enter distance AU of satellite from Sun'*

read(5,)satsun*

c Calculate the doppler shift relative to the Fraunhofer

*dopp=-rdot*19.67 ! milliangstroms. Note negative sign*

c Calculate the calibration factor from the V magnitude

c Brown and Yung calibration procedure

c For V magnitude, effective wavelength=5500 A

FV=(3.72E-9)(exp(2.303*(-0.4)*VMAG))! Units ergs/cm2secA*

c Correct to 5900 A

*FV=1.06*FV*

c Convert to photons/cm2secA at 5900 A

FV=FV/(3.3661E-12)

c Angular size of Gaussian intensity distribution

c Remembering that there are 10 arc secs across a slice

*sigma1=10*sigma/xnum !Brown and Yung specify FWHM*

c Central intensity in Gaussian intensity distribution

c Units of MR per A

*ci=((0.472)*FV)/(sigma1**2)*

c Write surface brightness of central peak

c Convert ci to MR per milliangstrom

FV=ci/1000.

c Convert to step width

*FV=FV*PIX(1) ! PIX(1) has units of mA/step*

c Convert to counts. This is the calibration factor

FV=FV/CONTMAX ! CONTMAX has units of counts/step

c Convert to kilorayleighs/count

*FV=1000.*FV*

c Read in the profile of the D1 and D2 Fraunhofer lines relative to

c the Doppler shift, and calculate the D1 and D2 solar continuum

c intensities under the Mercury emission lines. This profile

c is believed to be accurate, not include instrumental broadening.

DFILE='SOLAR.DAT'

114 FORMAT(I4,F6.4,F6.4)

OPEN(UNIT=4,FILE=DFILE,STATUS='OLD')

READ(4,114)(NLAM(I),DTWO(I),DONE(I),I=1,73)

CLOSE(UNIT=4)

SLAM=(FLOAT(DOPP))/10

LAM=NINT(SLAM)! NUMBER OF STEPS TO EMISSION LINE

DISIG=DONE(37+LAM)! Relative intensity continuum under D1 line

D2SIG=DTWO(37+LAM)! Relative intensity continuum under D2 line

c Calibration in terms of photons/cm2 sec atom for D2

c 0.049 is the D2 signal at the bottom of the solar Fraunhofer line

c 0.67 is the number of photons scattered per atom at 1 AU

c and at the bottom of the Fraunhofer line.

c ATCAL has dimensions of photons/cm2 sec per atom

ATCAL=0.67(D2SIG/0.049)/(SATSUN**2)*

write(6,)'Enter name of output file'*

read(5,10)ofile

```

20  format(f6.4,f8.2,f6.1,f10.6)
    open(unit=10,file=ofile,status='new')
    write(10,10)'g-factor, SysIII ,Seeing, Calibration, KR/count'
    write(10,20)atcal,sys3,sigma1/1.67,fv !Correct to gaussian sigma
    close(unit=10)

    WRITE(6,*)'G-FACTOR, photons/cm2 sec per atom =',ATCAL
    WRITE(6,*)'System III longitude = ',SYS3
    write(6,*)'Seeing (FWHM), arc seconds = ',sigma1/1.67
    WRITE(6,*)'Calibration factor, kilorayleighs/count = ',FV
    stop
    end

```

C.4 PROFIL.F

PROFIL extracts a profile through an iraf image along the line dimension and writes an ascii file. [column:line] Any number of columns can be averaged.

```

    character*40 image1,ofile,errmag,errmsg
    character*2 ques
    integer naxis,pixtype,axlen(7),nim,oim, ier
    real array1(600,1000),array2(600,1000)
    realina(1000)
15  format(40a)
20  format(i6,i6)
25  format(2a)

```

```

nim=30

oim=50

write(6,*)' Name the input image'

read(5,15)image1

write(6,*)'Name the output file'

read(5,15)ofile

write(6,*)'Enter start,stop columns for averaging'

read(5,20)istrt,istop

call imopen(image1,3,nim,ier)

call imgsiz(nim,axlen,naxis,pixtype,ier)

write(6,*)' Columns = ',axlen(1)

write(6,*)' Lines = ',axlen(2)

if(pixtype.eq.6)then

    write(6,*)' Pixels are in real format'

endif

if(pixtype.eq.3)then

    write(6,*)' Pixels are in short format'

endif

call imgs2r(nim,array1,1,axlen(1),1,axlen(2),ier)

call imclos(nim,ier)

c    Rearrange array to conventional format

do 30 i=1,axlen(1)

do 30 j=1,axlen(2)

```

```

        k=(j-1)*axlen(1)+i
        array2(i,j)=array1(k,1)
30    continue

        do 50 j=1,axlen(2)

            ina(j)=0

50    continue

        do 100 j=1,axlen(2)

            do 100 i=istrt,istop

                ina(j)=ina(j)+array2(i,j)

100   continue

            specmax=0.0

            do 110 j=1,axlen(2)

                ina(j)=ina(j)/(istop-istrt+1)

                if (specmax.lt.ina(j))then

                    specmax=ina(j)

                endif

110   continue

            write(6,*)'Want to normalize to maximum? (Y/N)'

            read(5,25)ques

            if((ques.eq.'Y').or.(ques.eq.'y')) then

                do 120 j=1,axlen(2)

                    ina(j)=ina(j)/specmax

120   continue

```



```

        endif
10    format(i6,f12.3)
c    Special format for input to wavelet program in mathcad
c 11  format(f12.3)
        write(6,*)'Enter start, stop points to be included in output'
        read(5,20)istart, istop
        open(unit=10,file=ofile,status='new')
        write(10,10)(j,ina(j), j=istart,istop)
        close(unit=10)
        stop
        end

```

C.5 EUROPARNA.F

EUROPANA.F will subtract a reference Europa reflection spectrum that is lacking any sodium emission from each spectrum in a 10-slicer spectral-spatial image of Europa sodium. The result is an spatial-spectral image showing only the sodium emission. The reference spectrum is determined using VFUDGIT to fit a high signal-to-noise spectrum drawn from the spatial-spectral image to be analyzed. The spectrum is first fit including the sodium emission, and then the sodium emission is zeroed out to get the reference spectrum for subtraction. The program also requires an input of a file from the calibrationprogram to allow output of signal intensity in kilorayleighs. For data older than 1999, you have to edit the KEYWRDs (lines 50 and 55 approximately) to be DATEOBS and EXPOSURE.

*character*80 image1,imav,errmag,pixdir,template*

*character*80 ofile,time,calib,title*

*character*8 keywrđ*

integer naxis,pixtype,axlen(7),nim,oim,ier,dtype,iedge(10)

real array1(512,512),array2(512,512),array3(512,512)

real krcount

dimension num(512),sod1(512),sod2(512),error(512),specav(512)

dimension d2(512),acont(512,1000),ad2(512,1000),bcont(512,1000)

dimension bd2(512,1000),ccont(512,1000),cd2(512,1000)

dimension dd2(512,1000),dcont(512,1000)

dimension xxcont(512,1000),xxd2(512,1000),exptime(1)

10 *format(i6)*

15 *format(80a)*

20 *format(i6,i6)*

nim=30

oim=50

c ***Read in the image***

write(6,)'If data are older than 1999, edit KEYWRDs'*

write(6,)' Name the input image'*

read(5,15)image1

c ***Open the Europa image and read in the data***

call imopen(image1,3,nim,ier)

call imgsiz(nim,axlen,naxis,pixtype,ier)

```

write(6,*)' Columns = ',axlen(1)
write(6,*)' Lines = ',axlen(2)
if(pixtype.eq.6)then
    write(6,*)' Pixels are in real format'
endif
if(pixtype.eq.3)then
    write(6,*)' Pixels are in short format'
endif
call imgs2r(nim,array1,1,axlen(1),1,axlen(2),ier)

```

c Extract keywords to identify the data

```
KEYWRD='DATE-NEW'
```

c KEYWRD='DATEOBS'

```
CALL IMGKWC (NIM,KEYWRD,TIME,IER)
```

```
KEYWRD='EXPTIME'
```

c KEYWRD='EXPOSURE'

```
CALL IMGKWR (NIM,KEYWRD,EXPTIME,IER)
```

```
call imclos(nim,ier)
```

c Arrange the data array to conventional format

```
do 30 i=1,axlen(1)
```

```
do 30 j=1,axlen(2)
```

```
k=(j-1)*axlen(1)+i
```

```
array2(i,j)=array1(k,1)
```

30 continue

```

write(6,*)'Name the data file from the calibration program'

read(5,15)calib

open(unit=4,file=calib,status='old')

read(4,15)title

40  format(f6.4,f8.2,f6.1,f10.6)

read(4,40)gfact,sys3,seeing,krcount

close(unit=4)

write(6,*)'Name the template file from vfudgit'

read(5,15)template

write(6,*)'Enter the number of data points in template file'

read(5,10)numdat

open(unit=4,file=template, status='old')

read(4,*)(num(i),sod1(i),sod2(i),error(i),i=1,numdat)

close(unit=4)

c  Calculate average value in template spectrum

sodav=0

do 50 i=1,numdat

sodav=sodav+sod1(i)

50  continue

sodav=sodav/numdat

c  Calculate average signal for each spectrum in the Europa file

do 100 i=1,axlen(1)

do 110 j=1,axlen(2)

```

```

                specav(i)=specav(i)+array2(i,j)
110          continue

                specav(i)=specav(i)/axlen(2)
100          continue
c      Scale the template, and subtract from each spectrum

                do 130 i=1,axlen(1)

                do 120 j=1,axlen(2)

                array2(i,j)=array2(i,j)-(specav(i)/sodav)*sod1(j)

120          continue

130          continue

c      Re-arrange the array to iraf image format

                do 140 i=1,axlen(1)

                do 140 j=1,axlen(2)

                k=(j-1)*axlen(1)+i

                array3(k,1)=array2(i,j)

140          continue

                write(6,*)'Name the output image'

                read(5,15)imav

c      Create the output image

                dtype=6

                call clargc(3,pixdir,ier)

                if(ier.eq.0)then

                pixdir='HDR$pixels/'

```

```

c   pixdir='duc0:[merc.jul94]'
    call immdir(pixdir)
    endif
    call imcrea(imav,axlen,naxis,dtype,ier)
    call imopen(imav,3,oim,ier)

c   Write in the data
    call imps2r(oim,array3,1,axlen(1),1,axlen(2),ier)
    call imclos(oim,ier)

c   Extract sodium emission
    write(6,*)' Enter the start, stop points for sodium'
    read(5,20)jstart,jstop
    do 150 i=1,axlen(1)

c   Assume continuum flat underneath emission line
        base=(array2(i,jstart)+array2(i,jstop))/2
        do 160 j=jstart,jstop
            d2(i)=d2(i)+array2(i,j)-base
160      continue
150      continue

c   Convert d2(i) to KR
        do 170 i=1,axlen(1)
            d2(i)=krcount*d2(i)

c   Compute overall average emission
        d2avg=d2avg+d2(i)

```

170 *continue*

d2avg=d2avg/axlen(1)

c *Get info for sodium image*

write(6,)' Enter starting column in the image file'*

read(5,10)istart

write(6,)' Enter number of slices'*

read(5,10)islice

write(6,)' Enter number of elements in each slice'*

read(5,10)idata

write(6,)' Enter slicer edge locations'*

do 180 i=1,islice

read(5,10)iedge(i)

180 *continue*

c *Write the data to a file*

write(6,)' Enter output data file name'*

read(5,15)ofile

open(unit=10,file=ofile,status='new')

300 *format(a23,f8.4)*

310 *format(a23,a18)*

320 *format(a23,f8.0)*

330 *format(a23,f8.1)*

340 *format(a23,f8.6)*

350 *format(a23,f8.2)*

```

write(10,310)'Date & Time ',time
write(10,350)'Avg Emission, KR ',d2avg
write(10,320)'Exposure Time, sec ',exptime
write(10,340)'Calibration, KR/count ',krcount
write(10,330)'System III longitude ',sys3
write(10,300)'g,photons/cm2sec atom ',gfact
write(10,300)'Seeing ',seeing
190  format(2x,i4,2x,f8.1,2x,f8.2)
write(10,190)(i,specav(i),d2(i),i=1,isllice*idata)
close(unit=10)
c  Select the data for the image file
do 200 i=1,isllice
do 200 j=1,idata
acont(i,j)=specav(iedge(i)-1+j)
ad2(i,j)=d2(iedge(i)-1+j)
200  continue
c  Resample the data to get 10 pixel elements per slice
n=idata
m=10
c  Expand to idata*10 samples
do 220 i=1,isllice
do 230 j=1,n ! n=idata
do 230 k=1,m ! m=10

```


$bcont(i, (j-1)*m+k) = acont(i, j)$

$bd2(i, (j-1)*m+k) = ad2(i, j)$

230 continue

220 continue

c Contract to 10 samples

do 240 i=1, islice

do 250 j=1, m ! m=10

do 250 k=1, n ! n=idata

$ccont(i, j) = ccont(i, j) + bcont(i, k+(j-1)*n)$

$cd2(i, j) = cd2(i, j) + bd2(i, k+(j-1)*n)$

250 continue

240 continue

c Compute single pixel values

do 783 i=1, islice

do 783 j=1, 10

$dcont(i, j) = ccont(i, j)/n$

$dd2(i, j) = cd2(i, j)/n$

c Zero out any negative d2 emissions

if($dd2(i, j).lt.0$) then

$dd2(i, j) = 0$

endif

783 continue

c Rearrange the data for input into image program

```

idata=10

do 260 i=1, islice

    do 270 j=1, idata

        xxcont(i, (idata+1-j))=dcont(i,j)

        xxd2(i, (idata+1-j))=dd2(i,j)

270    continue

260    continue

    write(6,*) 'Enter name of "image" file'

    read(5,15) ofile

    open(unit=10, file=ofile, status='new')

c Write in the data parameters

    write(10,310) 'Date & Time ', time

    write(10,350) 'Avg Emission KR ', d2avg

    write(10,320) 'Exposure Time, sec ', exptime

    write(10,300) 'Calibration, KR/count ', krcount

    write(10,330) 'System III longitude ', sys3

    write(10,300) 'g, photons/cm2sec atom ', gfact

    write(10,300) 'Seeing ', seeing

c Write in the data

98    format(2x,i6,i6,f8.1,f8.2)

    do 280 i=1, islice

        write(10,98)(j,i,xxcont(i,j),xxd2(i,j),j=1,idata)

280    continue

```

```

    stop
91  call imemsg(ier,errmag)
    write(*,(' Error: ',a80))errmsg
    stop
end

```

C.6 EUROPAIM.F

EUROPAIM takes *.img files made from EUROPANA and makes a 128x128 iraf image of continuum reflection and D2. The continuum image is scaled to match the peak signal in the Na D2 image. Each pixel is 1 arcsecond square. South is on the top and West is on the right in the images. These directions are as seen by a ground observer looking at the sky.

```

c    real exptime,sys3,gfact,seeing,krcount
c    character*60 image2,infile,errmsg,pixdir
c    character*40 infile
c    character*20 time1
c    character*20 time2
c    character*20 time3
    character*23 label
    character*18 time
    integer naxis, axlen(7)
    integer im,ier,dtype
    dimension sod1(400),sod2(400)

```

```

real surfarray(128,128), d2array(128,128)
real surfarrayd2(128,128)
real surf1array(128,128)
real d21array(128,128)
10  format(60a)
15  format(60a)
20  format(i8)
30  format(2x,i6,i6,f8.1,f8.1)
40  format(i6,i6)
45  format(f8.1,f8.1)
c   Read in the data file
write(6,*)' Enter name of input datafile (name.img)'
read(5,10)infile
write(6,*)' Enter number of slices'
read(5,20)nslice
write(6,*)' Number of points per slice assumed to be 10'
ndata=10
ntot=nslice*ndata
open(unit=4,file=infile,status='old')
c   do 47 i=1,ntot
c     sod1(i)=0.0
c     sod2(i)=0.0
c 47  continue

```

50 *format(i6)*
66 *FORMAT(2X,A23,A20)*
81 *format(a26,f10.2)*
82 *format(a26,i6)*
301 *format(a23,f8.4)*
311 *format(a23,a18)*
321 *format(a23,f8.0)*
331 *format(a23,f8.1)*
332 *format(a23,f8.2)*

c *Read in the data parameters*

read(4,311)label,time
read(4,332)label,d2avg
read(4,321)label,exptime
read(4,301)label,krcount
read(4,331)label,sys3
read(4,301)label,gfact
read(4,301)label,seeing

c *Read the data*

read(4,30)(m,n,sod1(i),sod2(i), i=1,ntot)
close(unit=4)

c *Zero out the arrays*

do 100 i=1,128
do 100 j=1,128

surfarray(i,j)=0.0

d2array(i,j)=0.0

100 *continue*

c ***Sort the data into 2 dimensional arrays***

ix=0

iy=0

do 200 i=1,nslice

do 200 j=1,ndata

*k=((i-1)*ndata+j)*

surfarray(58+i+ix,43+j+iy)=sod1(k)

d2array(58+i+ix,73+j+iy)=sod2(k)

200 *continue*

c ***Invert***

do 220 i=1,128

do 220 j=1,128

surf1array(i,j)=surfarray(129-j,i)

d21array(i,j)=d2array(129-j,i)

220 *continue*

c ***Initialize the maximum values***

surfmax=0.0

d2max=0.0

do 230 i=1,128

do 230 j=1,128

```

surfarray(i,j)=surf1array(i,j)
d2array(i,j)=d21array(i,j)
if(surfarray(i,j).gt.surfmax) then
  surfmax=surfarray(i,j)
endif
if(d2array(i,j).gt.d2max) then
  d2max=d2array(i,j)
endif

```

230 continue

c Deal with occasional zero values for surfmax

```

if(surfmax.eq.0)then
  surfmax=1.0
endif

```

c Normalize the surface array to the D1 and D2 arrays.

```

do 240 i=1,128
do 240 j=1,128
  surfarrayd2(i,j)=(d2max/surfmax)*surfarray(i,j)

```

240 continue

c Sum arrays

```

do 300 i=1,128
do 300 j=1,128
  d2array(i,j)=d2array(i,j)+surfarrayd2(i,j)

```

300 continue

```
write(6,*)' '  
write(*,'(Enter pixel directory = ",$)')
```

```
read(5,10)pixdir
```

```
write(6,*)' '
```

c *Get image name*

```
call clargc(1,image,ier)
```

```
if(ier.ne.0) then
```

```
  write(*,'(Enter name of D2 image: ",$)')
```

```
  read(5,15) image2
```

```
endif
```

c *Create the image*

```
axlen(1)=128
```

```
axlen(2)=128
```

```
naxis=2
```

```
call clargi(4,dtype,ier)
```

```
if(ier.ne.0)then
```

```
  dtype=6
```

```
endif
```

```
call imcrea(image2,axlen,naxis,dtype,ier)
```

```
if(ier.ne.0) then
```

```
  goto 91
```

```
endif
```

c *Open the image*


```

call imopen(image2,3,im,ier)
if(ier.ne.0) then
  goto 91
endif
call imakwc(im,'DATEOBS',time ,",ier)
call imakwr(im,'AVG EMSN KR',d2avg,",ier)
call imakwr(im,'EXPOSURE',exptime,",ier)
call imakwr(im,'CALIBRATION',krcount,",ier)
call imakwr(im,'GFACTOR',gfact,",ier)
call imakwr(im,'SYS3LONG',sys3,",ier)
call imakwr(im,'SEEING',seeing,",ier)
c Write date of observation into the header
c if(itrig.eq.2)then
c call imakwc(im,'DATE-OBS','D/M/Y =',time1,ier)
c call imakwc(im,'UT','UT HR =',time2,ier)
c else
c call imakwc(im,'DATE-OBS','UT Y/M/D/HR/MIN =',time3,ier)
c endif
c Write in the data
call imps2r(im,d2array,1,axlen(1),1,axlen(2),ier)
if(ier.ne.0) then
  goto 91
endif

```

c *call imakwi(im,'NUMBER',numpix,'PIXELS',ier)*

c *Close the image*

call imclos(im,ier)

if(ier.ne.0) then

goto 91

endif

stop

c *Error exit*

91 *call imemsg(ier,errmsg)*

write(,(' Error: ', a80)) errmsg*

stop

end

Bibliography

- Brown, M.E., and Hill, R.E. Discovery of an extended sodium atmosphere around Europa, *Nature* 380, 229-231, 1996.
- Brown, M.E. Potassium in Europa's Atmosphere, *Icarus* 151, 190, 2001.
- Brown, R.A., and Yung, Y.L. Io, its atmosphere and optical emissions, Jupiter, The University of Arizona Press, 1102-1145, 1976.
- Chamberlain, J.W. Theory of Planetary Atmospheres, IGS vol.22, Academic Press, 1978.
- De Pater, I., and Lissauer, J.J. Planetary Sciences, Cambridge University Press, 2001.
- Fink, U., and Larson, H.P. Temperature dependence of the water ice spectrum between 1 and 4 microns: Applications to Europa, Ganymede, and Saturn's rings, *Icarus* 24, 411-420, 1975.
- Frank, L.A., and Paterson W.R. Return to Io by the Galileo spacecraft: Plasma Observations, *J. Geophys. Res.* 105, 25 363-25 378, 2000.
- Frank, L.A., and Paterson W.R. Passage through Io's ionospheric plasmas by the Galileo spacecraft, *J. Geophys. Res.* 106, 26 209-26 204, 2001.
- Frank, L.A., and Paterson W.R. Plasma observed with the Galileo spacecraft during its flyby over Io's northern polar region, *J. Geophys. Res.* 107, 1029, 2002.
- Gault, W.A., and Rundle, H.N. Twilight observations of upper atmospheric sodium, potassium, and lithium, *Canadian Journal of Physics* 47, 85, 1969.
- Hall, D.T., Stroebel, D.F., Feldman, P.D., McGrath, M.A., and Weaver, H.A. Detection of an Oxygen atmosphere on Jupiter's moon Europa, *Nature* 373, 677-679, 1995.
- Intriligator, D.S., and Miller, W.D. First Evidence for a Europa Plasma Torus, *J. Geophys. Res.* 87, 8081-8090, 1982.
- Keller C.U., Plymate C., and Ammons S.M. Low-cost solar adaptive optics in the infrared, *SPIE* 4853, 2002.

- Killen, R.M. Curve-of-Growth Model for Sodium D2 Emission at Mercury, *Publ. Ast. Soc. Pacific* 118, 1347-1353, 2006.
- Kimmel, G.A., and Petrik, N.G. Electron-stimulated reactions in thin water films on Pt(111), *PHYS 125*, 231st ACS National Meeting, 2006.
- Kliore, A.J., Herrera, R.G., Hinson, D.P., Twicken J.D., Flasar, F.M., and Schinder, P.D. The Ionosphere of Io and the plasma environments of Europa, Ganymede and Callisto, *BAAS* 30, 55.P09, 1998.
- Leblanc, F., Johnson, R.E., and Brown, M. Europa's sodium atmosphere: An ocean source? *Icarus* 159, 134-144, 2002.
- Lodders, K., and Fegley, B. *The planetary scientist's companion*, Oxford University Press, 1998.
- Pierce, A.K. Notes from Observatories: Construction of a Bower Image Slicer, *Publ. Ast. Soc. Pacific* 77, 456, 216-117, 1965.
- Potter, A.E., and Morgan, T.H. Discovery of sodium and potassium vapor in the atmosphere of the moon, *Science* 241, 675-680, 1988.
- Potter, A.E., Anderson, C.M., Killen, R.M., and Morgan, T.H. Ratio of sodium to potassium in the Mercury exosphere, *J. Geophys. Res. (Planets)* 107, E6, 2002.
- Press, W.H., Flannery, B.P., Teukolsky, S.A., and Vetterling, W.T. *Numerical Recipes: The Art of Scientific Computing*, Cambridge University Press, 1986.
- Saur, J., Neubauer, F.M., Connerney, J.E.P., Zarka, P., and Kivelson, M.G. *Plasma Interaction of Io with its Plasma Torus, Jupiter*. Cambridge University Press, 537-560, 2004.
- U.S. Standard Atmosphere, 1976. NASA, U.S Airforce NOAA-S/T, 76-1562. U.S. Government Printing Office, Washington, D.C., 1976.
- Woodward, R.C. Jr. V-FUDGIT 4.2: A Voigt fitting function and macro package for FUDGIT, 1998.